

Applications with the Newest Multi-spectral Environmental Satellites

Lectures and Labs in Madison from 25 to 29 Mar 2013



Paul Menzel

RS Bootcamp Agenda for 25 – 29 March 2013 in Room 1411

Monday 9 – 11 am and 1 – 4 pm

Planck function, BTs in mixels, Intro to HYDRA, reflected solar and thermal emission, 4 vs 11 um

Tuesday 9 – 11 am and 1 – 4 pm

RTE, land-ocean-atm spectral signatures in MODIS & VIIRS

Wednesday 9 – 11 am and 1 – 4 pm

Hyperspectral IR, MW Sounder, VIIRS, CrIS, & ATMS split window estimates of low level moisture.

Thursday 1- 4 pm

Group projects on winter storm over USA on their own

Friday 9 – 11 am

Group presentations, Quiz, Summary Lecture.

Lectures am, Labs pm

180 min labs will include student presentations

Lectures and Labs

Lectures and laboratory exercises emphasize investigation of high spatial resolution visible and infrared data (from MODIS and VIIRS), high spectral resolution infrared data (from AIRS and CrIS), and microwave sounding data (AMSU and ATMS). Text for the classroom and a visualization tool for the labs are provided free; “Applications with Meteorological Satellites” is used as a resource text from <ftp://ftp.ssec.wisc.edu/pub/menzel/> and HYDRA is used to interrogate and view multispectral data in the labs from <http://www.ssec.wisc.edu/rink/hydra2>. Homework assignments and classroom tests are administered to verify that good progress is being made in learning and mastering the materials presented.

Lectures



Applications with Meteorological Satellites is used as a resource text

It is available for free at *ftp://ftp.ssec.wisc.edu/pub/menzel/*

CHAPTER 1 - EVOLUTION OF SATELLITE METEOROLOGY

CHAPTER 2 - NATURE OF RADIATION *

CHAPTER 3 - ABSORPTION, EMISSION, REFLECTION, AND SCATTERING *

CHAPTER 4 - THE RADIATION BUDGET

CHAPTER 5 - THE RADIATIVE TRANSFER EQUATION (RTE) *

CHAPTER 6 - DETECTING CLOUDS *

CHAPTER 7 - SURFACE TEMPERATURE *

CHAPTER 8 - TECHNIQUES FOR DETERMINING ATMOSPHERIC PARAMETERS *

CHAPTER 9 - TECHNIQUES FOR DETERMINING ATMOSPHERIC MOTIONS

CHAPTER 10 - AN APPLICATION OF GEOSTATIONARY SATELLITE SOUNDING DATA

CHAPTER 11 - SATELLITE ORBITS

CHAPTER 12 - RADIOMETER DESIGN CONSIDERATIONS *

CHAPTER 13 - ESTABLISHING CLIMATE RECORDS FROM MULTISPECTRAL MODIS MEASUREMENTS

CHAPTER 14 - THE NEXT GENERATION OF SATELLITE SYSTEMS

CHAPTER 15 – INVESTIGATING LAND, OCEAN, AND ATMOSPHERE WITH MULTISPECTRAL
MEASUREMENTS *

* indicates chapters covered

References, problems sets, and quizzes are included in the Appendices

Agenda includes material from Chapters 2, 3, 5, 11, and 12

CHAPTER 2 - NATURE OF RADIATION

2.1	Remote Sensing of Radiation	2-1
2.2	Basic Units	2-1
2.3	Definitions of Radiation	2-2
2.5	Related Derivations	2-5

CHAPTER 3 - ABSORPTION, EMISSION, REFLECTION, AND SCATTERING

3.1	Absorption and Emission	3-1
3.2	Conservation of Energy	3-1
3.3	Planetary Albedo	3-2
3.4	Selective Absorption and Emission	3-2
3.7	Summary of Interactions between Radiation and Matter	3-6
3.8	Beer's Law and Schwarzschild's Equation	3-7
3.9	Atmospheric Scattering	3-9
3.10	The Solar Spectrum	3-11
3.11	Composition of the Earth's Atmosphere	3-11
3.12	Atmospheric Absorption and Emission of Solar Radiation	3-11
3.13	Atmospheric Absorption and Emission of Thermal Radiation	3-12
3.14	Atmospheric Absorption Bands in the IR Spectrum	3-13
3.15	Atmospheric Absorption Bands in the Microwave Spectrum	3-14
3.16	Remote Sensing Regions	3-14

CHAPTER 5 - THE RADIATIVE TRANSFER EQUATION (RTE)

5.1	Derivation of RTE	5-1
5.10	Microwave Form of RTE	5-28

CHAPTER 11 - SATELLITE ORBITS

11.2	The Geostationary Orbit	11-2
11.5	Sunsynchronous Polar Orbit	11-4

CHAPTER 12 - RADIOMETER DESIGN CONSIDERATIONS

12.3	Design Considerations	12-1
------	-----------------------	------

Lectures are given with powerpoint presentations

Radiative Transfer in the Atmosphere

Lecture notes available at
www.met.rdg.ac.uk/~met1001

Part 1 notes at
www.met.rdg.ac.uk/~met1001

1

Outline

Statistical Radiation
 Planck Function
 Continuum Absorption, Scattering
 Radiative Transfer Equation
 Radiative Transfer Models
 Observational Evidence

2

Open 1 Elements of Energy Balance and Energy Cycle

3

Thermology of radiative energy

4

Continuum Radiation

Wavelength	Wavenumber	Frequency
1000 cm	1000 cm ⁻¹	3000 GHz
100 cm	100 cm ⁻¹	300 GHz
10 cm	10 cm ⁻¹	30 GHz
1 cm	1 cm ⁻¹	3 GHz
1 mm	1 mm ⁻¹	300 GHz
1 μm	10000 cm ⁻¹	300 THz
1 nm	10000000 cm ⁻¹	300 PHz

5

Thermostatic Radiation Power Capable proportional to σT^4

Open 1 Power available from σT^4 at d, θ, ϕ, ψ

$P = \sigma T^4 \cdot A \cdot \Omega$

[Power 4, 4-5, 45, 45]

6

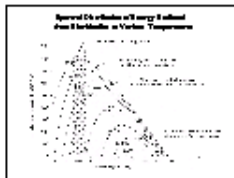
Blackbody

Planck's Law: $B_{\lambda}(T) = \frac{2hc^2}{\lambda^5} \frac{1}{e^{hc/\lambda kT} - 1}$

Wien's Displacement Law: $\lambda_{max} T = b$

Stefan-Boltzmann Law: $F = \sigma T^4$

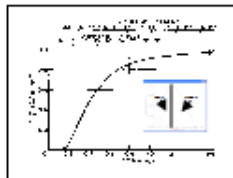
7



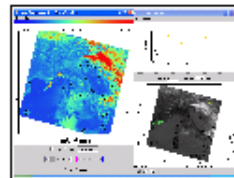
8



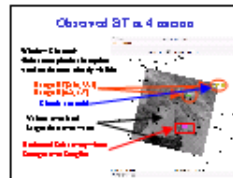
9



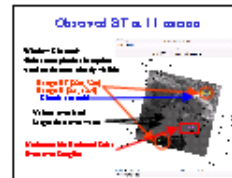
10



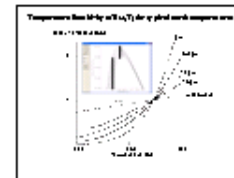
11



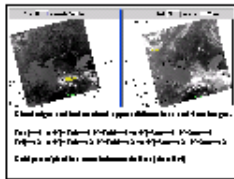
12



13



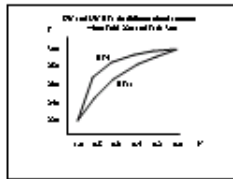
14



15

Wavelength (cm)	Wavenumber (cm ⁻¹)	Frequency (GHz)
1000	1000	300
100	100	30
10	10	3
1	1	0.3
0.1	0.1	0.03

16



17

Blackbody

Planck's Law: $B_{\lambda}(T) = \frac{2hc^2}{\lambda^5} \frac{1}{e^{hc/\lambda kT} - 1}$

Wien's Displacement Law: $\lambda_{max} T = b$

Stefan-Boltzmann Law: $F = \sigma T^4$

18

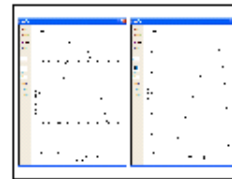
Blackbody

Planck's Law: $B_{\lambda}(T) = \frac{2hc^2}{\lambda^5} \frac{1}{e^{hc/\lambda kT} - 1}$

Wien's Displacement Law: $\lambda_{max} T = b$

Stefan-Boltzmann Law: $F = \sigma T^4$

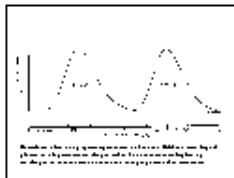
19



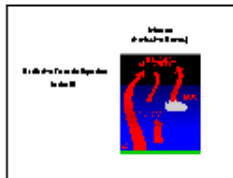
20



21



22



23

Blackbody Radiation

Wavelength (cm)	Wavenumber (cm ⁻¹)	Frequency (GHz)
1000	1000	300
100	100	30
10	10	3
1	1	0.3
0.1	0.1	0.03

24

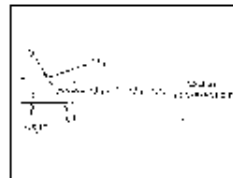
Blackbody Radiation

Planck's Law: $B_{\lambda}(T) = \frac{2hc^2}{\lambda^5} \frac{1}{e^{hc/\lambda kT} - 1}$

Wien's Displacement Law: $\lambda_{max} T = b$

Stefan-Boltzmann Law: $F = \sigma T^4$

25



26

Blackbody

Planck's Law: $B_{\lambda}(T) = \frac{2hc^2}{\lambda^5} \frac{1}{e^{hc/\lambda kT} - 1}$

Wien's Displacement Law: $\lambda_{max} T = b$

Stefan-Boltzmann Law: $F = \sigma T^4$

27

Blackbody Radiation

Planck's Law: $B_{\lambda}(T) = \frac{2hc^2}{\lambda^5} \frac{1}{e^{hc/\lambda kT} - 1}$

Wien's Displacement Law: $\lambda_{max} T = b$

Stefan-Boltzmann Law: $F = \sigma T^4$

28

Material includes equations

$$\text{Planck's Law} \quad B(\lambda, T) = \frac{c_1}{\lambda^5} \left[e^{-\frac{c_2}{\lambda T}} - 1 \right]^{-1} \quad (\text{mW/m}^2/\text{ster/cm})$$

where

λ = wavelengths in cm

T = temperature of emitting surface (deg K)

$c_1 = 1.191044 \times 10^{-5}$ (mW/m²/ster/cm⁻⁴)

$c_2 = 1.438769$ (cm deg K)

Wien's Law

$$dB(\lambda_{\max}, T) / d\lambda = 0 \text{ where } \lambda(\max) = .2897/T$$

indicates peak of Planck function curve shifts to shorter wavelengths (greater wavenumbers) with temperature increase. Note $B(\lambda_{\max}, T) \sim T^5$.

$$\text{Stefan-Boltzmann Law} \quad E = \pi \int_0^{\infty} B(\lambda, T) d\lambda = \sigma T^4, \text{ where } \sigma = 5.67 \times 10^{-8} \text{ W/m}^2/\text{deg}^4.$$

states that irradiance of a black body (area under Planck curve) is proportional to T^4 .

Brightness Temperature

$$T = \frac{c_2}{\lambda \ln\left(\frac{c_1}{\lambda^5 B_\lambda} + 1\right)} \text{ is determined by inverting Planck function}$$

And some derivations,

$$I_{\lambda} = \varepsilon_{\lambda}^{\text{sfc}} B_{\lambda}(T(p_s)) \tau_{\lambda}(p_s) + \sum_p \varepsilon_{\lambda}(\Delta p) B_{\lambda}(T(p)) \tau_{\lambda}(p)$$

The emissivity of an infinitesimal layer of the atmosphere at pressure p is equal to the absorptance (one minus the transmittance of the layer). Consequently,

$$\varepsilon_{\lambda}(\Delta p) \tau_{\lambda}(p) = [1 - \tau_{\lambda}(\Delta p)] \tau_{\lambda}(p)$$

Since transmittance is an exponential function of depth of absorbing constituent,

$$\tau_{\lambda}(\Delta p) \tau_{\lambda}(p) = \exp \left[- \int_p^{p+\Delta p} k_{\lambda} q g^{-1} dp \right] * \exp \left[- \int_0^p k_{\lambda} q g^{-1} dp \right] = \tau_{\lambda}(p + \Delta p)$$

Therefore

$$\varepsilon_{\lambda}(\Delta p) \tau_{\lambda}(p) = \tau_{\lambda}(p) - \tau_{\lambda}(p + \Delta p) = - \Delta \tau_{\lambda}(p) .$$

So we can write

$$I_{\lambda} = \varepsilon_{\lambda}^{\text{sfc}} B_{\lambda}(T(p_s)) \tau_{\lambda}(p_s) - \sum_p B_{\lambda}(T(p)) \Delta \tau_{\lambda}(p) .$$

which when written in integral form reads

$$I_{\lambda} = \varepsilon_{\lambda}^{\text{sfc}} B_{\lambda}(T(p_s)) \tau_{\lambda}(p_s) - \int_0^{p_s} B_{\lambda}(T(p)) [d\tau_{\lambda}(p) / dp] dp .$$

Labs



HYperspectral viewer for Development of Research Applications – HYDRA2

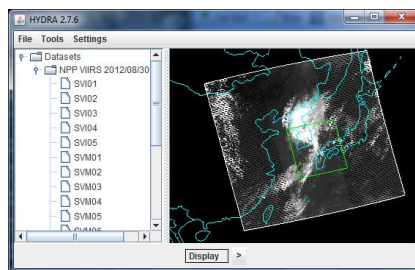
MODIS,
VIIRS, CrIS,
ATMS

Developed at CIMSS by
Tom Rink

With programming
support from
Tommy Jasmin,
Ghansham Sangar
(ISRO)

With guidance from
Liam Gumley
Kathy Strabala
Paul Menzel

Freely available gui-driven software
For researchers and educators
Computer platform independent
Extendable to more sensors and applications
Uses Java-based technologies
Interactive, high-performance 2D/3D animations
derived from SSEC VisAD api
On-going development effort



<ftp://ftp.ssec.wisc.edu/rink/HYDRA2>

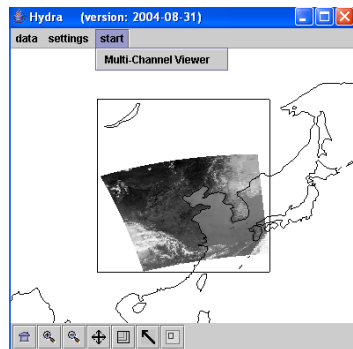
HYperspectral viewer for Development of Research Applications - HYDRA

MSG,
GOES



Freely available software
For researchers and educators
Computer platform independent
Extendable to more sensors and applications
Based in VisAD
(Visualization for Algorithm Development)
Uses Jython (Java implementation of Python)
runs on most machines

Rink et al, BAMS 2007



MODIS,
AIRS, IASI,
AMSU,
CALIPSO

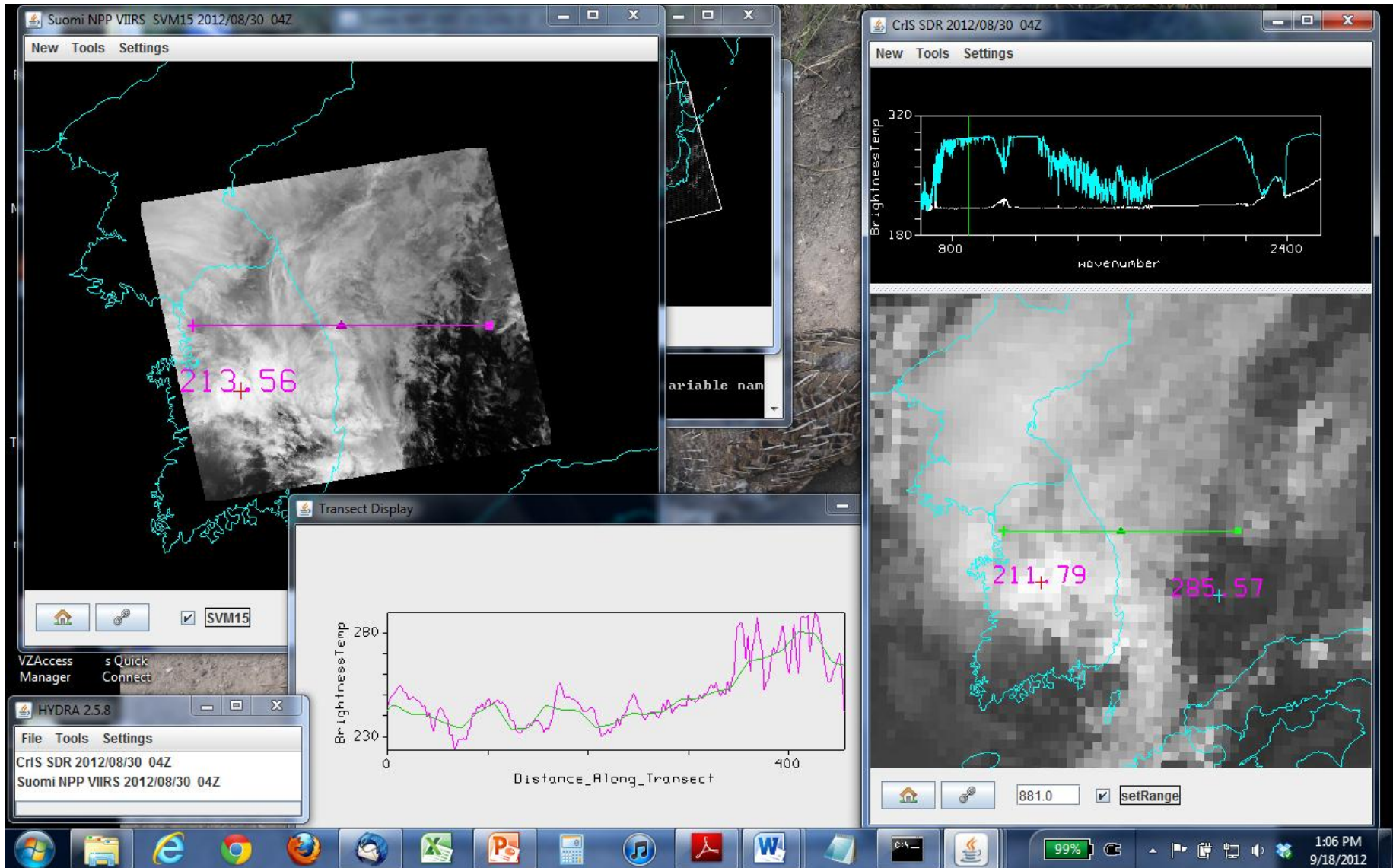
Developed at CIMSS by
Tom Rink
Tom Whittaker
Kevin Baggett

With guidance from
Paolo Antonelli
Liam Gumley
Paul Menzel
Allen Huang



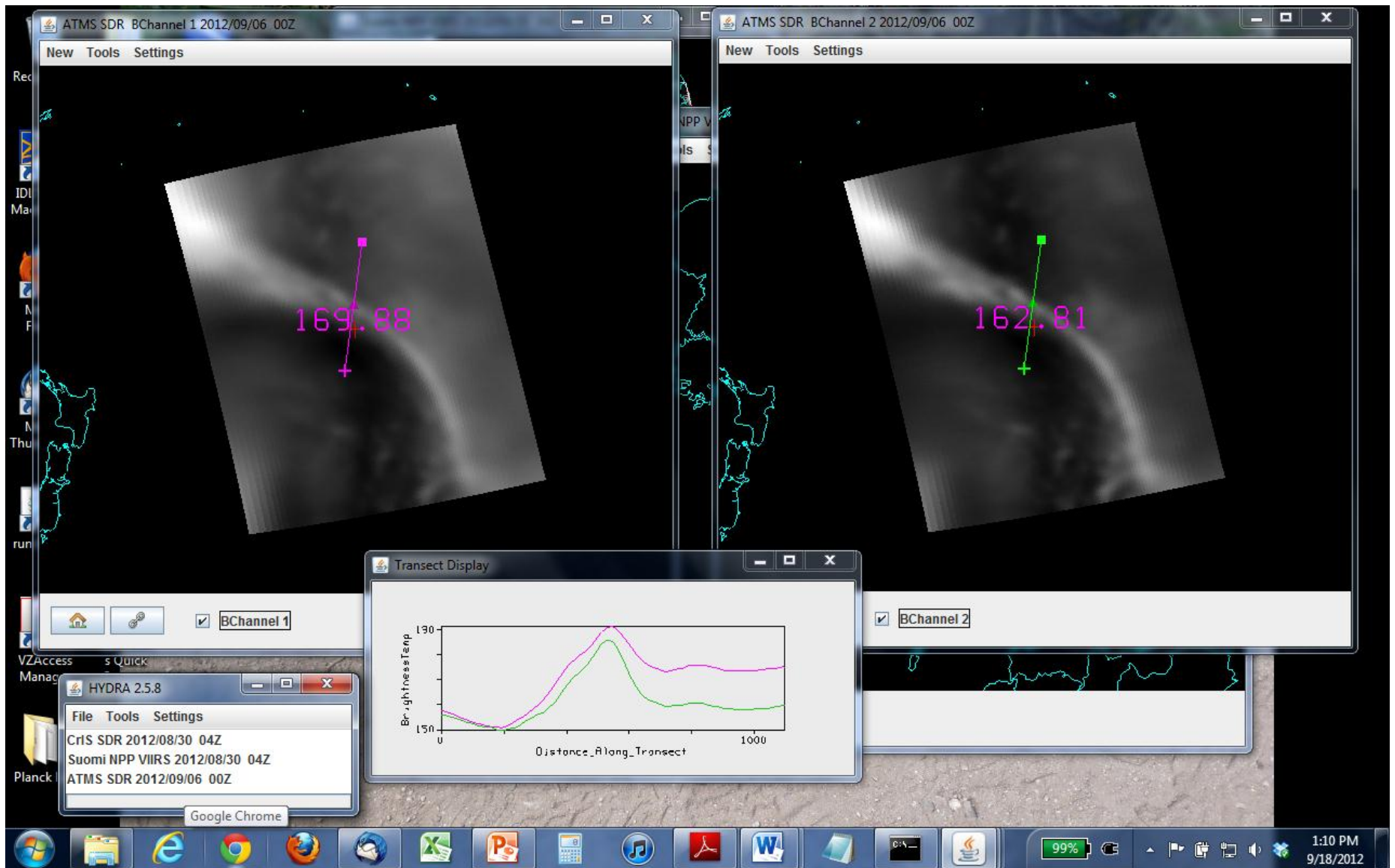
<http://www.ssec.wisc.edu/hydra/>

View remote sensing data with HYDRA2



VIIRS and CrIS

ATMS



Access to visualization tools and data

For hydra2 <ftp://ftp.ssec.wisc.edu/rink/hydra2/>

For MODIS data and quick browse images

<http://rapidfire.sci.gsfc.nasa.gov/realtime>

For MODIS data <http://ladsweb.nascom.nasa.gov/>

For AIRS data <http://daac.gsfc.nasa.gov/>

For VIIRS, CrIS, and ATMS data, orbit tracks, guide

<http://www.nsof.class.noaa.gov>

<http://www.ssec.wisc.edu/datacenter/npp/>

http://www.class.ncdc.noaa.gov/notification/faq_npp.htm

See tutorial "How do I order NPP data in CLASS (11/28/11)"

Orbits and Instruments

Lectures in Madison

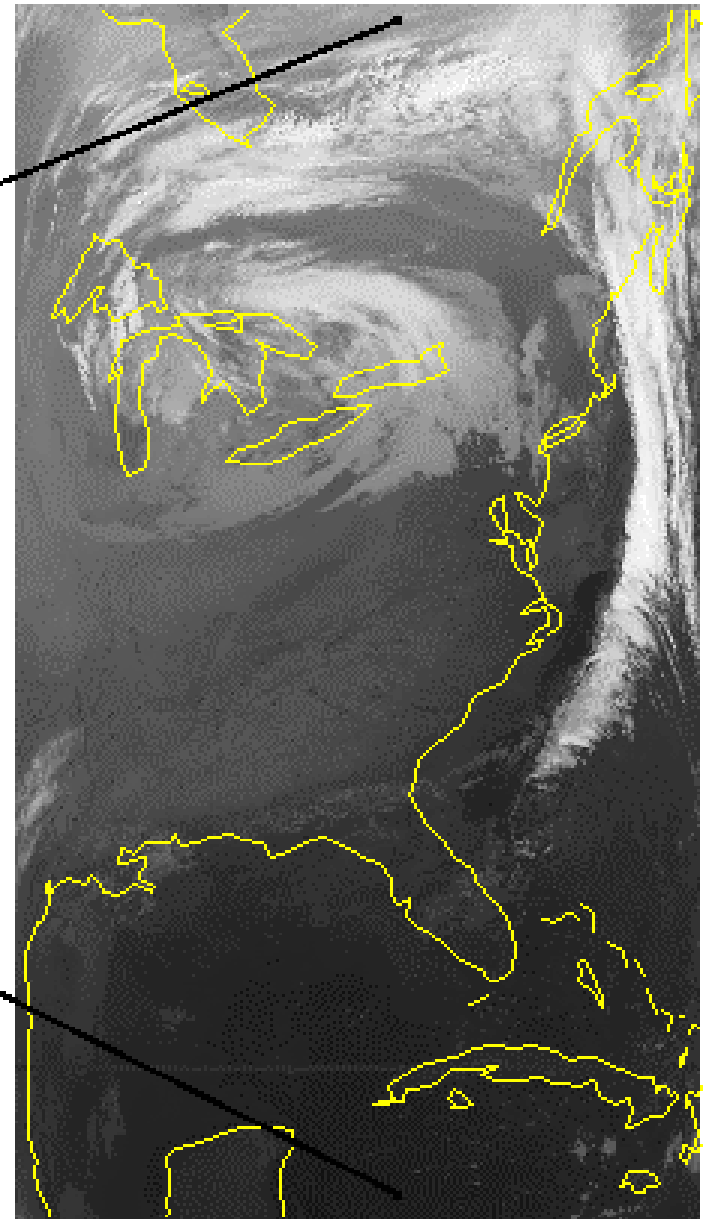
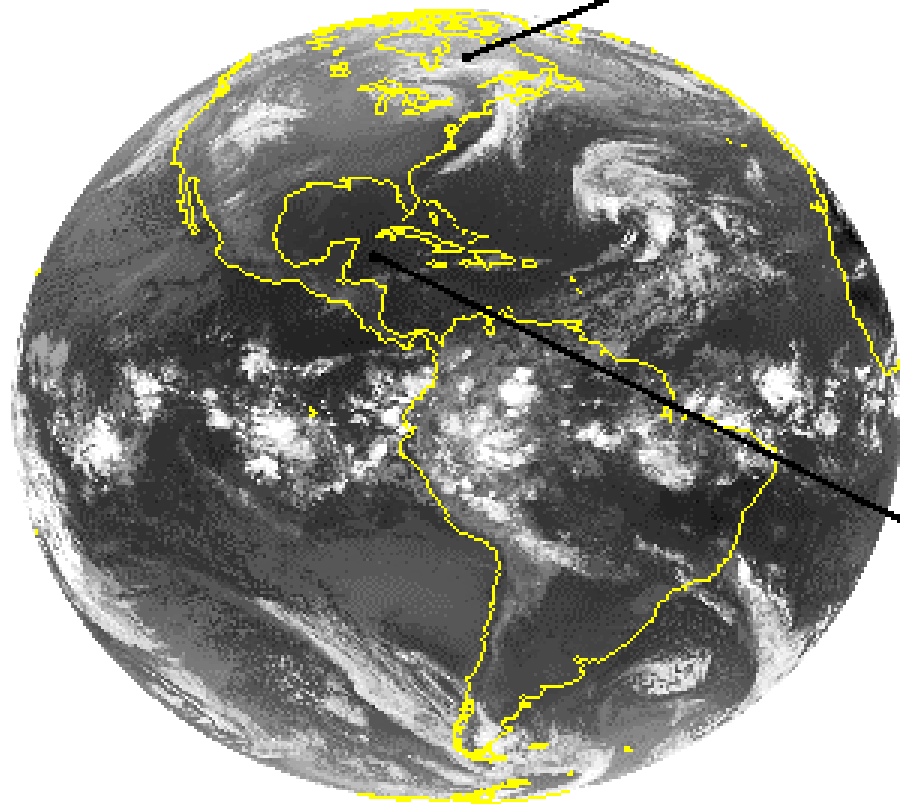
25 Mar 2013

Paul Menzel

UW/CIMSS/AOS

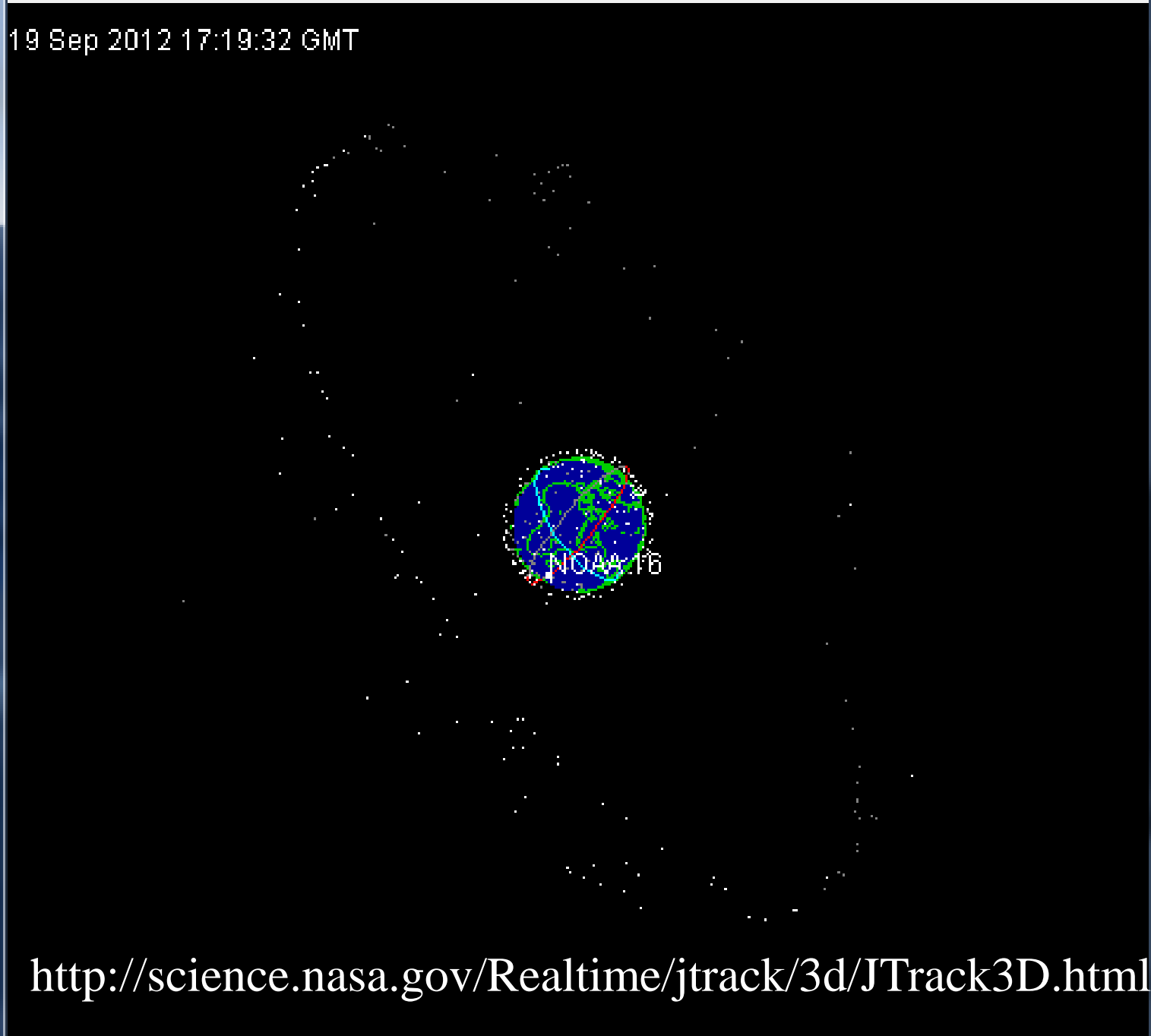


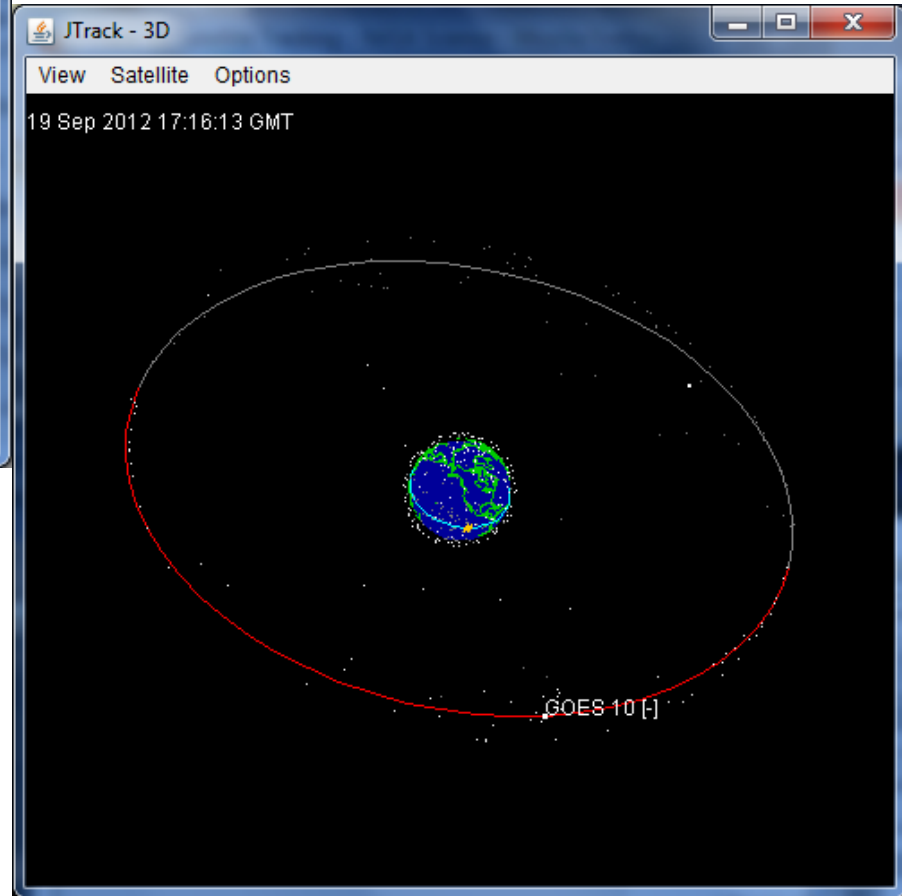
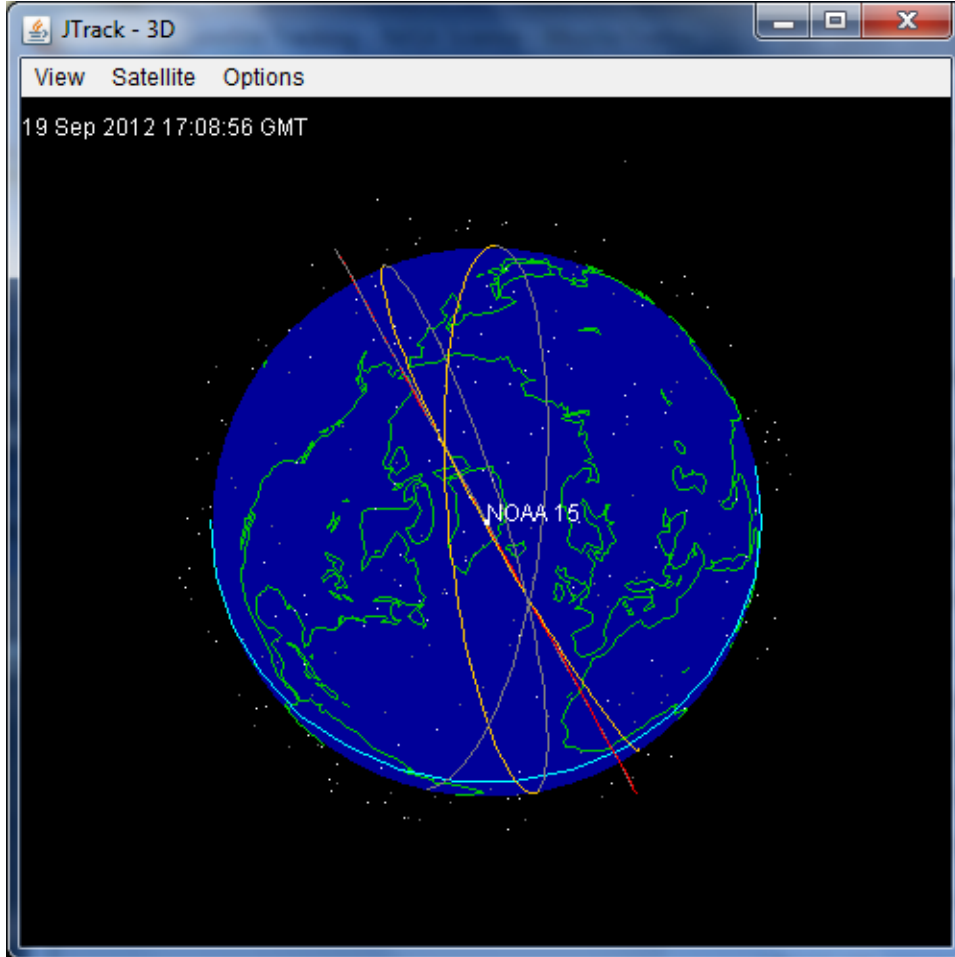
GEO vs LEO



19 Sep 2012 17:19:32 GMT

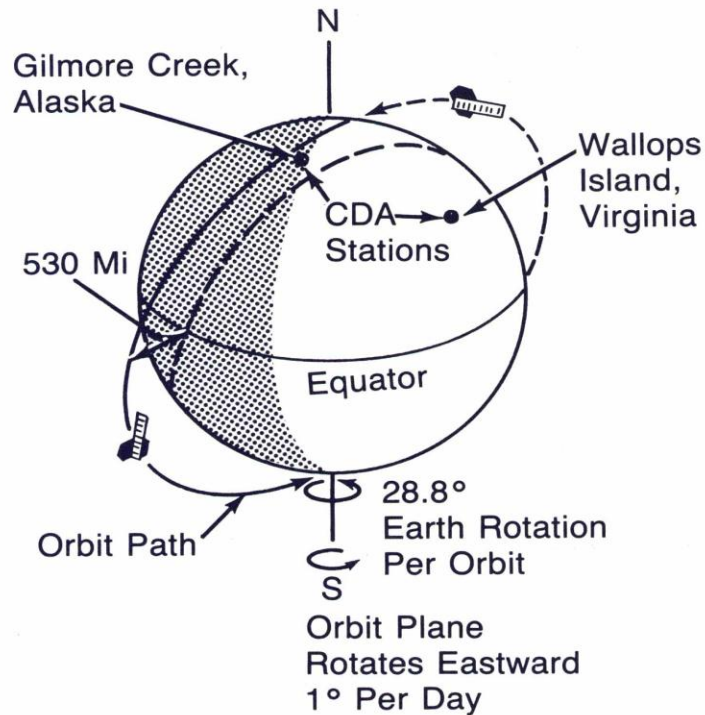
**All
Sats
on
NASA
J-track**



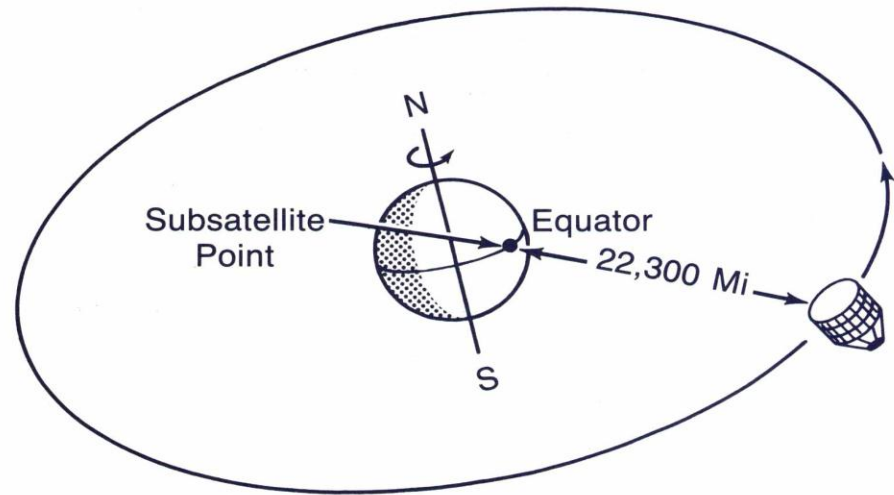


Polar (LEO) & Geostationary (GEO) Orbits

Polar Orbiting Satellites



Geostationary Satellites



Geo Orbit

Let us continue our discussion of the circular orbit. Using the definition of angular velocity $\omega = 2\pi/\tau$ where τ is the period of the orbit, then

$$GMm/r^2 = m\omega^2r$$

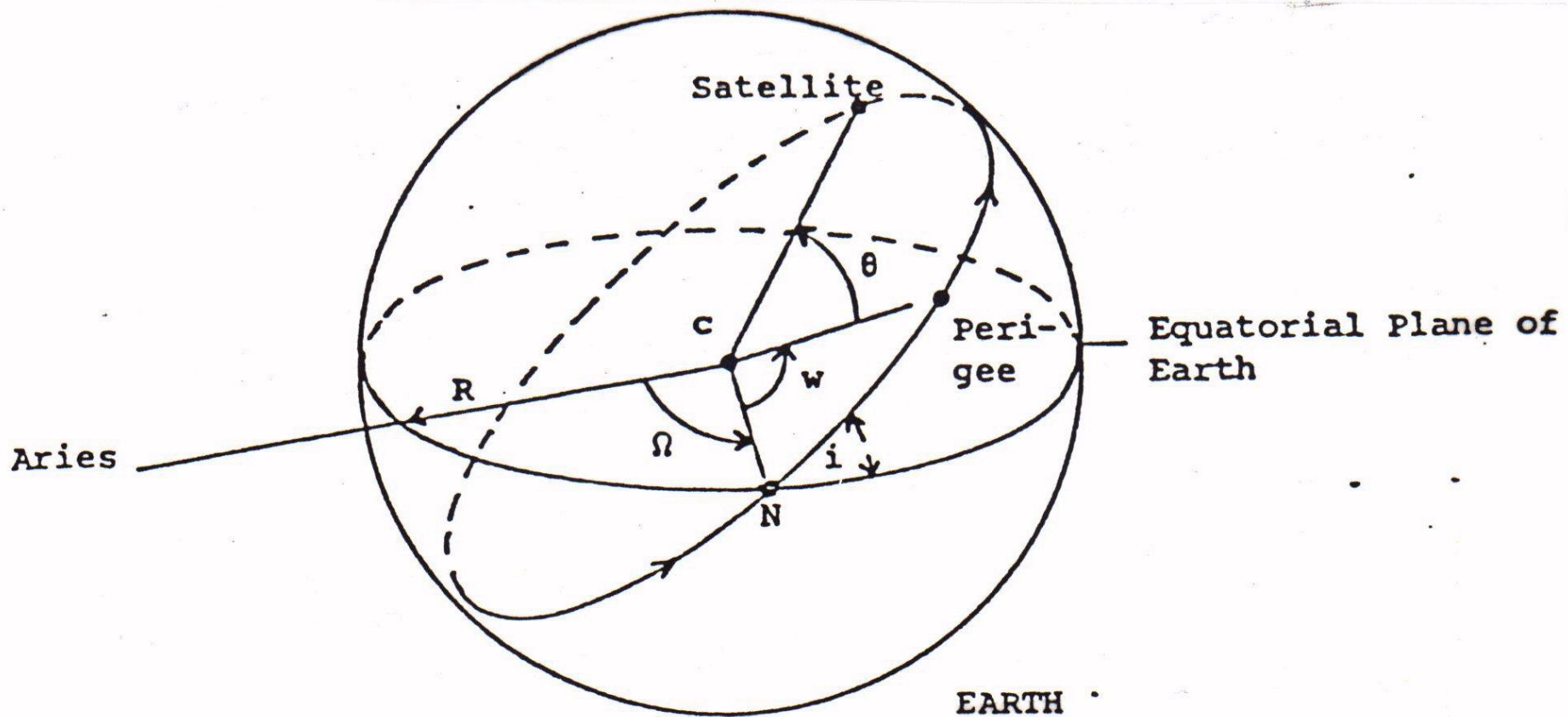
becomes

$$GM/r^3 = 4\pi^2/\tau^2 .$$

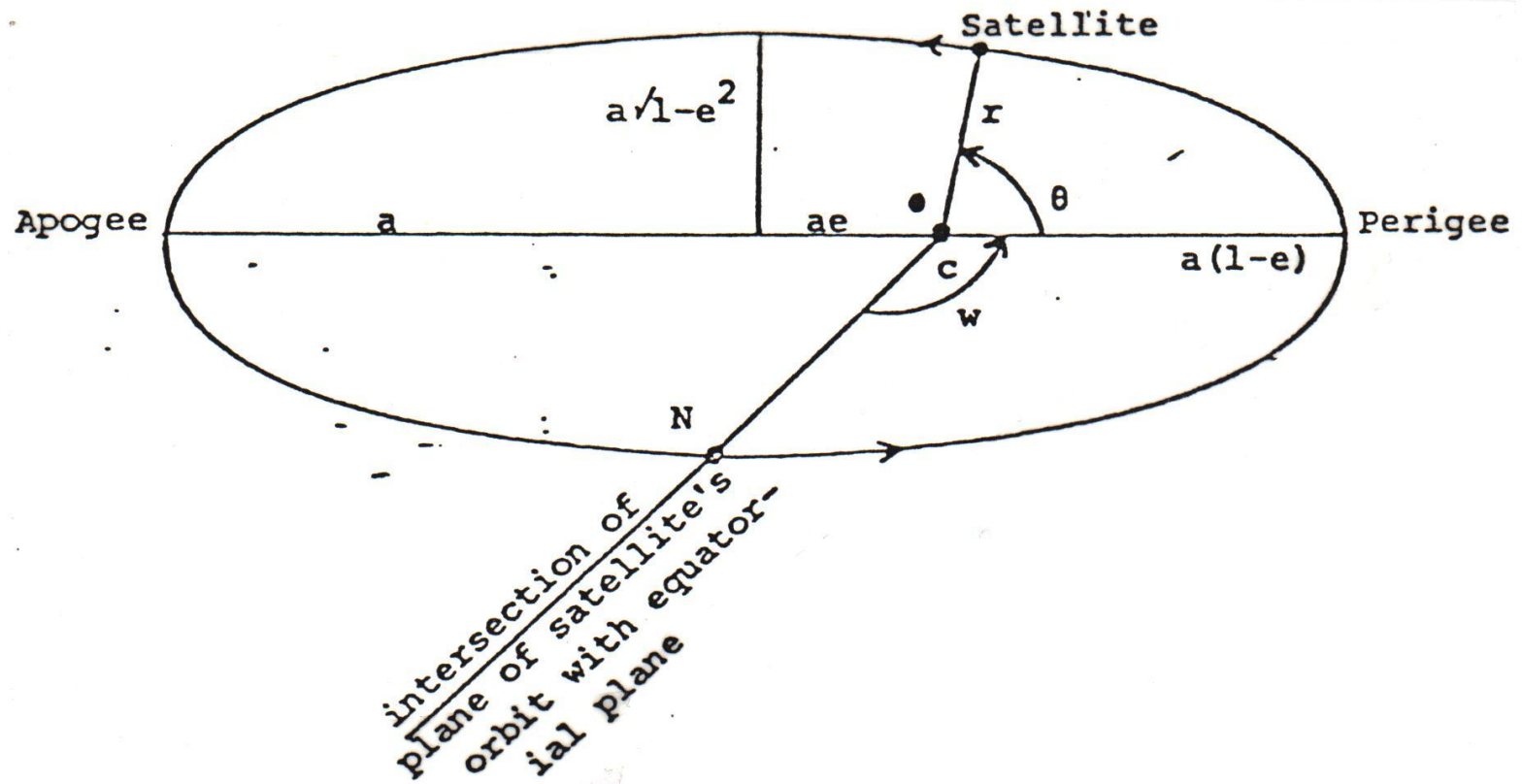
For the geostationary orbit, the period of the satellite matches the rotational period of the earth so that the satellite appears to stay in the same spot in the sky. This implies that $\tau = 24$ hours = 8.64×10^4 seconds, and the associated radius of the orbit $r = 4.24 \times 10^7$ meters or a height of about 36,000 km. The geostationary orbit is possible at only one orbit radius.

Leo Orbit

For a polar circular orbit with $\tau = 100$ minutes = 6×10^4 seconds, we get $r = 7.17 \times 10^6$ metres or a height of about 800 km. Polar orbits are not confined to a unique radius, however the type of global coverage usually suggests a range of orbit radii.



Orbital elements for an elliptical orbit showing the projection of the orbit on the surface of a spherical earth. C is the centre of the earth and R is the equatorial radius. i is the inclination of the orbit relative to the equatorial plane, Ω is the right ascension of the ascending node with respect to Aries, a is the semi-major axis of the ellipse, ϵ is the eccentricity, w is the argument of the perigee, and Θ is the angular position of the satellite in its orbit.



The orientation of the satellite orbit plane is described by (a) the inclination of the satellite orbit plane with respect to the earth equatorial plane denoted by i , and (b) the right ascension of the ascending node, Ω , measured eastwards relative to Aries (representing a fixed point in the heavens). The shape and size of the satellite orbit is given by (c) the semi-major axis of the ellipse denoted by a , and (d) the eccentricity of the ellipse, denoted by e . The orientation of the orbit in the orbit plane is given by (e) the argument of the perigee or the angle between the ascending node and the perigee denoted by w . And finally (f) θ denotes the angular position of the satellite in its orbit. These are the six orbital elements that are necessary to calculate the trajectory of the satellite in its orbit

Effects of Non-spherical Earth

The earth's gravitational field is not that of a point mass, rather it is the integrated sum over the bulging earth. The potential energy for a satellite of mass m a distance r from the centre of mass of the earth is written

$$PE = - Gm \int_{\text{earth}} \frac{dM}{s}$$

where the integration is over the mass increment dM of the earth which is a distance s from the satellite. This integration yields a function in the form

$$PE = -GMm/r [1 - \sum_{n=2, \dots} J_n (R/r)^n P_n(\cos\theta)]$$

where the J_n are coefficients of the n^{th} zonal harmonics of the earth's gravitational potential energy and the $P_n(\cos\theta)$ are Legendre polynomials defined by

$$P_n(x) = \frac{1}{n2^n} \frac{d^n}{dx^n} [(x^2-1)^n]$$

The most significant departure from the spherically symmetric field comes from the $n=2$ term, which corrects for most of the effects of the equatorial bulge. Therefore

$$PE = -GMm/r [1 - J_2 (R/r)^2 (3\cos^2\theta - 1)/2 + \dots]$$

where $J_2 = 1082.64 \times 10^{-6}$. At the poles $P_2 = 2$ and at the equator $P_2 = -1$. The coefficients for the higher zonal harmonics are three orders of magnitude reduced from the coefficient of the second zonal harmonic.

Equatorial bulge primarily makes the angle of the ascending node vary with time.

Sun-synchronous Polar Orbit

The equatorial bulge primarily makes the angle of the ascending node vary with time. The variation is given by

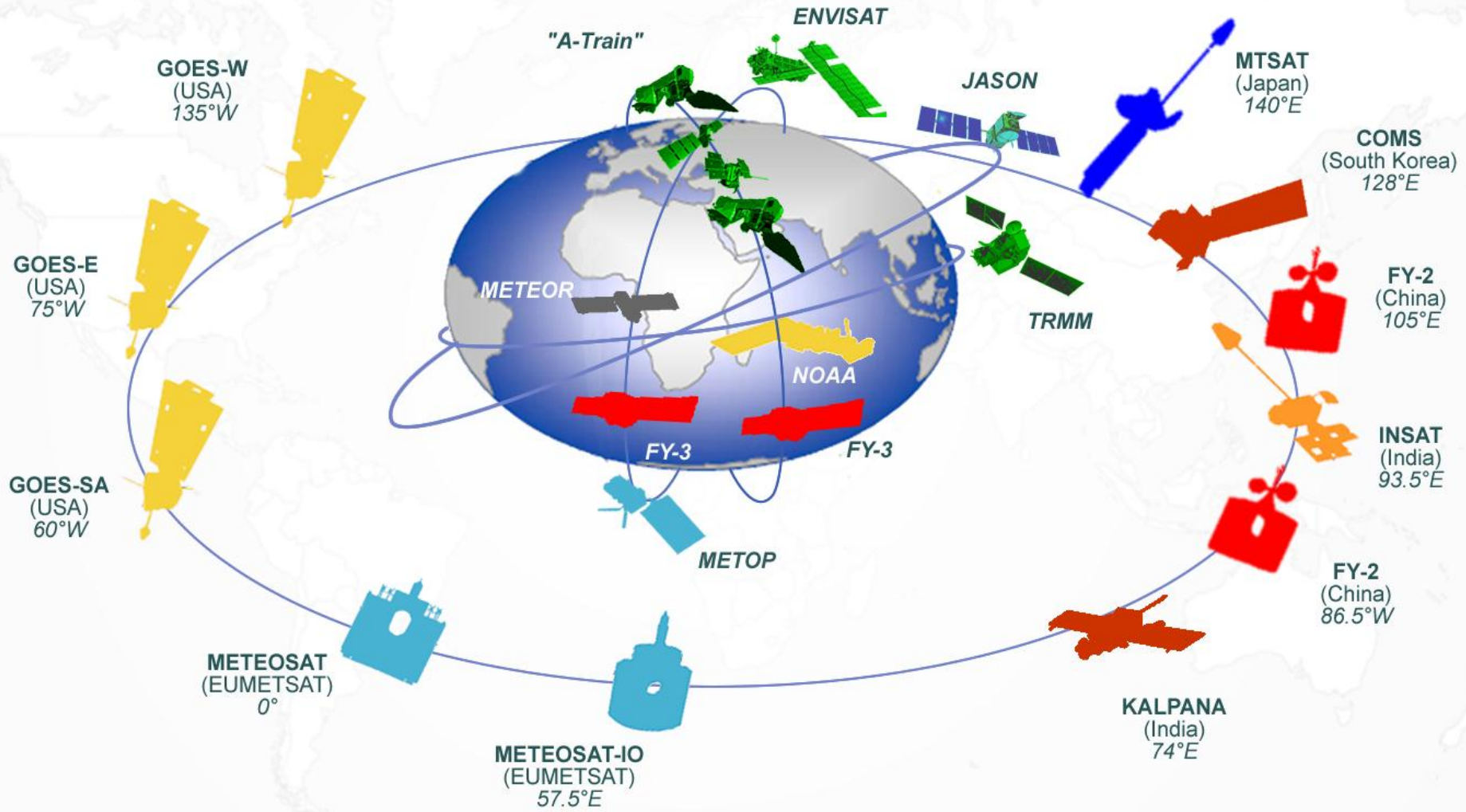
$$d\Omega/dt = -3/2 J_2 (GM)^{1/2} R^2 a^{-7/2} (1-\epsilon^2)^{-2} \cos i$$

Through suitable selection of the orbital inclination i , the rotation of the orbital plane can be made to match the rotation of the earth around the sun, yielding an orbit that is sun synchronous. The negative sign indicates a retrograde orbit, one with the satellite moving opposite to the direction of the earth's rotation. The rotation rate for sun synchronous orbit is given by

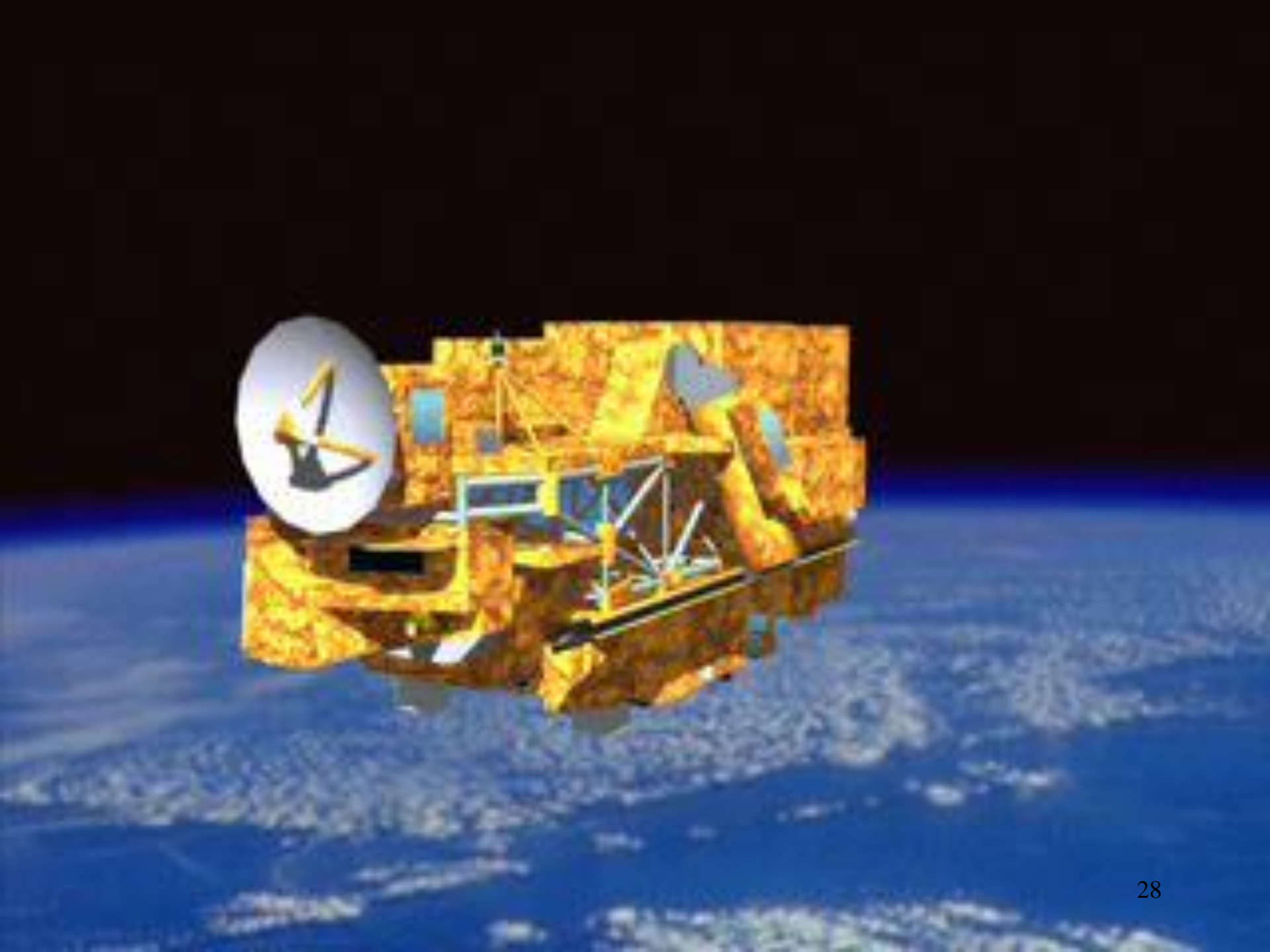
$$\Omega = 2\pi/365.24 \text{ radians/year} = 2 \times 10^{-7} \text{ rad/sec} .$$

which is approximately one degree per day. Such a rate is obtained by placing the satellite into an orbit with a suitable inclination; for a satellite at a height of 800 km (assuming the orbit is roughly circular so that $a = r$), we find $i = 98.5$ degrees which is a retrograde orbit inclined at 81.5 degrees. The inclination for sun synchronous orbits is only a weak function of satellite height; the high inclination allows the satellite to view almost the entire surface of the earth from pole to pole.

Space-based Global Observing System 2012



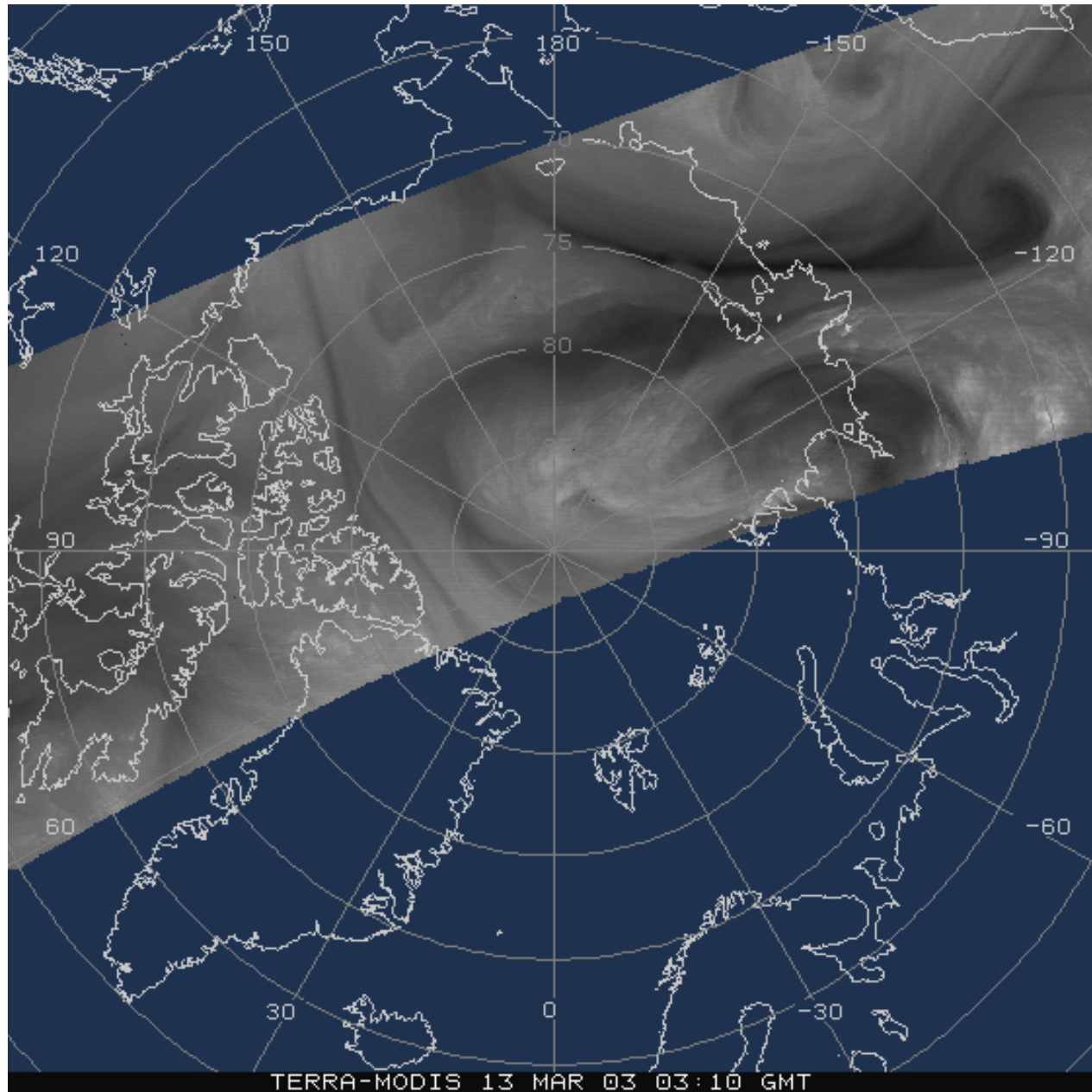




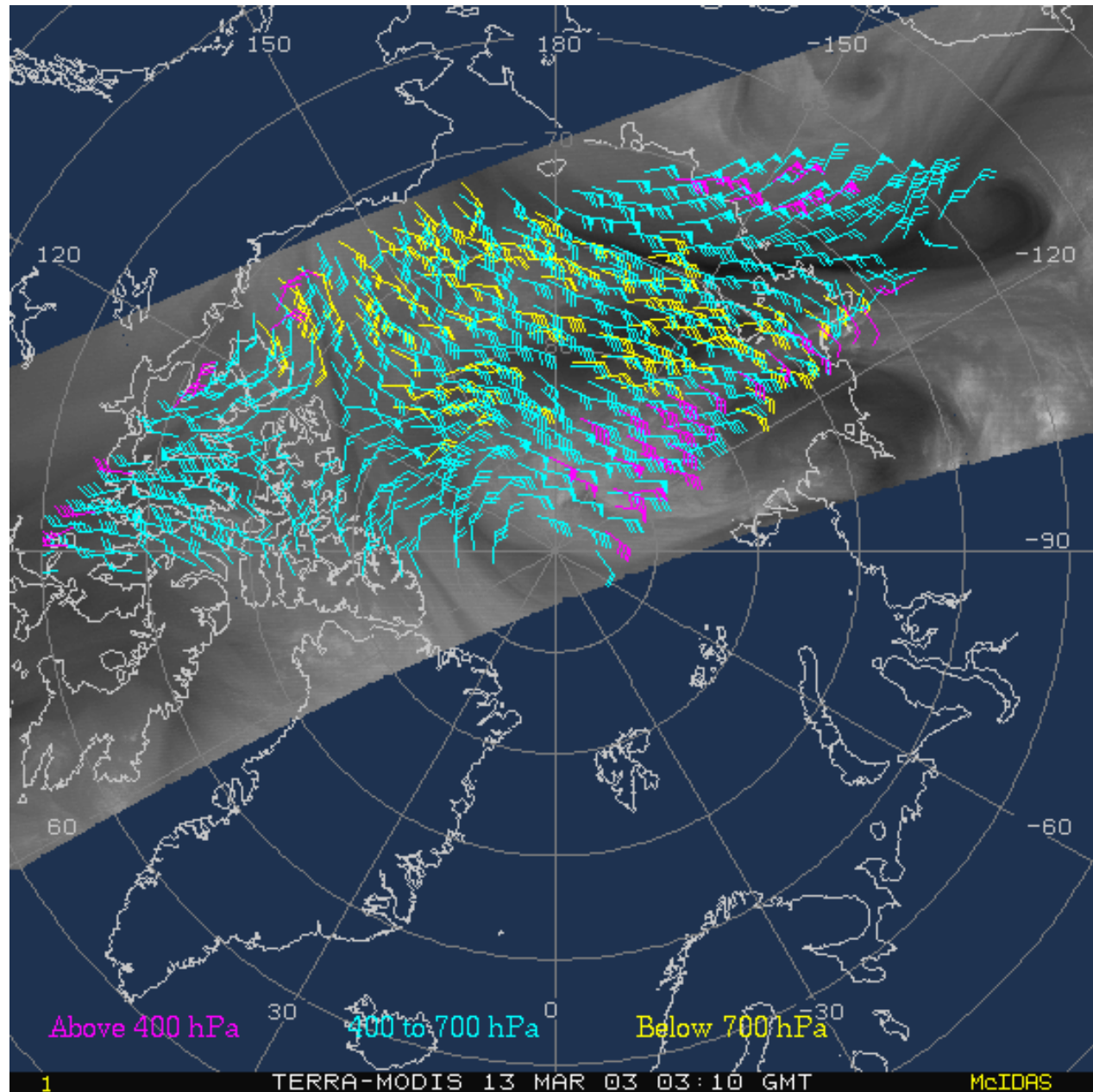




Leo coverage of poles every 100 minutes



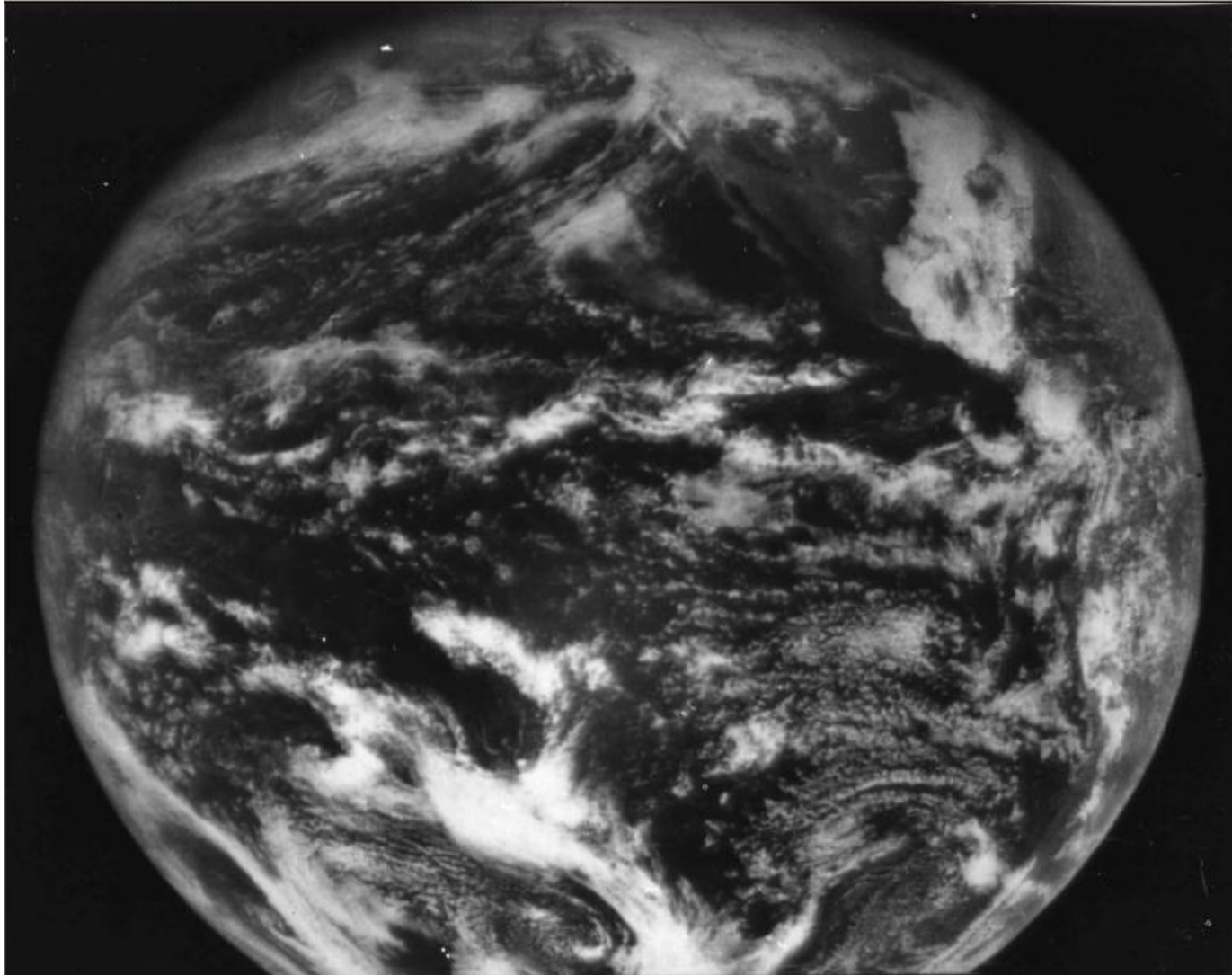
Tracking Polar Atmospheric Motion from Leo Obs



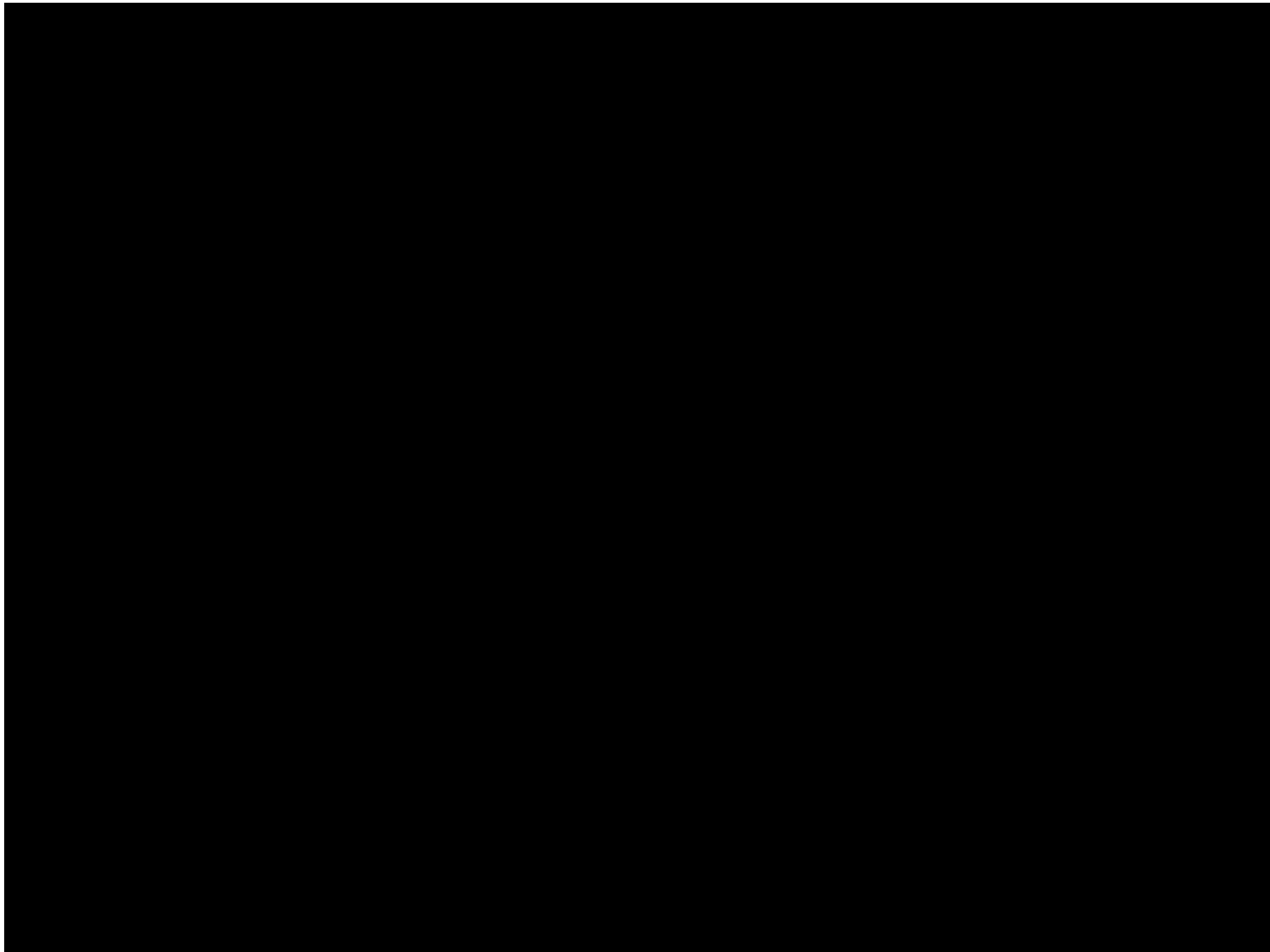
Getting to Geostationary Orbit

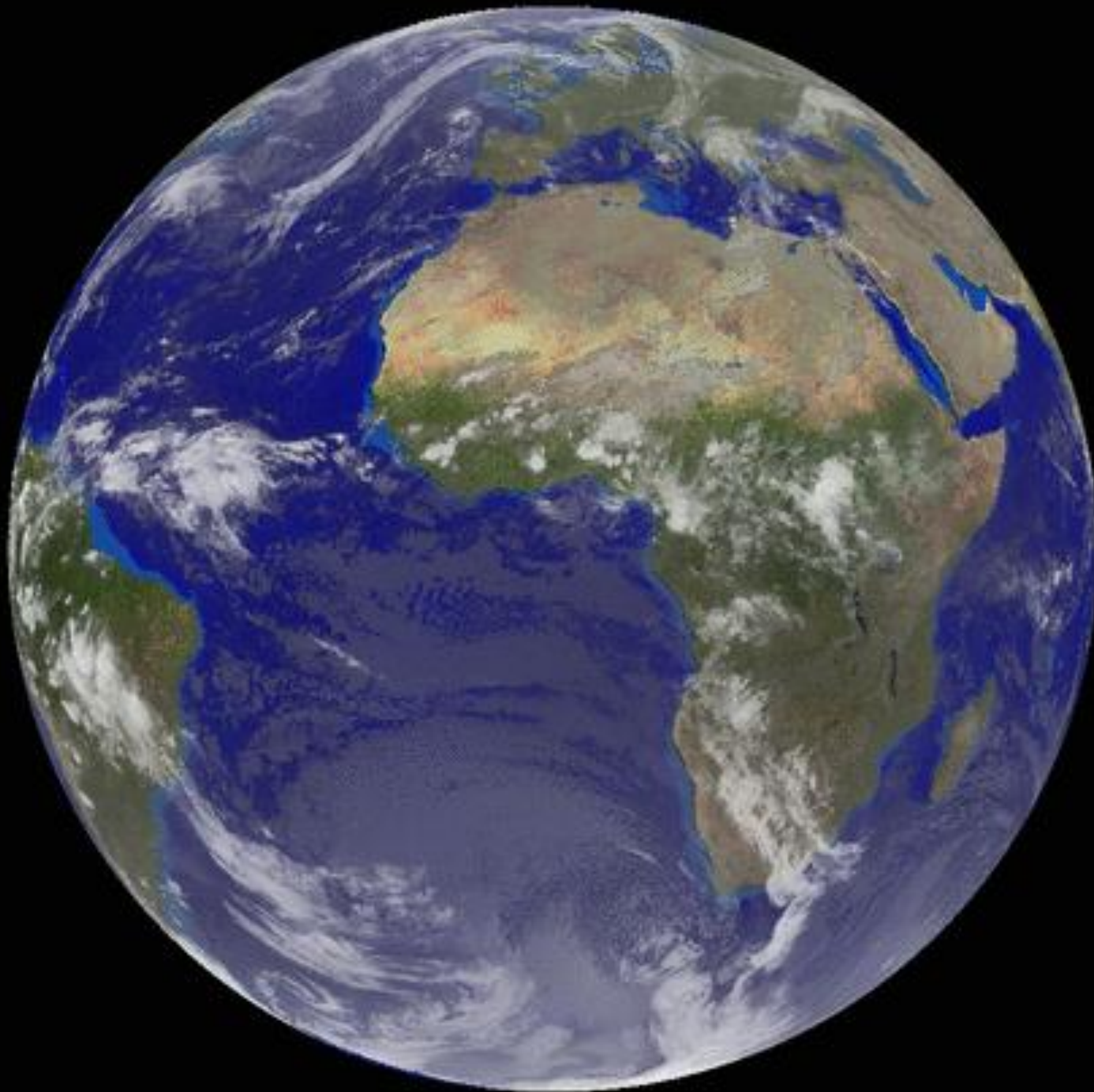


Observations from geostationary orbit

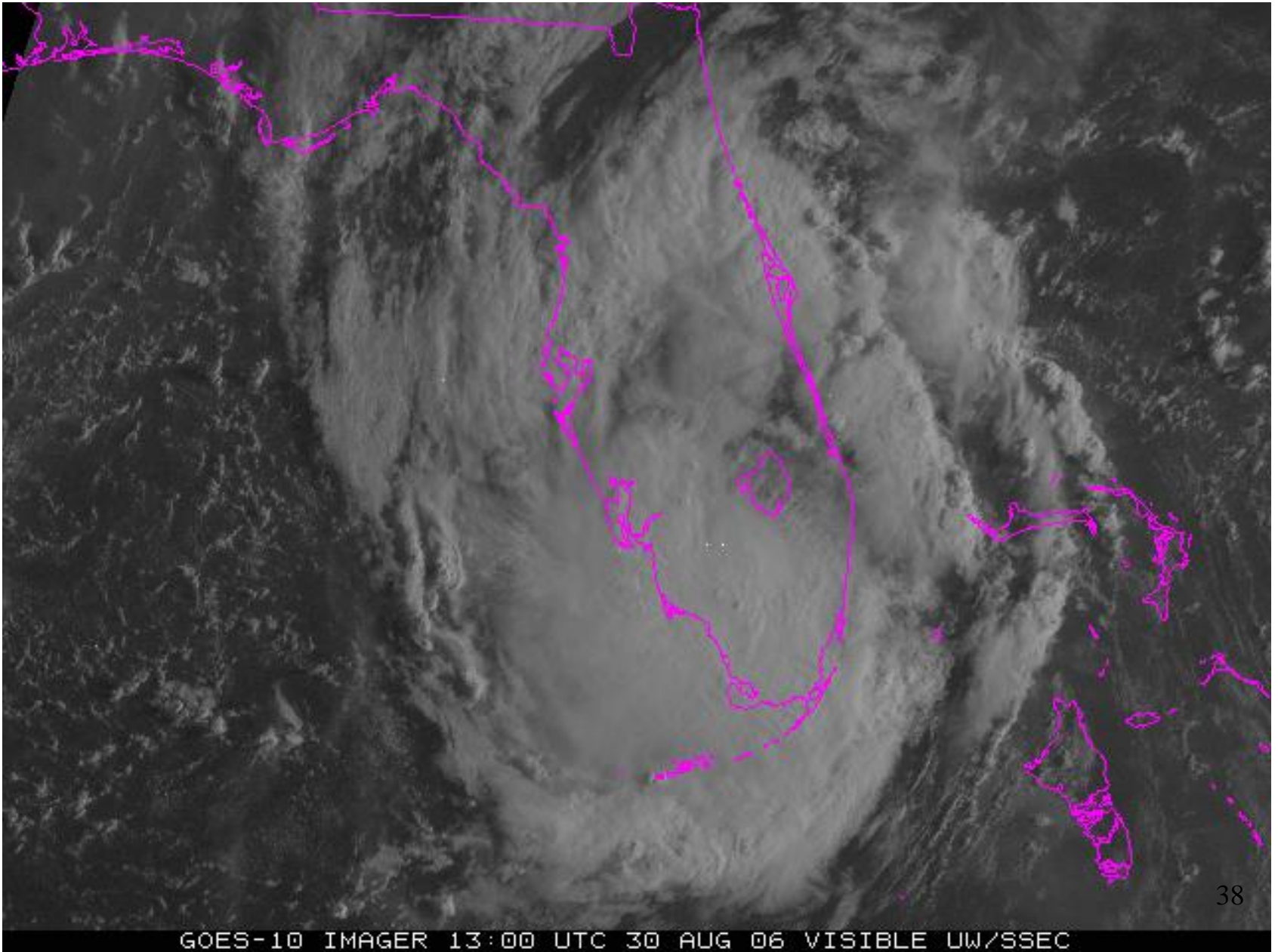


“the weather moves - not the satellite”
Verner Suomi





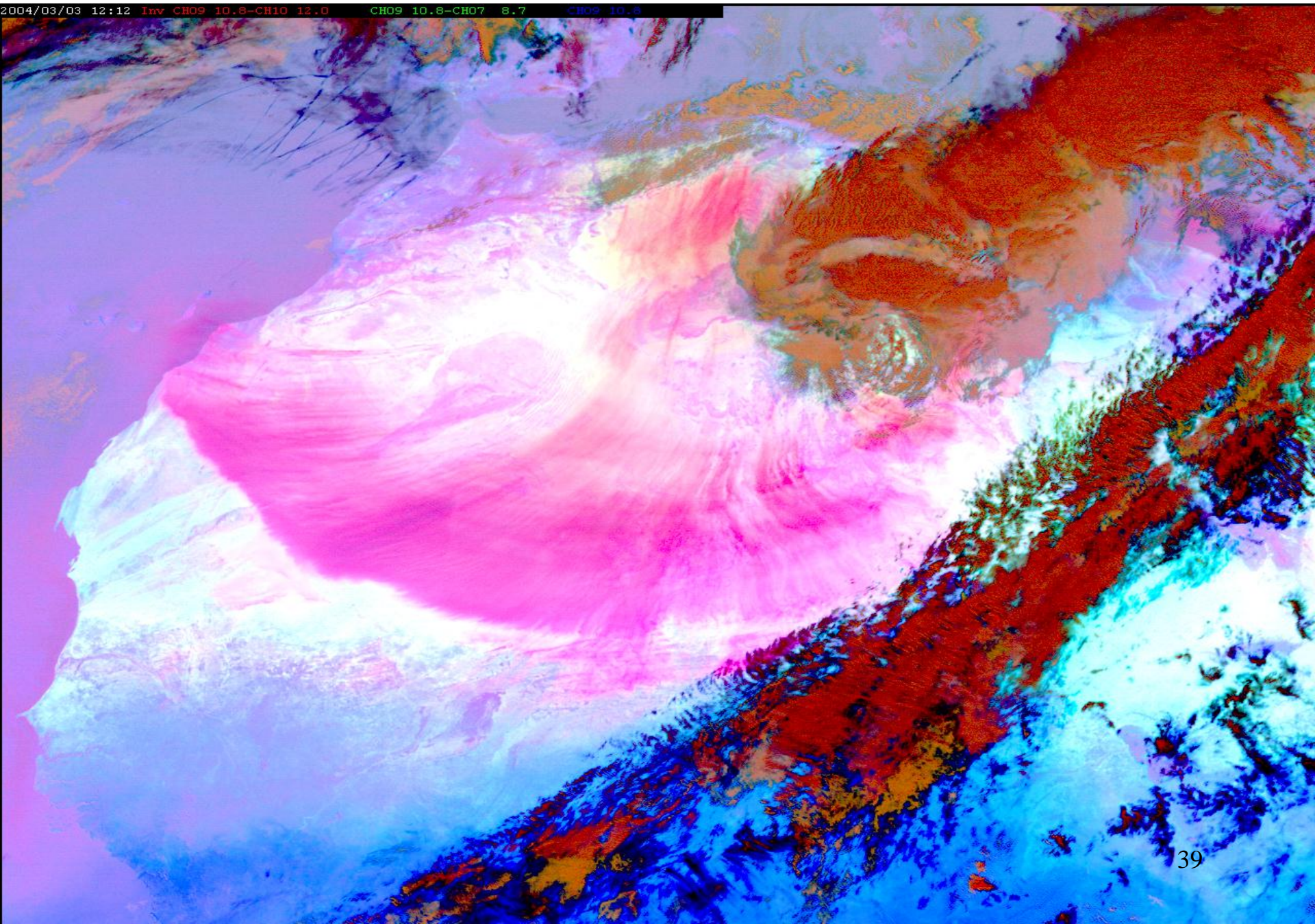
One minute imaging over Florida



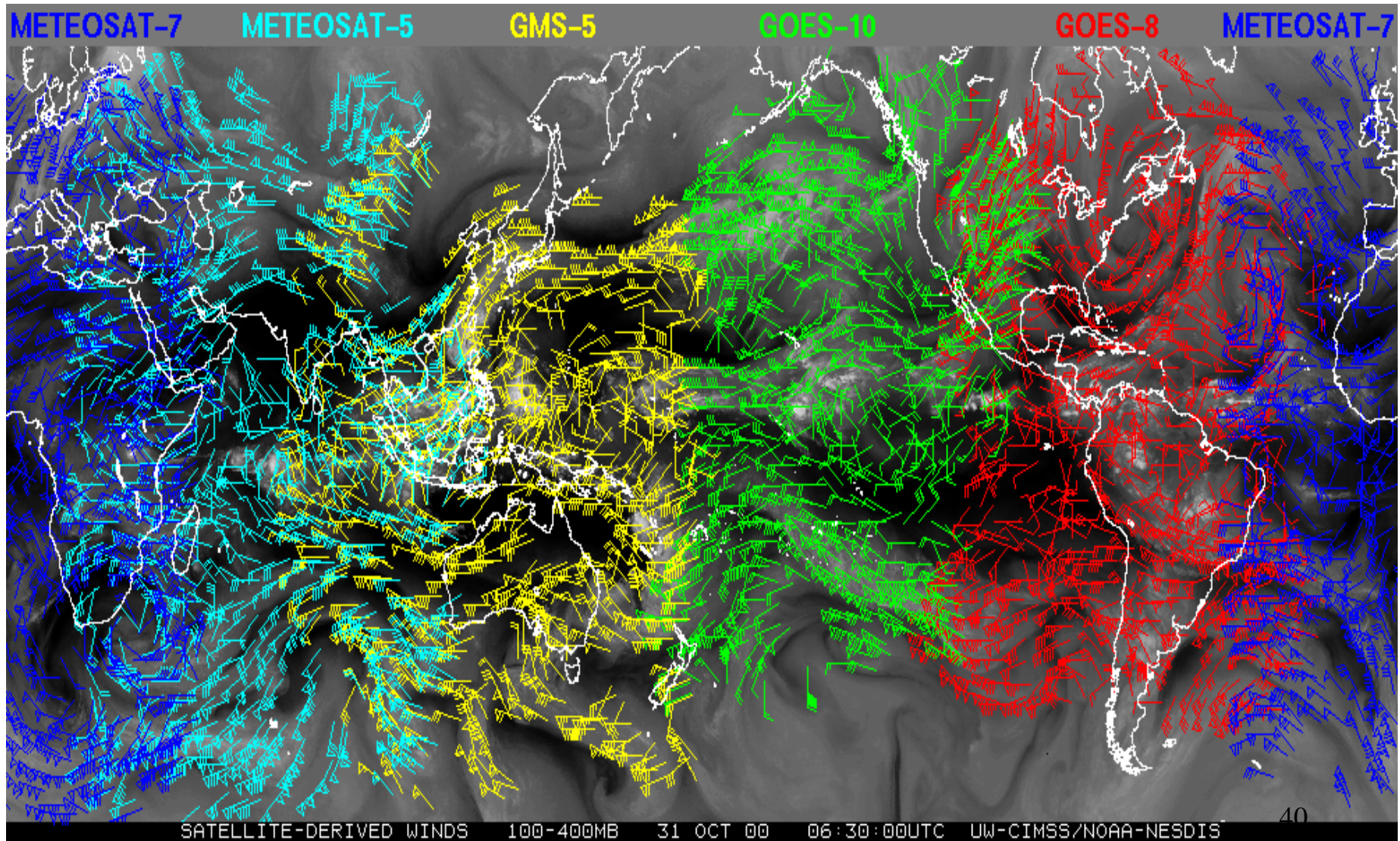
GOES-10 IMAGER 13:00 UTC 30 AUG 06 VISIBLE UW/SSEC

SEVIRI sees dust storm over Africa

2004/03/03 12:12 Inv CH09 10.8-CH10 12.0 CH09 10.8-CH07 8.7 CH09 10.8



Five geos are providing global coverage for winds in tropics and mid-lats



Comparison of geostationary (geo) and low earth orbiting (leo) satellite capabilities

Geo

observes process itself
(motion and targets of opportunity)

repeat coverage in minutes
($\Delta t \leq 15$ minutes)

near full earth disk

best viewing of tropics & mid-latitudes

same viewing angle

differing solar illumination

visible, NIR, IR imager
(1, 4 km resolution)

IR only sounder
(8 km resolution)

filter radiometer

diffraction more than leo

Leo

observes effects of process

repeat coverage twice daily
($\Delta t = 12$ hours)

global coverage

best viewing of poles

varying viewing angle

same solar illumination

visible, NIR, IR imager
(1, 1 km resolution)

IR and microwave sounder
(1, 17, 50 km resolution)

filter radiometer,
interferometer, and
grating spectrometer

diffraction less than geo

Leo Observations

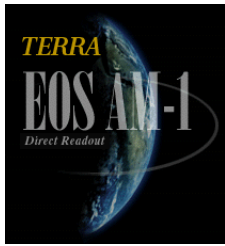
**Terra was launched in 1999
and the EOS Era began**

**MODIS, CERES, MOPITT,
ASTER, and MISR
reach polar orbit**

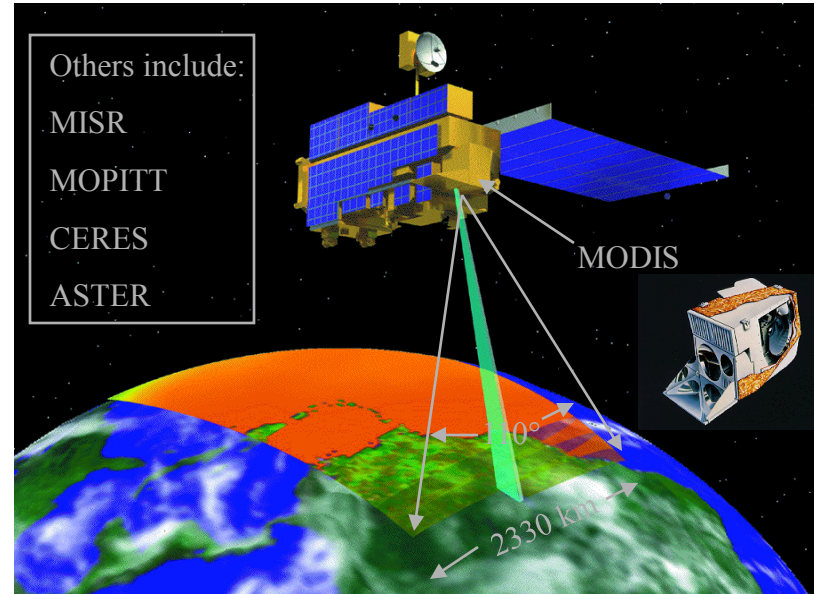
**Aqua and ENVISAT
followed in 2002**

**MODIS and MERIS
to be followed by VIIRS
AIRS and IASI
to be followed by CrIS
AMSU leading to ATMS**





Launch of EOS-Terra (EOS-AM) Satellite - A New Era Begins



MODIS instrument Specifications:

Bands 1-2 (0.66, 0.86 μm): 250 m

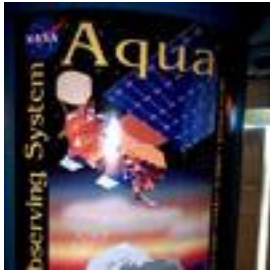
Bands 3-7 (0.47, 0.55, 1.24, 1.64, 2.13 μm): 500 m

Bands 8-36: 1 km

Launch date: December 18, 1999, 1:57 PT
Earth viewdoor open date: February 24, 2001

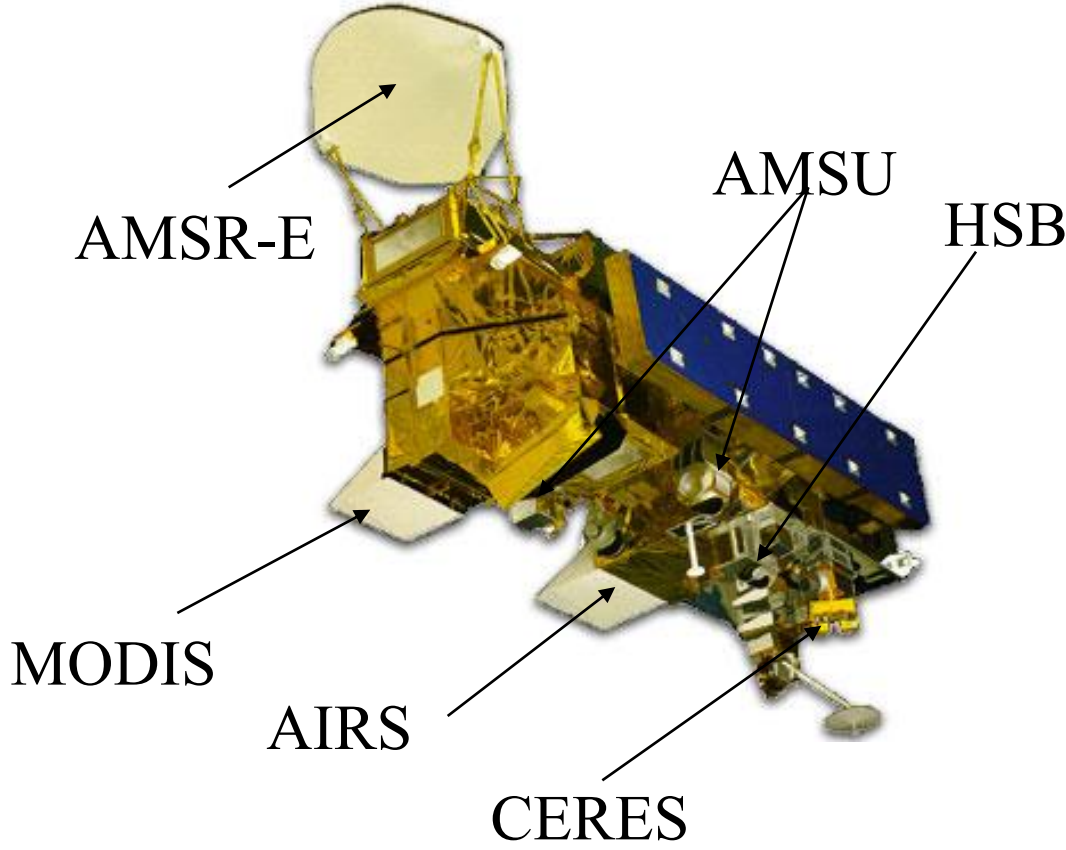


Followed by the launch of
EOS-Aqua (EOS-PM) Satellite



Launch date: May 4, 2002, 2:55 PDT
Earth view door open date: June 25, 2002

“Thermometer in the Sky”



NOAA-J/14

for over 12 years of service to the Nation and the World!

Launched : **December 30, 1994**
 Deactivated : **May 23, 2007**
 Approximately **4,528 days** and **63,925 orbits**

Data visualizations are courtesy of the NASA/Goddard Scientific Visualization Studio including Sea Surface Temp/Anomalies, Sea Surface Temp/Heights and Fires and Aerosols, each created in part from NOAA J/14 data.

Joint Polar System

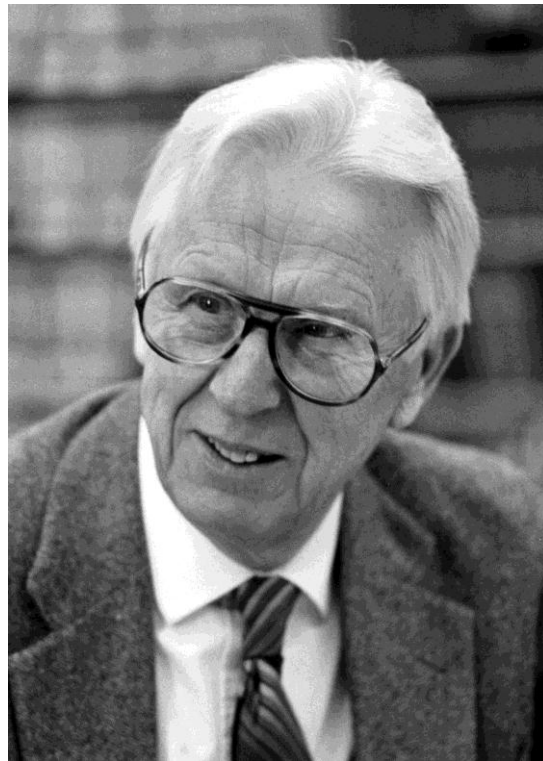
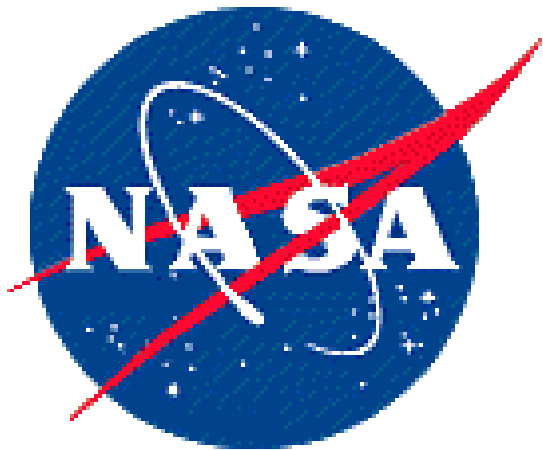
Welcome METOP

Congratulations ESA / EUMETSAT

MetOp-A Launch on 19 October, 16h28 UTC
 Soyuz 2-1a, Baikonour

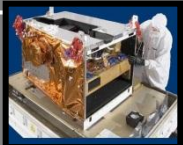
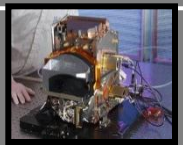
Suomi National Polar-orbiting Partnership (NPP)

launched 28 Oct 2011



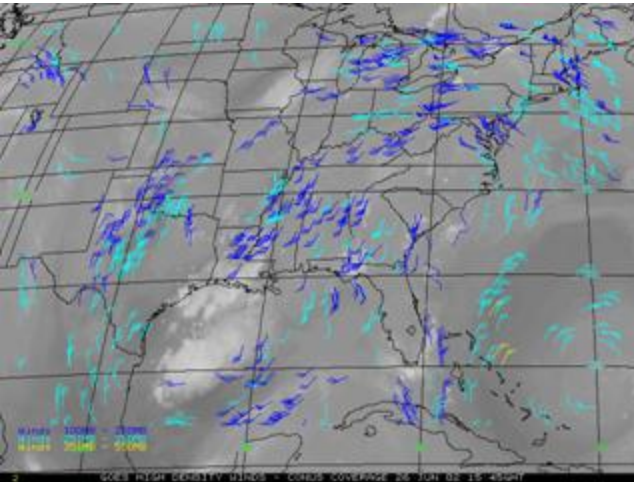
NPP was re-named Suomi NPP on 24 Jan 2012

SNPP/JPSS Instruments

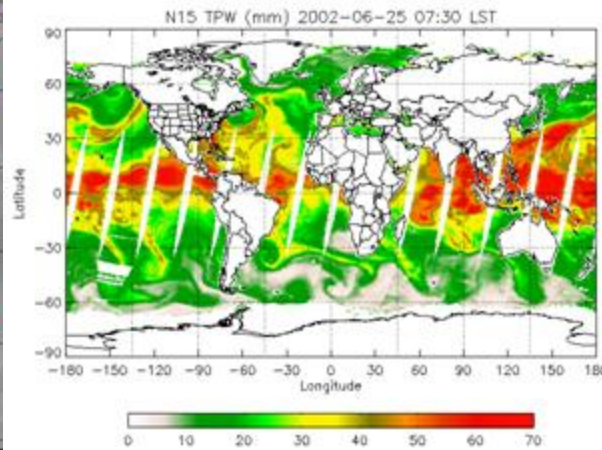
JPSS Instrument	Measurement	NOAA Heritage	NASA Heritage
	ATMS and CrIS together provide profiles of high vertical resolution atmospheric temperature and water vapor information	AMSU	AMSU
		HIRS	AIRS
	Provides daily high-resolution imagery and radiometry across the visible to long-wave infrared spectrum for a multitude of environmental assessments	AVHRR	MODIS
	Spectrometers with UV bands for ozone total column measurements	SBUV-2	OMI
	Scanning radiometer which supports studies of Earth Radiation Budget		CERES

Atmospheric Products: Examples

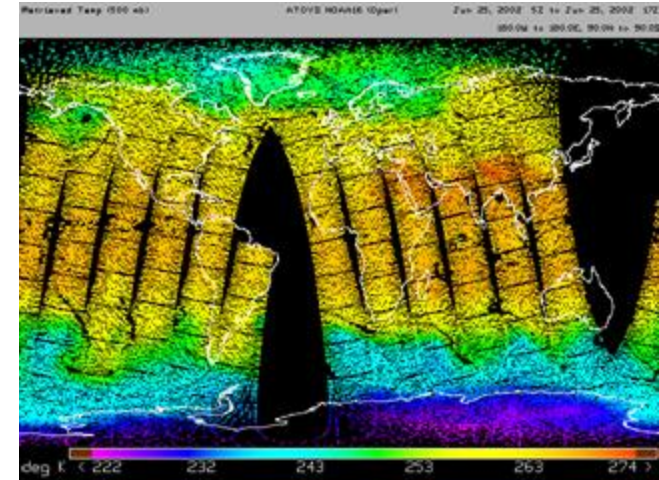
Winds



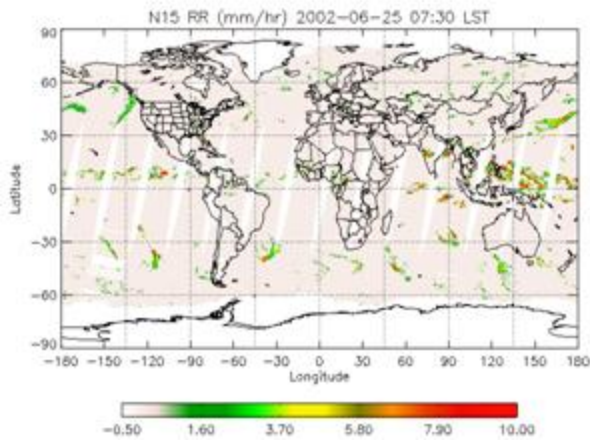
Total Water Vapor



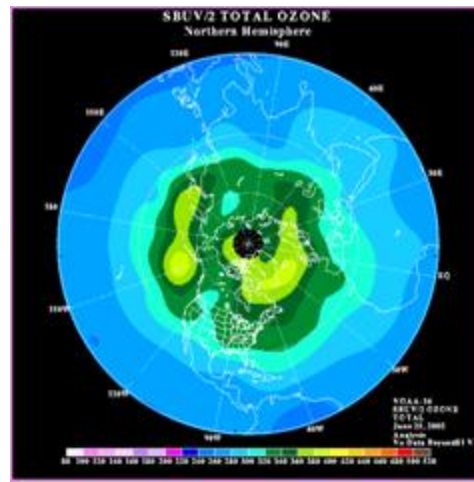
Temperature 500 mb



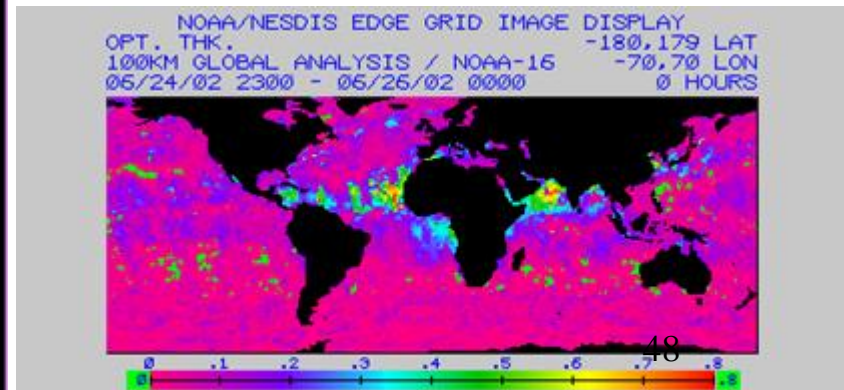
Rain Rate



Ozone

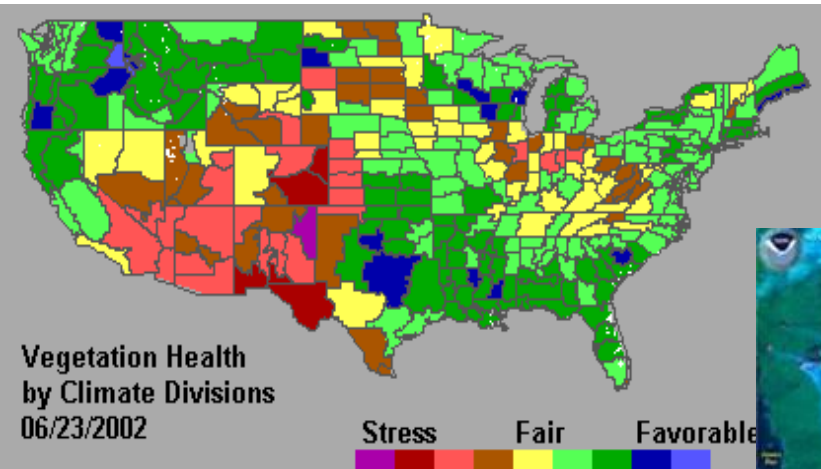


Aerosol Optical Thickness

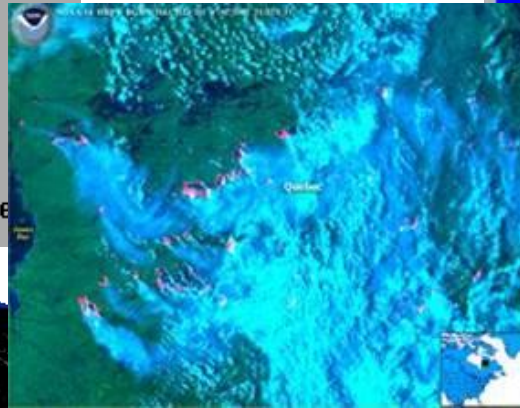


Land Surface Products: Examples

Vegetation Health



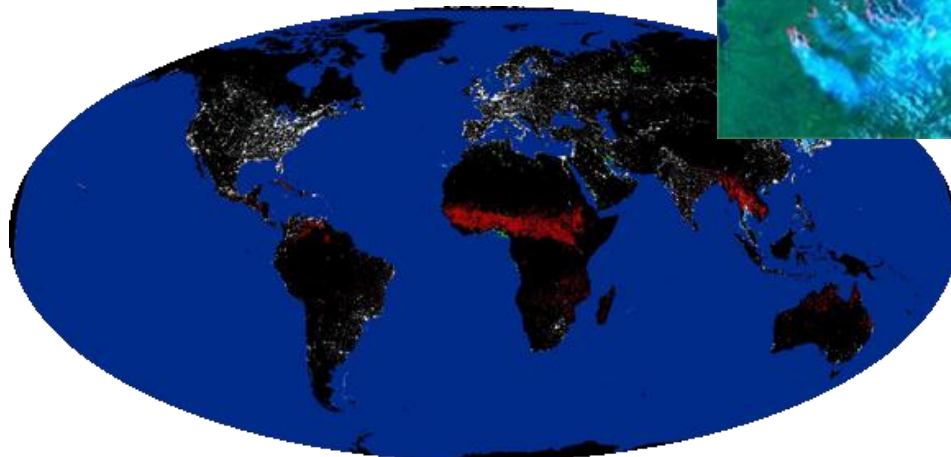
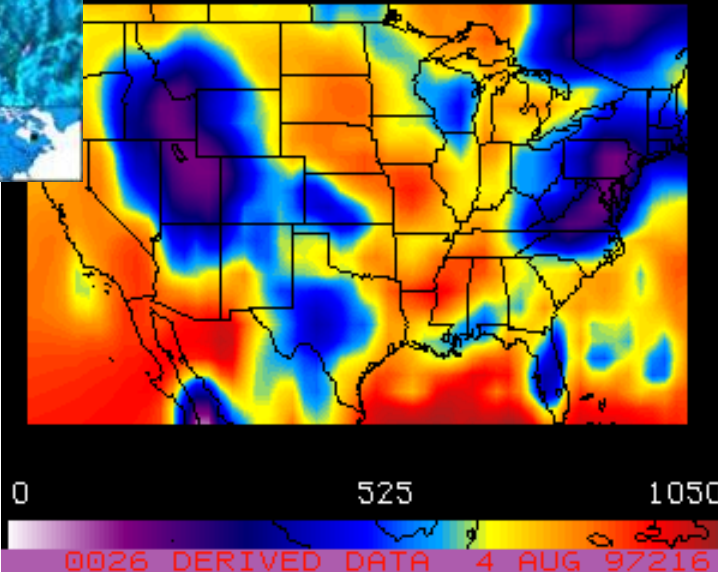
Quebec Fires/Smoke



Snow

Solar Radiation

RFACE DOWNWARD FLUX (W/M2)

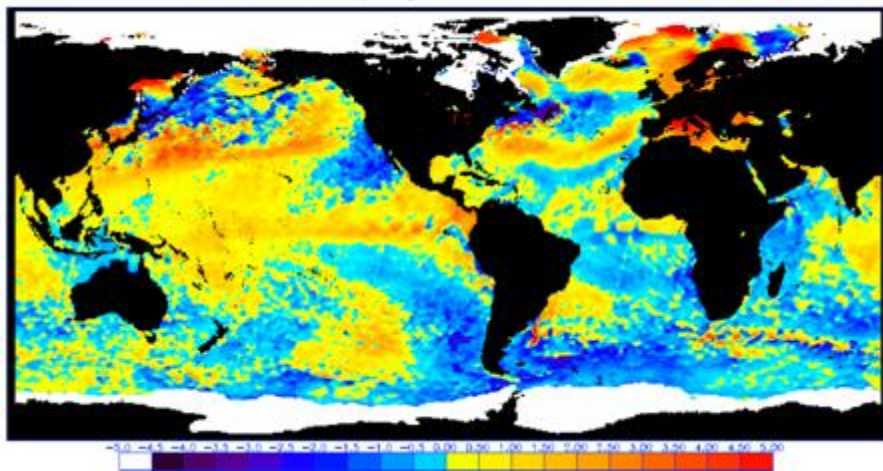


Global Lights/Fires

Ocean Products: Examples

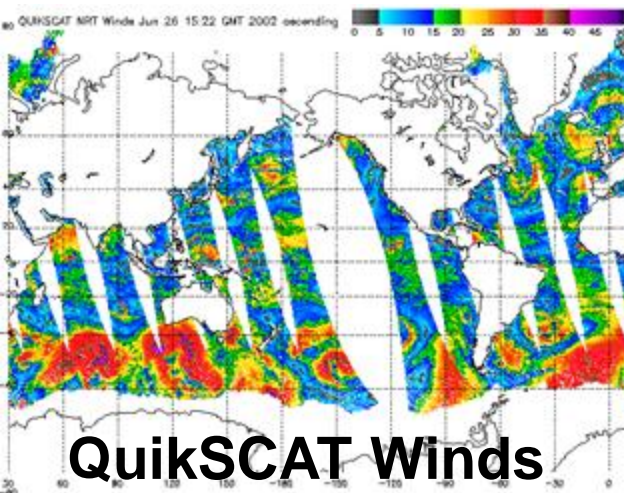
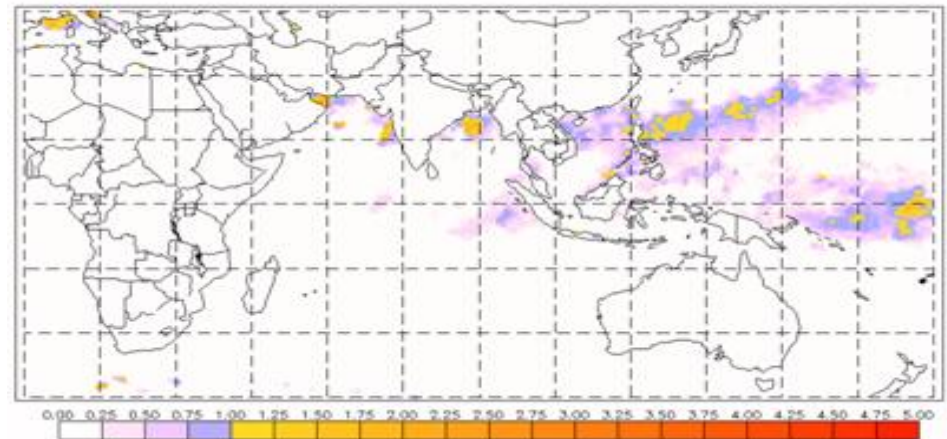
SST Anomalies

NOAA 50KM GLOBAL ANALYSIS: SST - Climatology (C), 6/24/2002
(white regions indicate sea-ice)

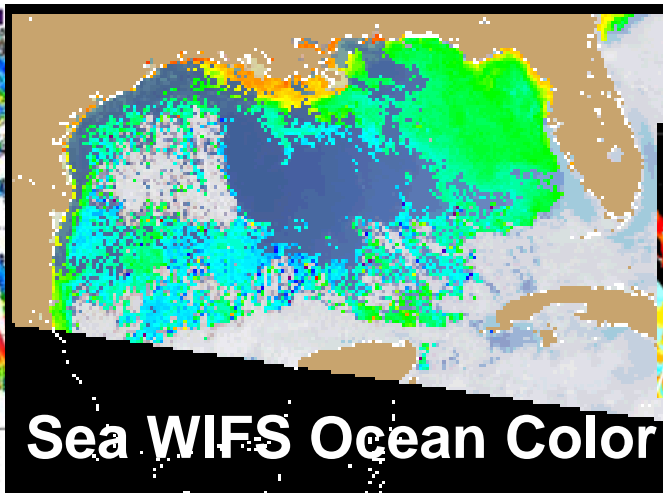


Hot Spots: Potential Coral Bleaching

NOAA/NESDIS 50km SST - Maximum Monthly Climatology (C), 6/24/2002

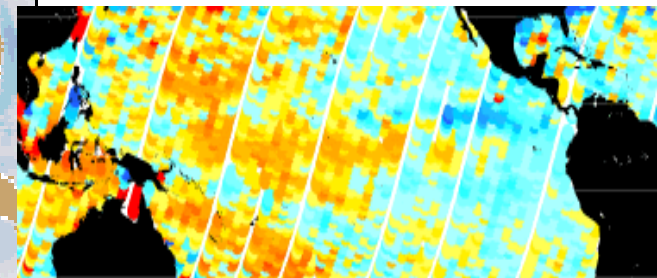


QuikSCAT Winds



Sea WIFS Ocean Color

TOPEX Sea Level



Remote Sensing Advantages

- * provides a regional view
- * enables one to observe & measure the causes & effects of climate & environmental changes (both natural & human-induced)
- * provides repetitive geo-referenced looks at the same area
- * covers a broader portion of the spectrum than the human eye
- * can focus in on a very specific bandwidth in an image
- * can also look at a number of bandwidths simultaneously
- * operates in all seasons, at night, and in bad weather

Intro to VIS-IR Radiation

Lectures in Madison

25 March 2013

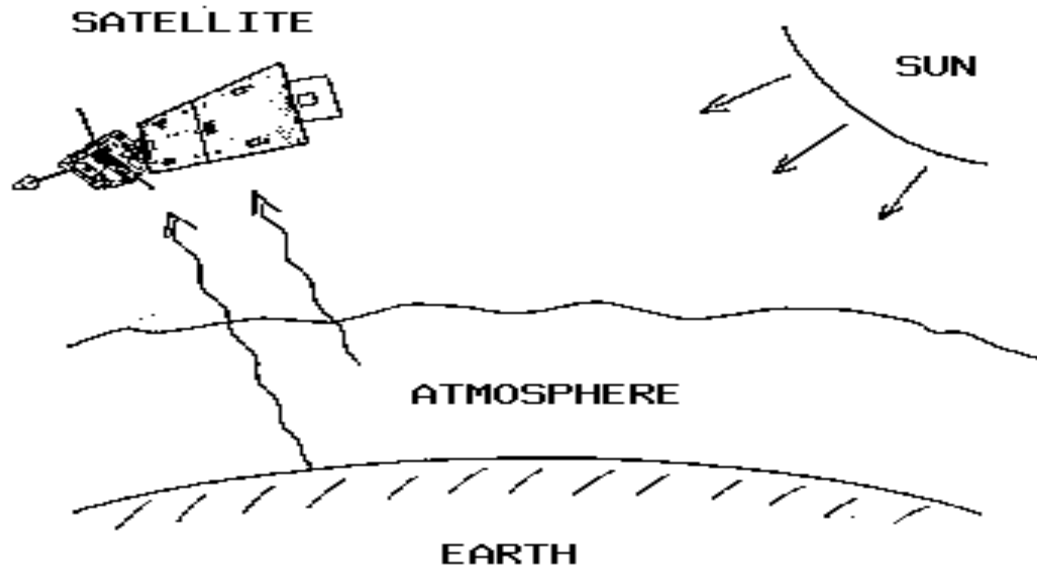
Paul Menzel

UW/CIMSS/AOS

Relevant Material in Applications of Meteorological Satellites

→	CHAPTER 2 - NATURE OF RADIATION	
2.1	Remote Sensing of Radiation	2-1
2.2	Basic Units	2-1
2.3	Definitions of Radiation	2-2
2.5	Related Derivations	2-5
	CHAPTER 3 - ABSORPTION, EMISSION, REFLECTION, AND SCATTERING	
3.1	Absorption and Emission	3-1
3.2	Conservation of Energy	3-1
3.3	Planetary Albedo	3-2
3.4	Selective Absorption and Emission	3-2
3.7	Summary of Interactions between Radiation and Matter	3-6
3.8	Beer's Law and Schwarzschild's Equation	3-7
3.9	Atmospheric Scattering	3-9
3.10	The Solar Spectrum	3-11
3.11	Composition of the Earth's Atmosphere	3-11
3.12	Atmospheric Absorption and Emission of Solar Radiation	3-11
3.13	Atmospheric Absorption and Emission of Thermal Radiation	3-12
3.14	Atmospheric Absorption Bands in the IR Spectrum	3-13
3.15	Atmospheric Absorption Bands in the Microwave Spectrum	3-14
3.16	Remote Sensing Regions	3-14
	CHAPTER 5 - THE RADIATIVE TRANSFER EQUATION (RTE)	
5.1	Derivation of RTE	5-1
5.10	Microwave Form of RTE	5-28

Satellite remote sensing of the Earth-atmosphere

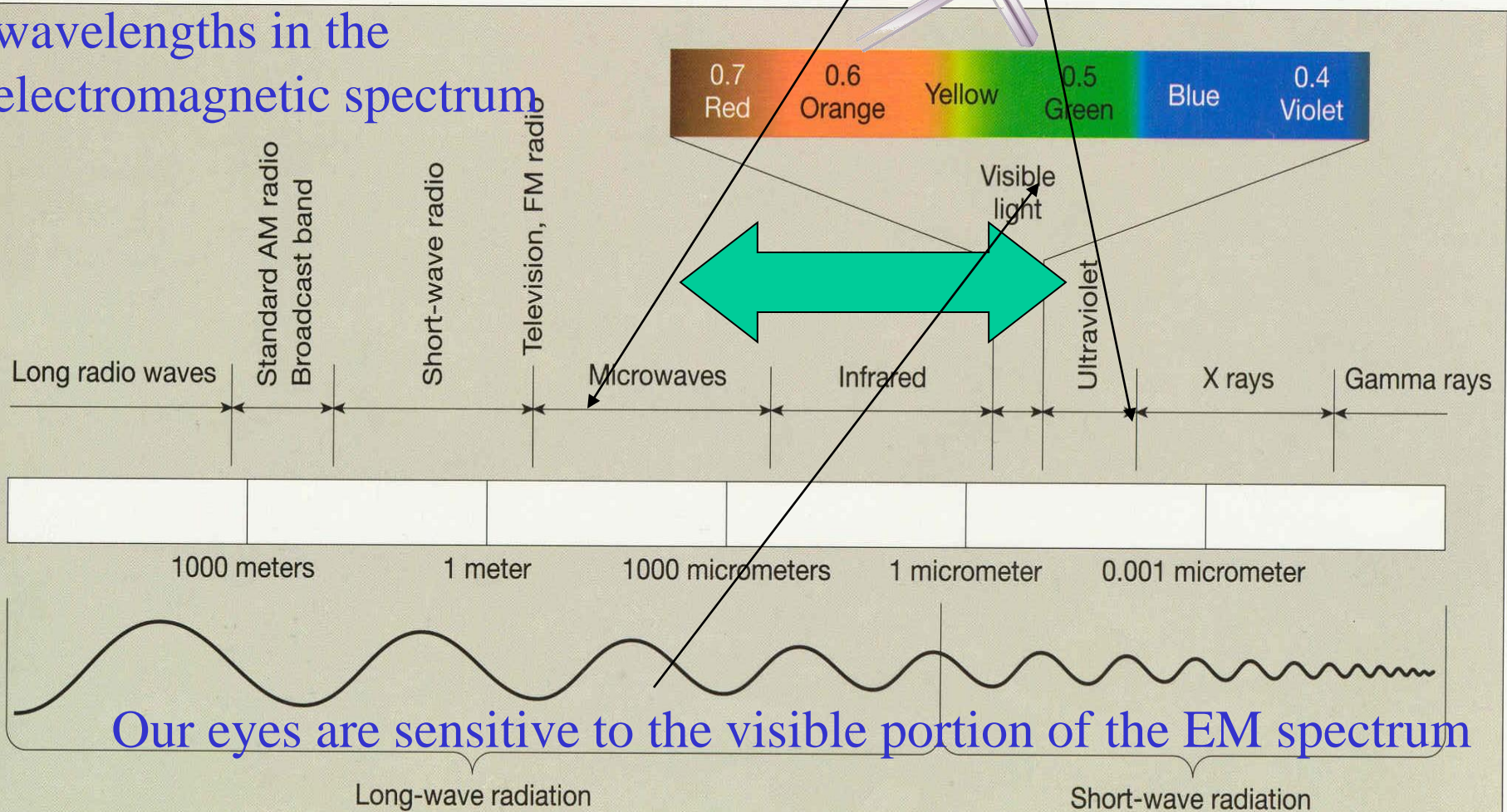
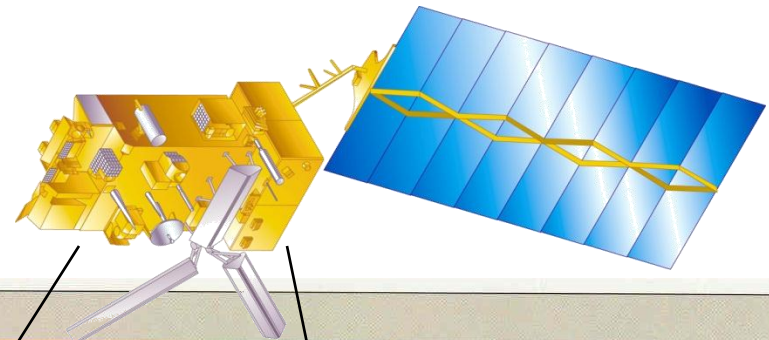


Observations depend on

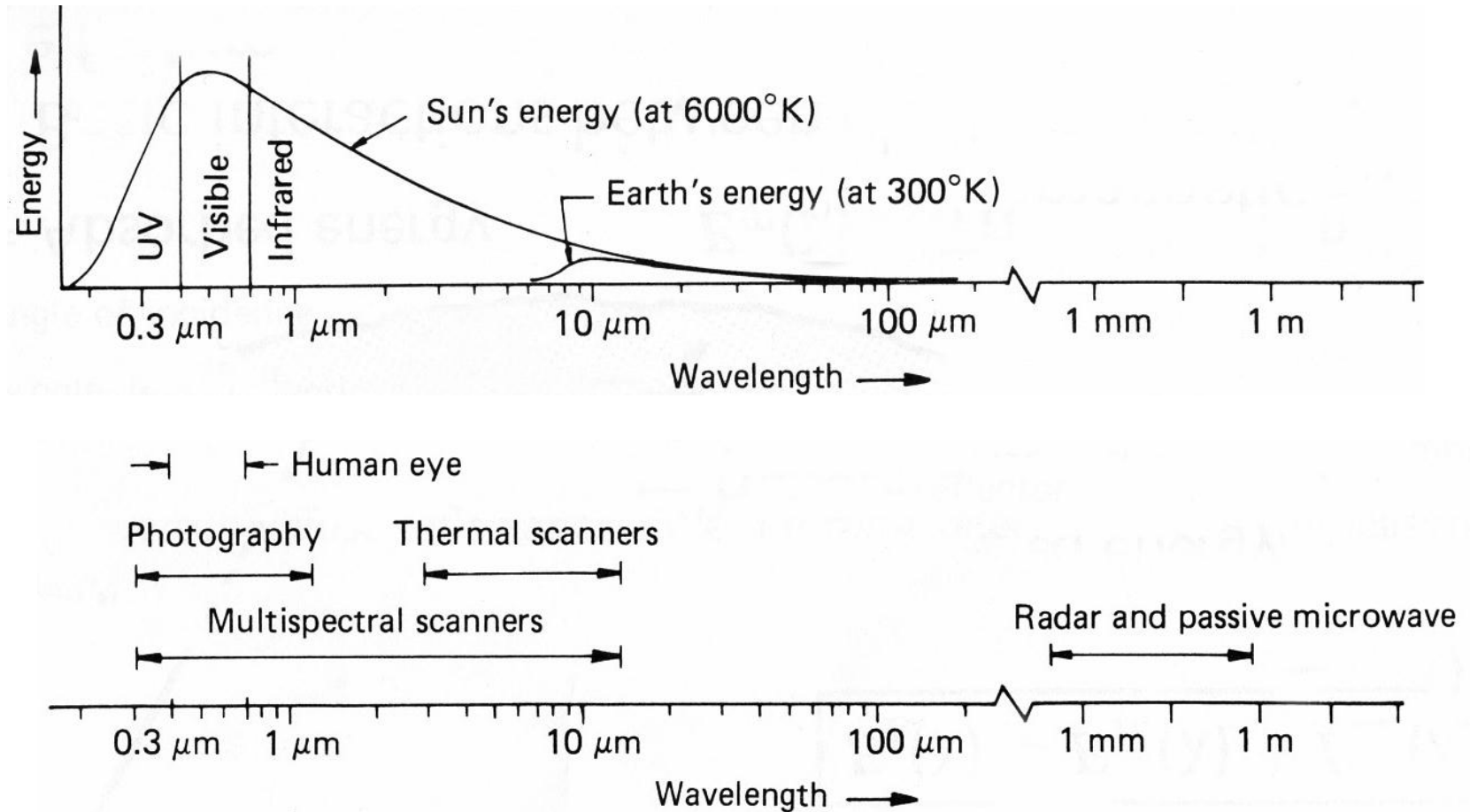
- telescope characteristics (resolving power, diffraction)
- detector characteristics (field of view, signal to noise)
- communications bandwidth (bit depth)
- spectral intervals (window, absorption band)
- time of day (daylight visible)
- atmospheric state (T, Q, clouds)
- earth surface (Ts, vegetation cover)

Electromagnetic spectrum

Remote sensing uses radiant energy that is reflected and emitted from Earth at various wavelengths in the electromagnetic spectrum



Spectral Characteristics of Energy Sources and Sensing Systems



Definitions of Radiation

QUANTITY	SYMBOL	UNITS
Energy	dQ	Joules
Flux	dQ/dt	Joules/sec = Watts
Irradiance	dQ/dt/dA	Watts/meter²
Monochromatic Irradiance	dQ/dt/dA/dλ	W/m²/micron
	or	
	dQ/dt/dA/dν	W/m²/cm⁻¹
Radiance	dQ/dt/dA/dλ/dΩ	W/m²/micron/ster
	or	
	dQ/dt/dA/dν/dΩ	W/m²/cm⁻¹/ster

Using wavelengths

$$\text{Planck's Law} \quad B(\lambda, T) = \frac{c_1}{\lambda^5} \left[e^{-c_2/\lambda T} - 1 \right]^{-1} \quad (\text{mW/m}^2/\text{ster/cm})$$

where

λ = wavelengths in cm

T = temperature of emitting surface (deg K)

$c_1 = 1.191044 \times 10^{-5}$ (mW/m²/ster/cm⁻⁴)

$c_2 = 1.438769$ (cm deg K)

$$\text{Wien's Law} \quad dB(\lambda_{\max}, T) / d\lambda = 0 \text{ where } \lambda(\max) = .2897/T$$

indicates peak of Planck function curve shifts to shorter wavelengths (greater wavenumbers) with temperature increase. Note $B(\lambda_{\max}, T) \sim T^5$.

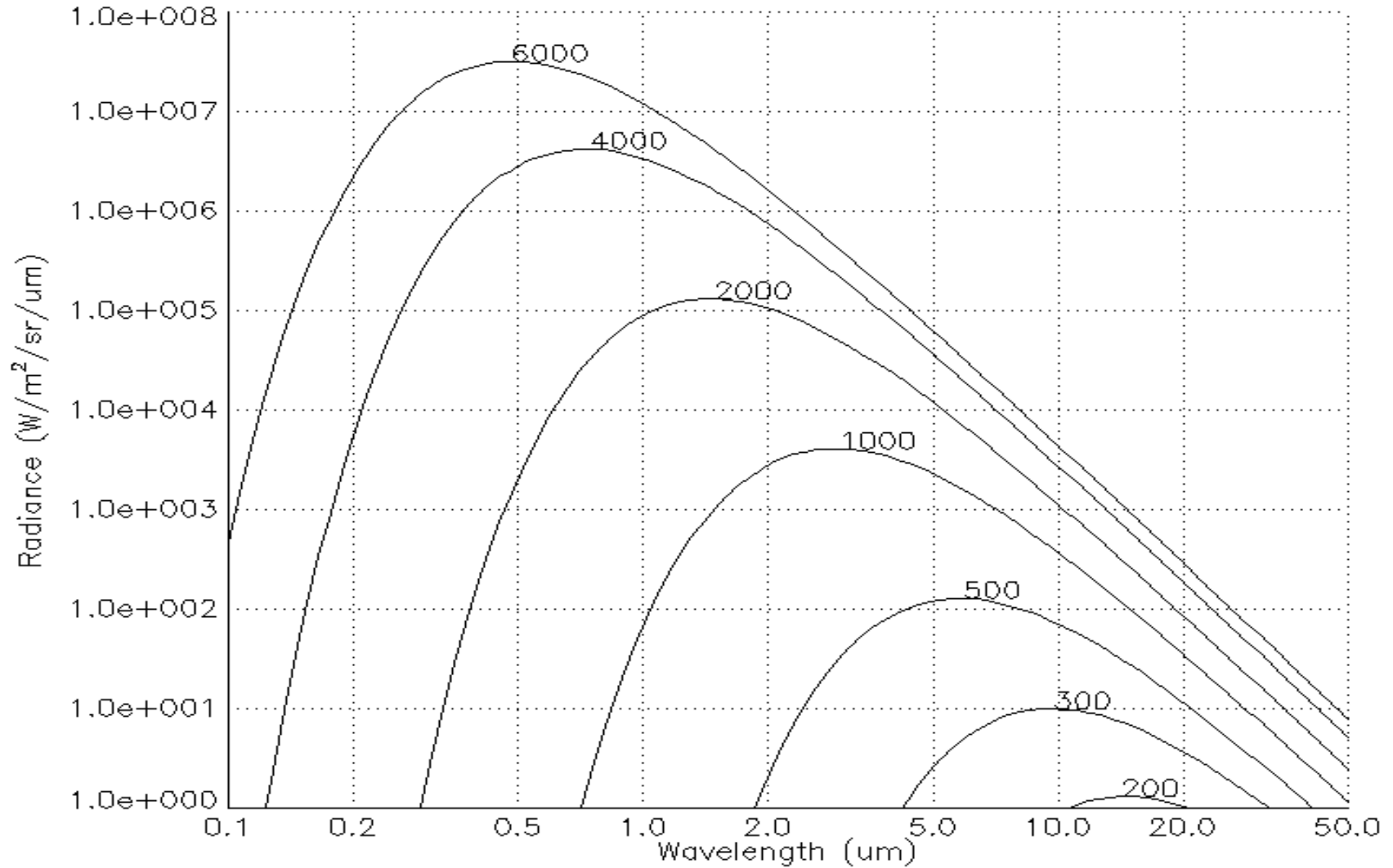
$$\text{Stefan-Boltzmann Law} \quad E = \pi \int_0^{\infty} B(\lambda, T) d\lambda = \sigma T^4, \text{ where } \sigma = 5.67 \times 10^{-8} \text{ W/m}^2/\text{deg}^4.$$

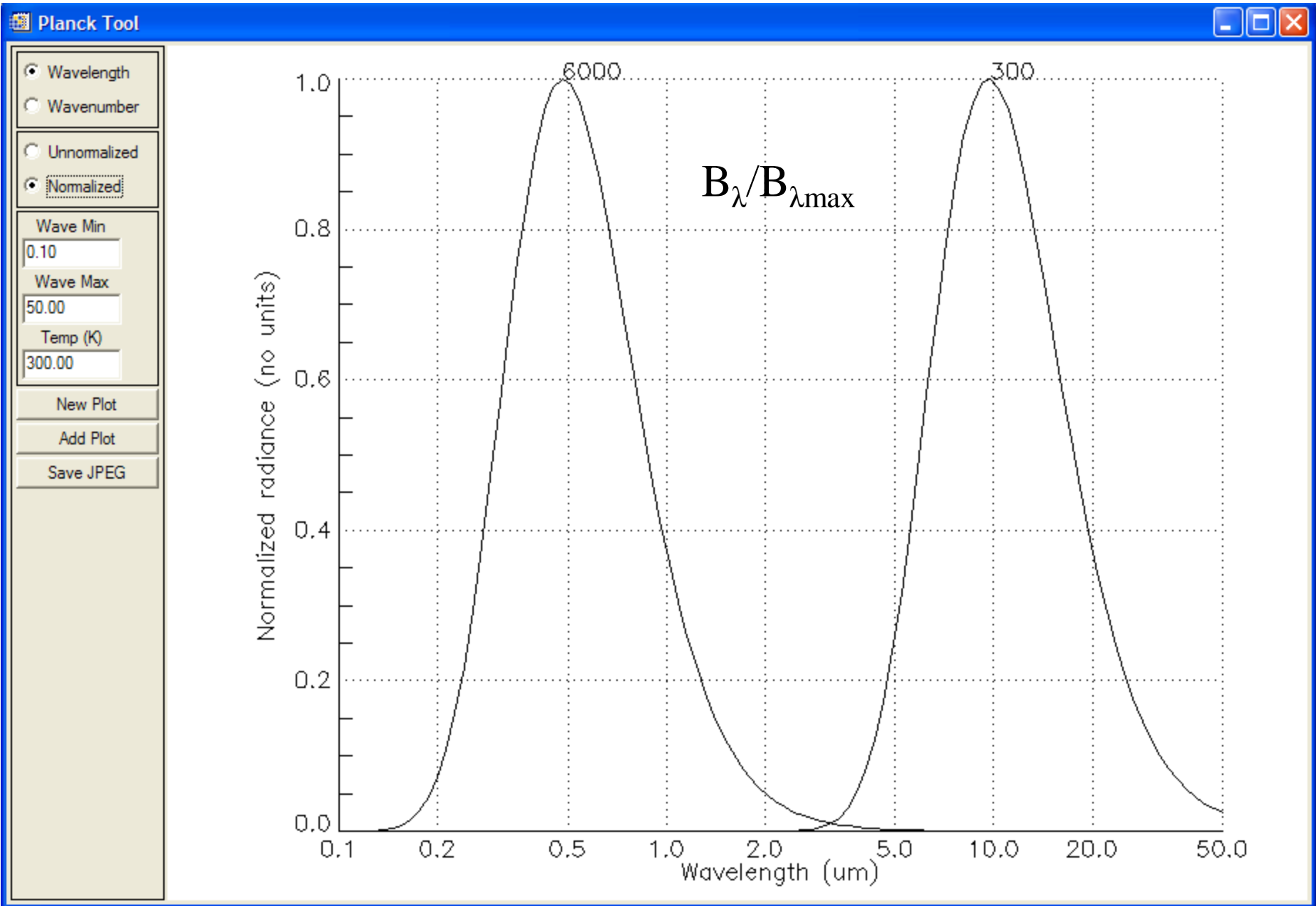
states that irradiance of a black body (area under Planck curve) is proportional to T^4 .

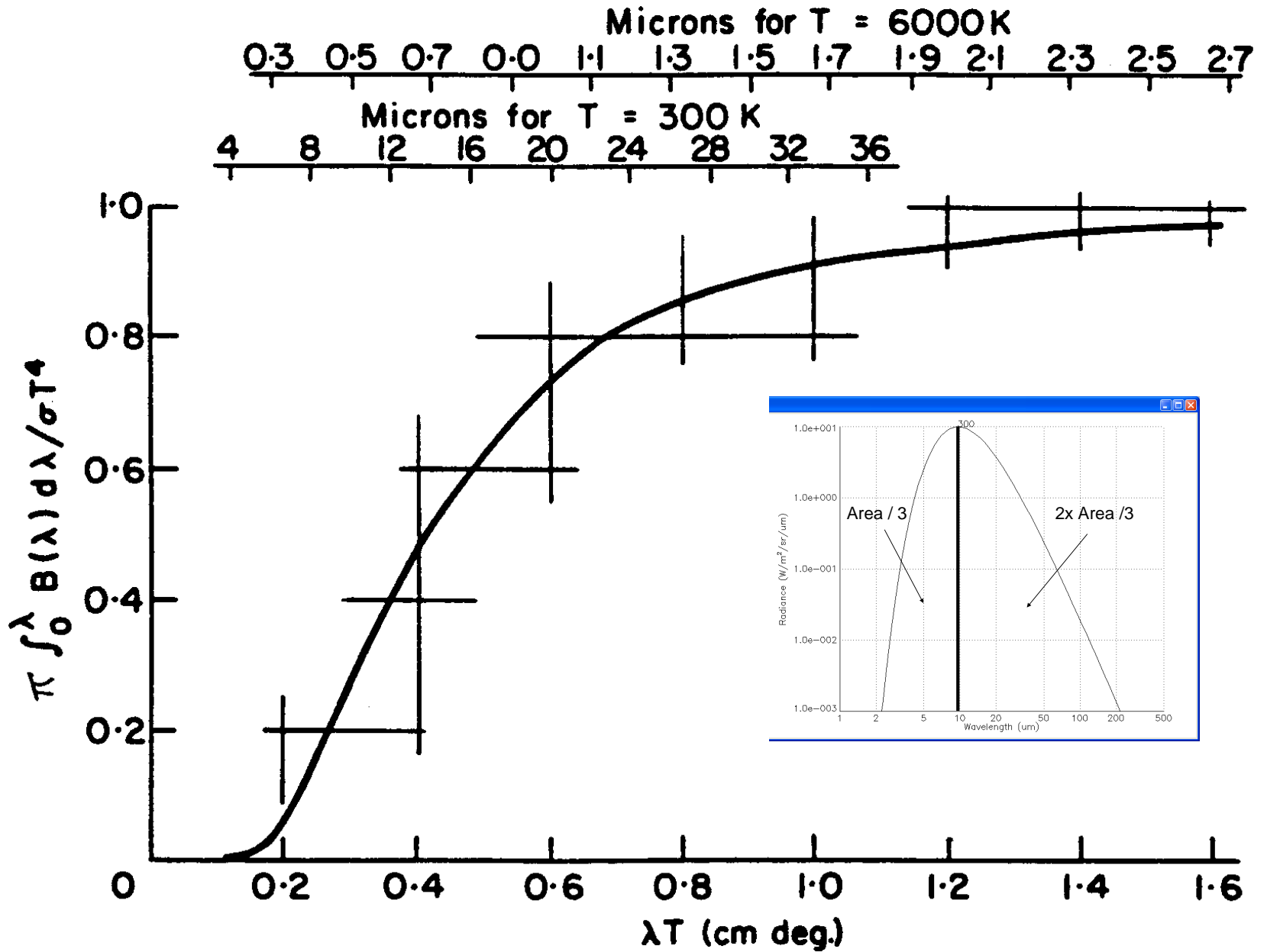
Brightness Temperature

$$T = \frac{c_2}{\lambda \ln\left(\frac{c_1}{\lambda^5 B_\lambda} + 1\right)} \text{ is determined by inverting Planck function}$$

Spectral Distribution of Energy Radiated from Blackbodies at Various Temperatures







Using wavenumbers

Planck's Law
$$B(\nu, T) = \frac{c_1 \nu^3}{[e^{c_2 \nu / T} - 1]} \quad (\text{mW/m}^2/\text{ster/cm}^{-1})$$

where

ν = # wavelengths in one centimeter (cm⁻¹)

T = temperature of emitting surface (deg K)

$c_1 = 1.191044 \times 10^{-5}$ (mW/m²/ster/cm⁻⁴)

$c_2 = 1.438769$ (cm deg K)

Wien's Law
$$dB(\nu_{\max}, T) / d\nu = 0 \text{ where } \nu_{\max} = 1.95T$$

indicates peak of Planck function curve shifts to shorter wavelengths (greater wavenumbers) with temperature increase.

Stefan-Boltzmann Law
$$E = \pi \int_0^{\infty} B(\nu, T) d\nu = \sigma T^4, \text{ where } \sigma = 5.67 \times 10^{-8} \text{ W/m}^2/\text{deg}^4.$$

states that irradiance of a black body (area under Planck curve) is proportional to T⁴.

Brightness Temperature

$$T = \frac{c_2 \nu}{[\ln(\frac{c_1 \nu^3}{B_\nu} + 1)]}$$

is determined by inverting Planck function

Using wavenumbers

$$c_2 \nu / T$$

$$B(\nu, T) = c_1 \nu^3 / [e^{c_2 \nu / T} - 1]$$

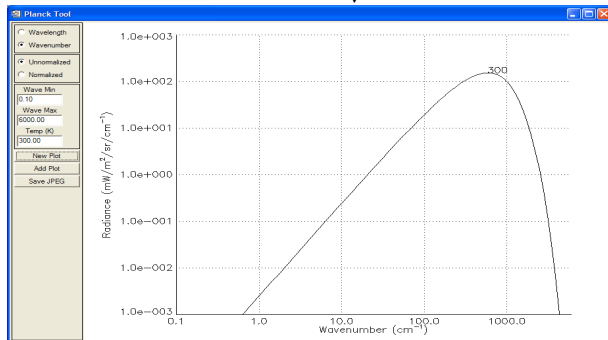
(mW/m²/ster/cm⁻¹)

$$\nu(\text{max in cm}^{-1}) = 1.95T$$

$$B(\nu_{\text{max}}, T) \sim T^{**3}.$$

$$E = \pi \int_0^{\infty} B(\nu, T) d\nu = \sigma T^4,$$

$$T = c_2 \nu / [\ln(\frac{c_1 \nu^3}{B_\nu} + 1)]$$



Using wavelengths

$$c_2 / \lambda T$$

$$B(\lambda, T) = c_1 / \{ \lambda^5 [e^{c_2 / \lambda T} - 1] \}$$

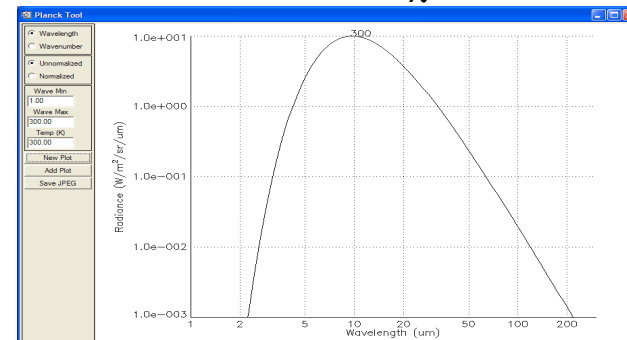
(mW/m²/ster/μm)

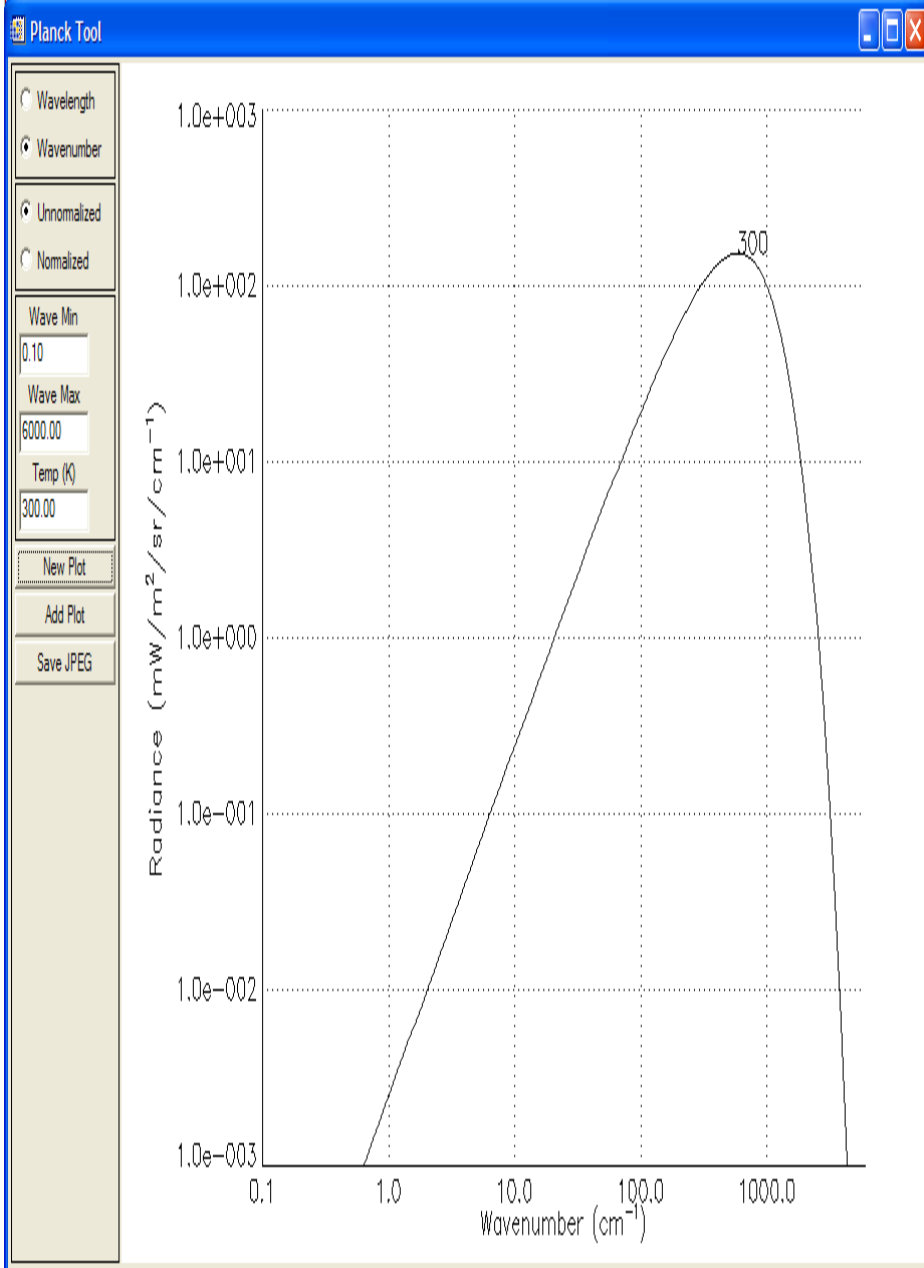
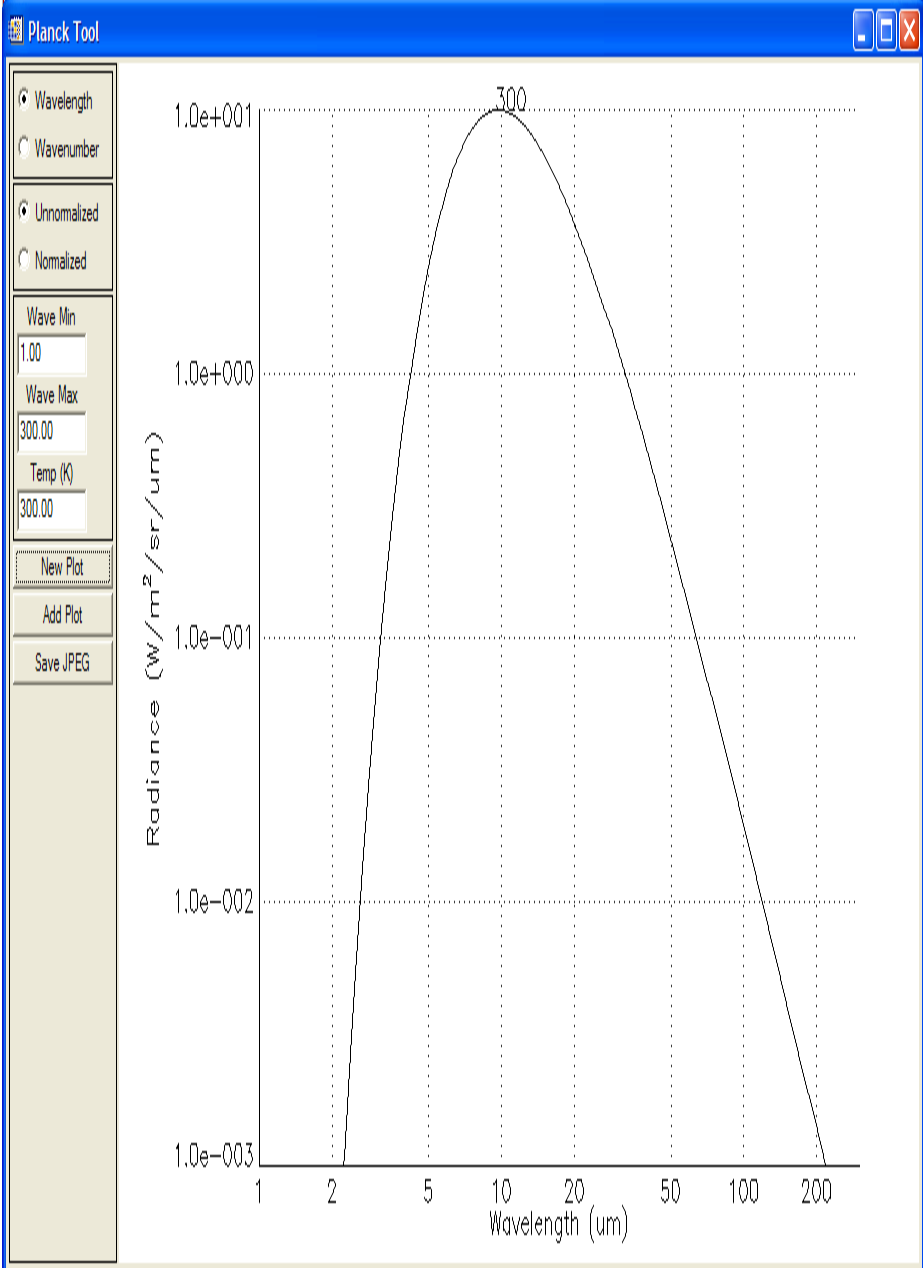
$$\lambda(\text{max in cm})T = 0.2897$$

$$B(\lambda_{\text{max}}, T) \sim T^{**5}.$$

$$E = \pi \int_0^{\infty} B(\lambda, T) d\lambda = \sigma T^4,$$

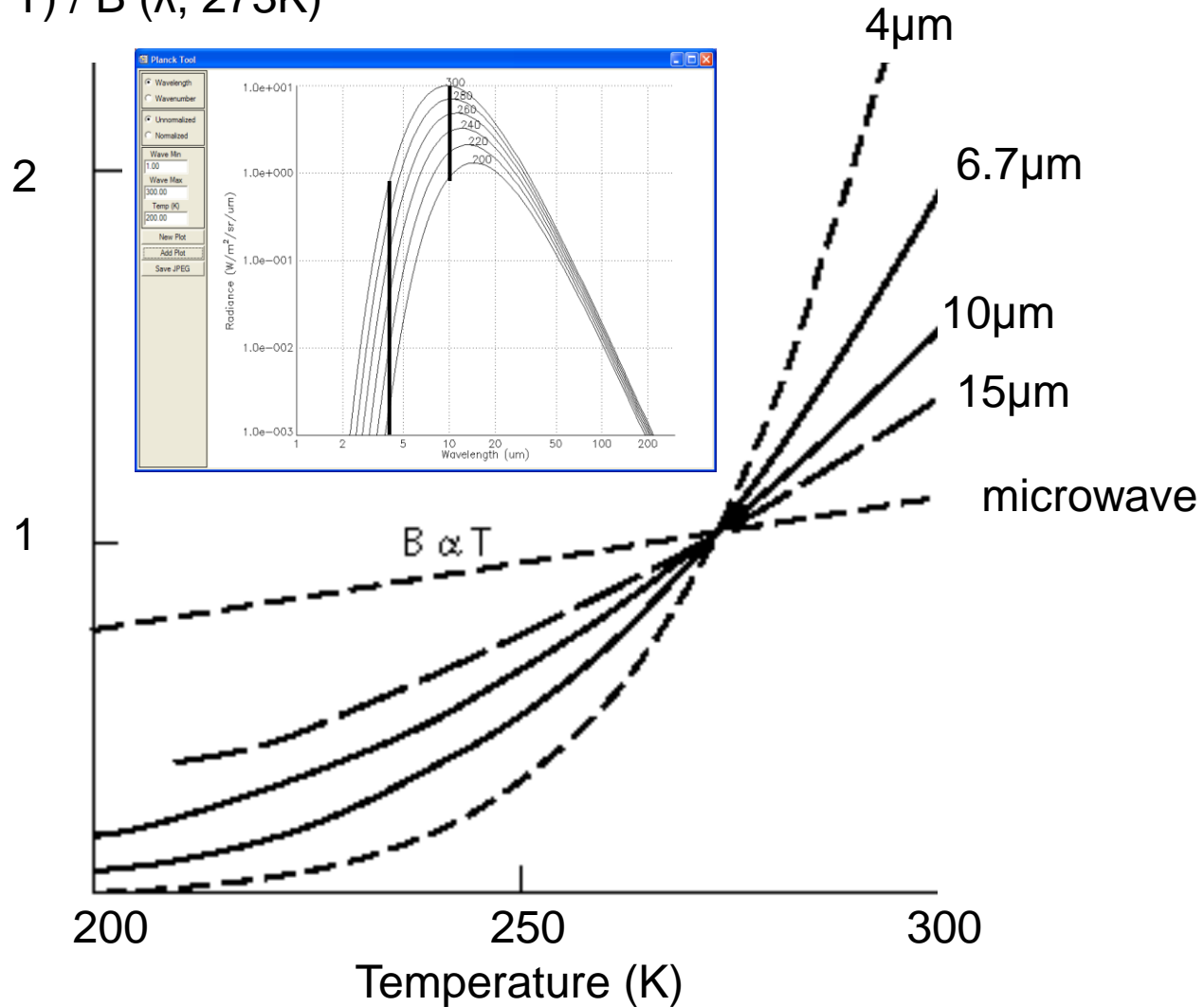
$$T = c_2 / [\lambda \ln(\frac{c_1}{\lambda^5 B_\lambda} + 1)]$$





Temperature Sensitivity of $B(\lambda, T)$ for typical earth temperatures

$B(\lambda, T) / B(\lambda, 273K)$



(Approximation of) B as function of α and T

$$\Delta B/B = \alpha \Delta T/T$$

Integrating the Temperature Sensitivity Equation
Between T_{ref} and T (B_{ref} and B):

$$B = B_{\text{ref}} (T/T_{\text{ref}})^{\alpha}$$

Where $\alpha = c_2 \nu / T_{\text{ref}}$ (in wavenumber space)

$$B = B_{\text{ref}} \left(\frac{T}{T_{\text{ref}}} \right)^\alpha$$

$$\Downarrow$$

$$B = \left(\frac{B_{\text{ref}}}{T_{\text{ref}}^\alpha} \right) T^\alpha$$

$$\Downarrow$$

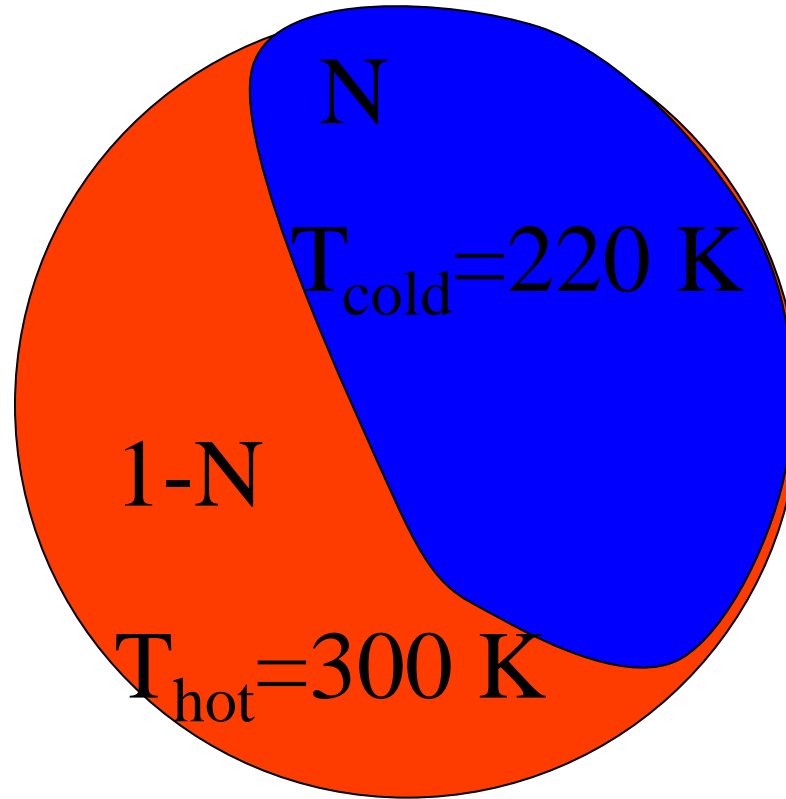
$$B \propto T^\alpha$$

The temperature sensitivity indicates the power to which the Planck radiance depends on temperature, since B proportional to T^α satisfies the equation. For infrared wavelengths,

$$\alpha = c_2 \nu / T = c_2 / \lambda T.$$

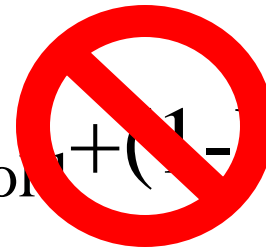
Wavenumber	Typical Scene Temperature	Temperature Sensitivity
900	300	4.32
2500	300	11.99

Non-Homogeneous FOV



$$B = N * B(T_{\text{cold}}) + (1 - N) * B(T_{\text{hot}})$$

$$BT = N * T_{\text{cold}} + (1 - N) * T_{\text{hot}}$$

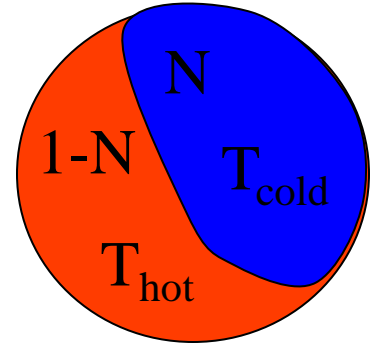


For NON-UNIFORM FOVs:

$$B_{\text{obs}} = NB_{\text{cold}} + (1-N)B_{\text{hot}}$$

$$B_{\text{obs}} = N B_{\text{ref}} (T_{\text{cold}}/T_{\text{ref}})^{\alpha} + (1-N) B_{\text{ref}} (T_{\text{hot}}/T_{\text{ref}})^{\alpha}$$

$$B_{\text{obs}} = B_{\text{ref}} (1/T_{\text{ref}})^{\alpha} (N T_{\text{cold}}^{\alpha} + (1-N) T_{\text{hot}}^{\alpha})$$



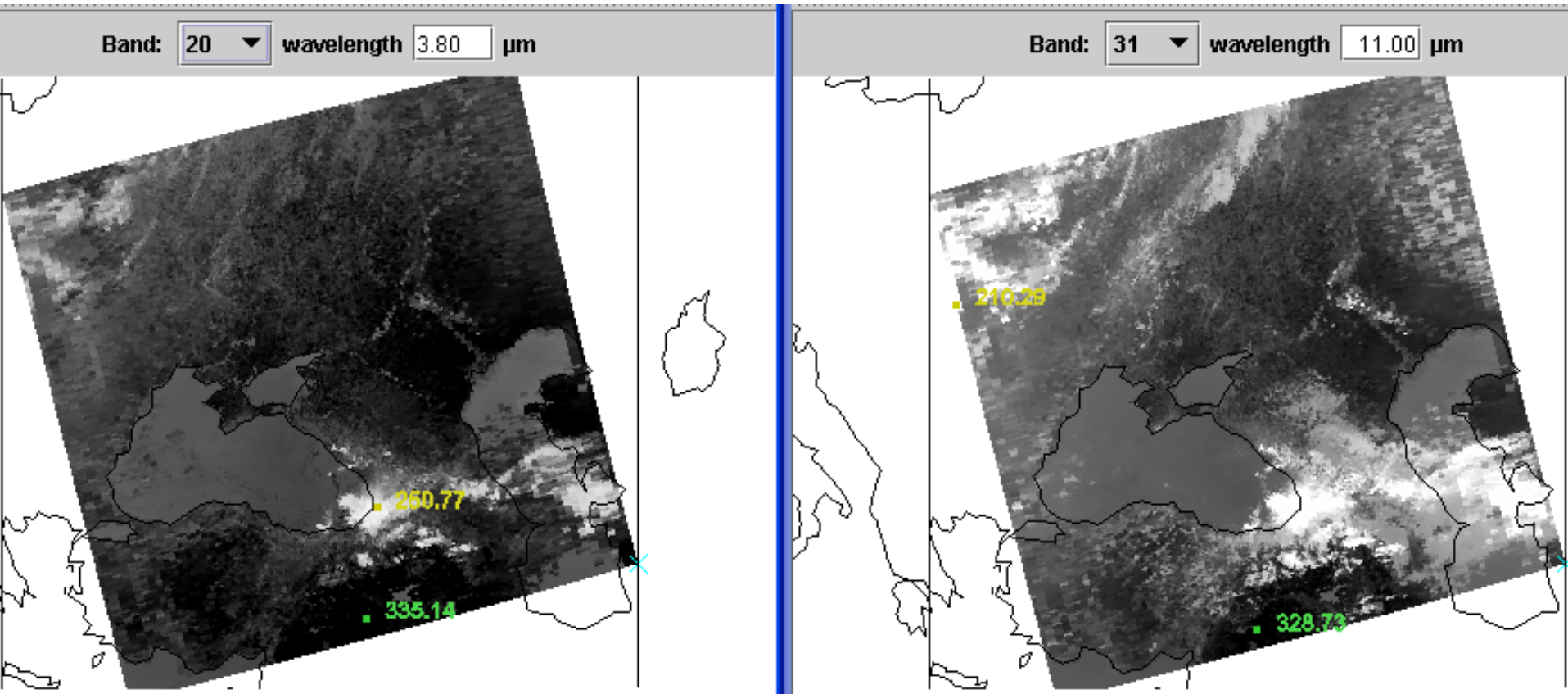
For $N=.5$

$$B_{\text{obs}}/B_{\text{ref}} = .5 (1/T_{\text{ref}})^{\alpha} (T_{\text{cold}}^{\alpha} + T_{\text{hot}}^{\alpha})$$

$$B_{\text{obs}}/B_{\text{ref}} = .5 (1/T_{\text{ref}} T_{\text{cold}})^{\alpha} (1 + (T_{\text{hot}}/T_{\text{cold}})^{\alpha})$$

The greater α the more predominant the hot term

At $4 \mu\text{m}$ ($\alpha=12$) the hot term more dominating than at $11 \mu\text{m}$ ($\alpha=4$)



Cloud edges and broken clouds appear different in 11 and 4 um images.

$$T(11)**4=(1-N)*Tclr**4+N*Tcld**4\sim(1-N)*300**4+N*200**4$$

$$T(4)**12=(1-N)*Tclr**12+N*Tcld**12\sim(1-N)*300**12+N*200**12$$

Cold part of pixel has more influence for B(11) than B(4)

Relevant Material in Applications of Meteorological Satellites

CHAPTER 2 - NATURE OF RADIATION

2.1	Remote Sensing of Radiation	2-1
2.2	Basic Units	2-1
2.3	Definitions of Radiation	2-2
2.5	Related Derivations	2-5

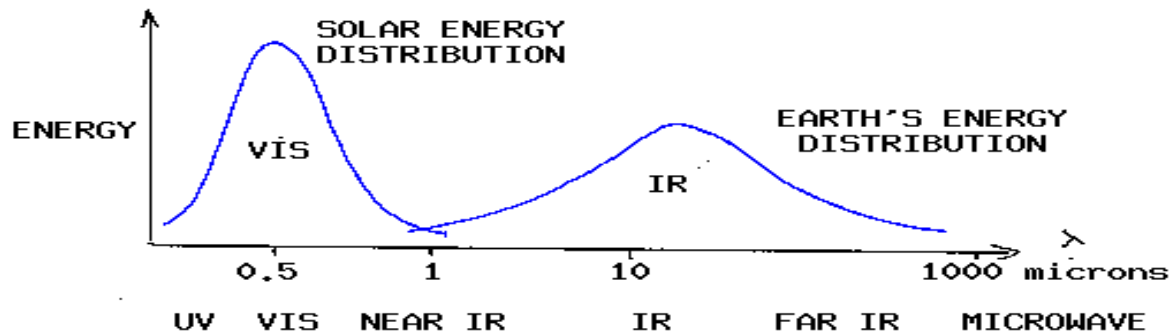
→ CHAPTER 3 - ABSORPTION, EMISSION, REFLECTION, AND SCATTERING

3.1	Absorption and Emission	3-1
3.2	Conservation of Energy	3-1
3.3	Planetary Albedo	3-2
3.4	Selective Absorption and Emission	3-2
3.7	Summary of Interactions between Radiation and Matter	3-6
3.8	Beer's Law and Schwarzschild's Equation	3-7
3.9	Atmospheric Scattering	3-9
3.10	The Solar Spectrum	3-11
3.11	Composition of the Earth's Atmosphere	3-11
3.12	Atmospheric Absorption and Emission of Solar Radiation	3-11
3.13	Atmospheric Absorption and Emission of Thermal Radiation	3-12
3.14	Atmospheric Absorption Bands in the IR Spectrum	3-13
3.15	Atmospheric Absorption Bands in the Microwave Spectrum	3-14
3.16	Remote Sensing Regions	3-14

CHAPTER 5 - THE RADIATIVE TRANSFER EQUATION (RTE)

5.1	Derivation of RTE	5-1
5.10	Microwave Form of RTE	5-28

Solar (visible) and Earth emitted (infrared) energy

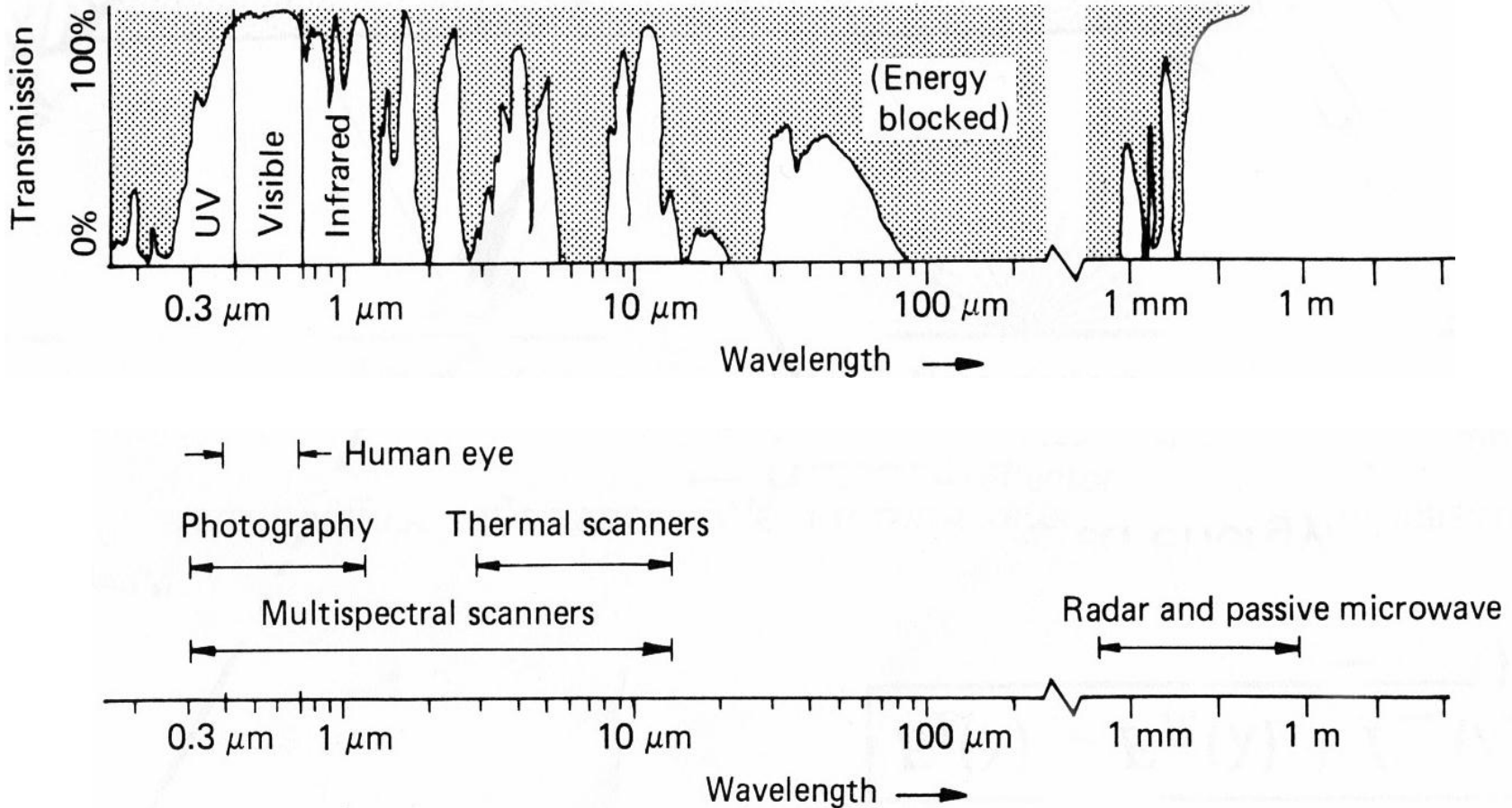


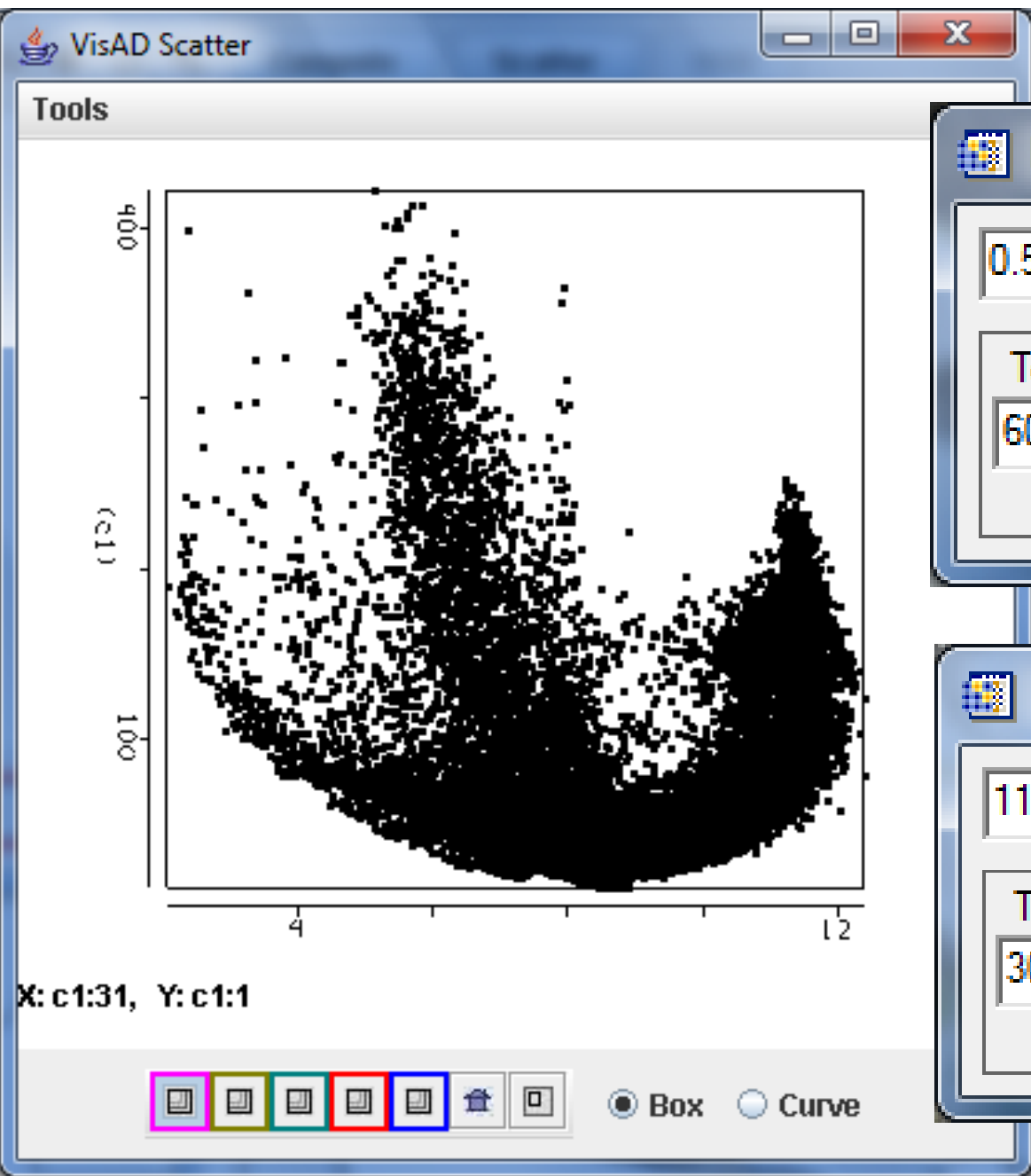
Incoming solar radiation (mostly visible) drives the earth-atmosphere (which emits infrared).

Over the annual cycle, the incoming solar energy that makes it to the earth surface (about 50 %) is balanced by the outgoing thermal infrared energy emitted through the atmosphere.

The atmosphere transmits, absorbs (by H₂O, O₂, O₃, dust) reflects (by clouds), and scatters (by aerosols) incoming visible; the earth surface absorbs and reflects the transmitted visible. Atmospheric H₂O, CO₂, and O₃ selectively transmit or absorb the outgoing infrared radiation. The outgoing microwave is primarily affected by H₂O and O₂.

Spectral Characteristics of Atmospheric Transmission and Sensing Systems





Planck Calc...

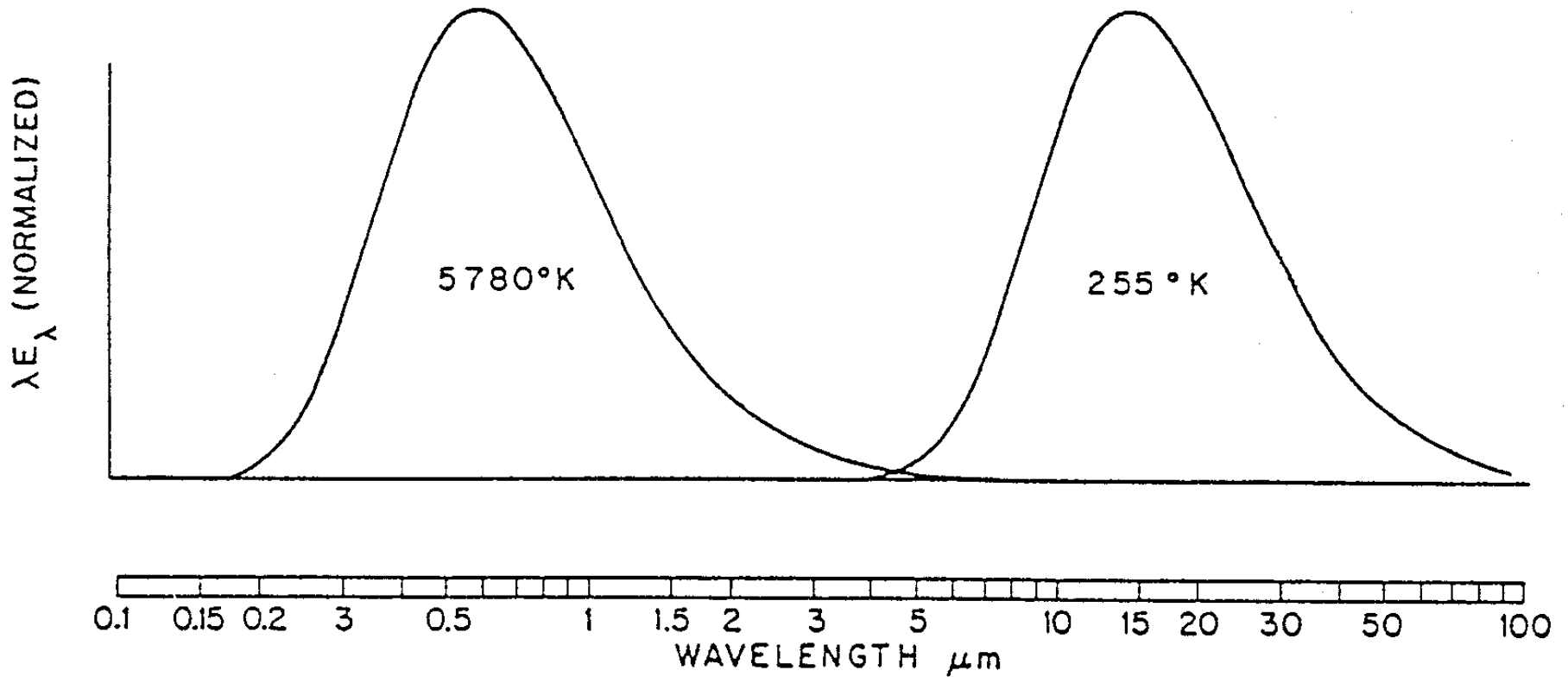
0.50 microns

Temperature	Radiance
6000.00	3.175708e+007
Kelvin	W/m ² /sr/um

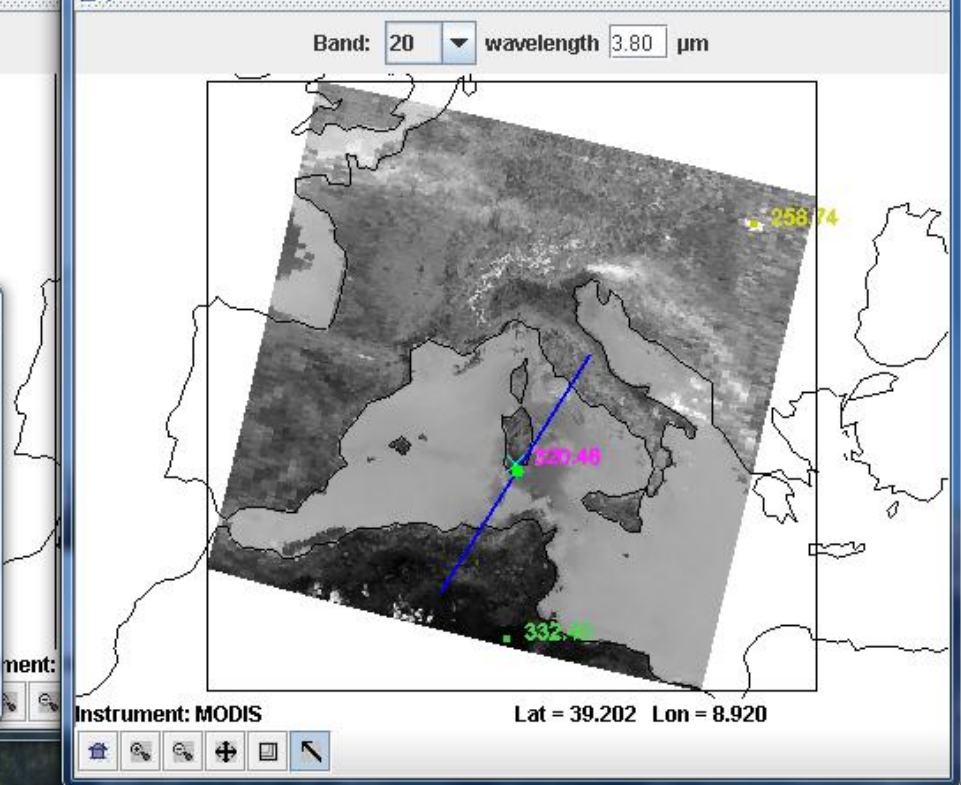
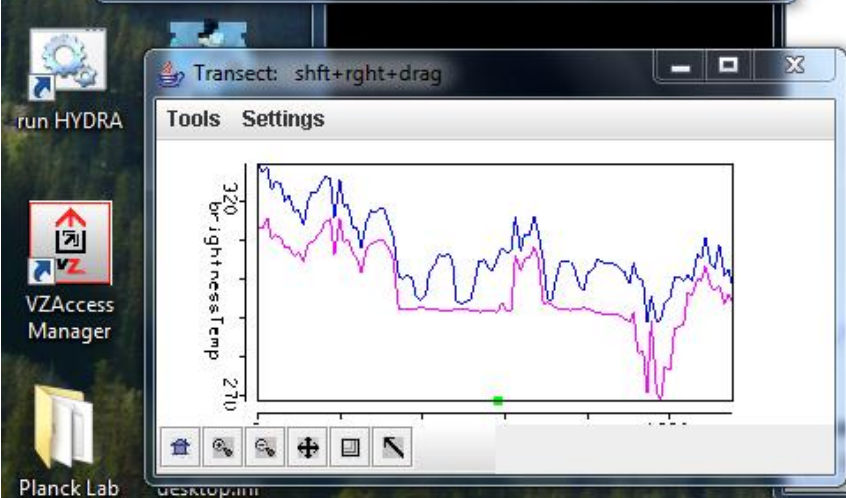
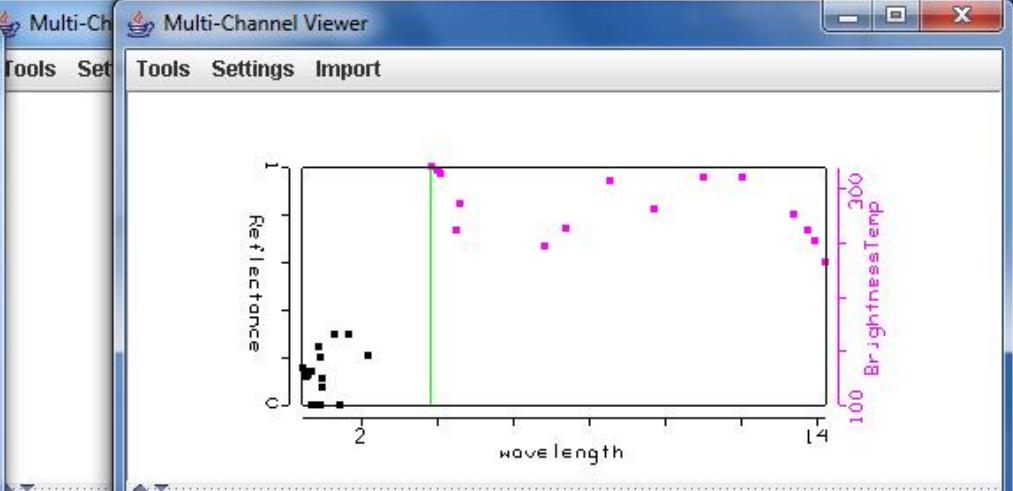
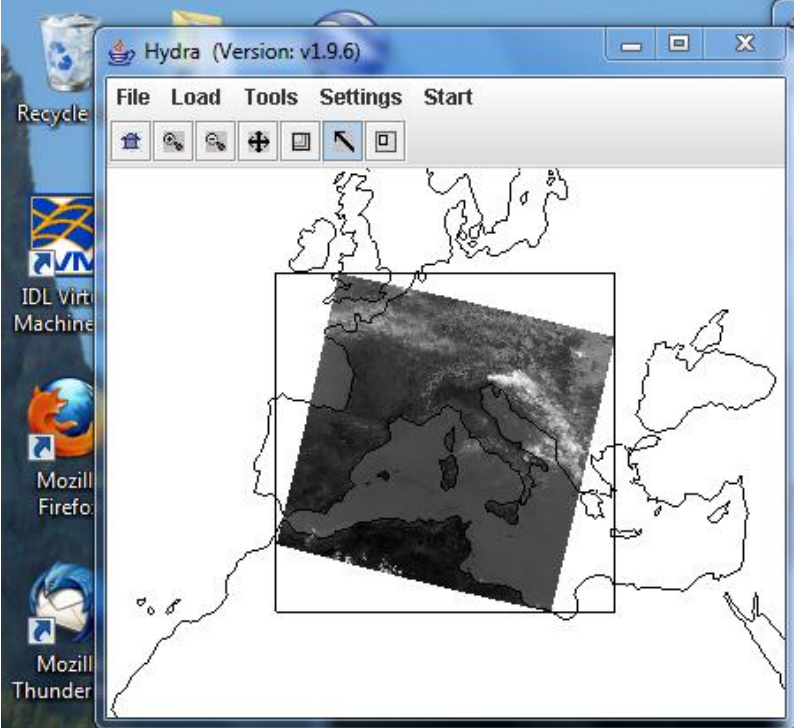
Planck Calc...

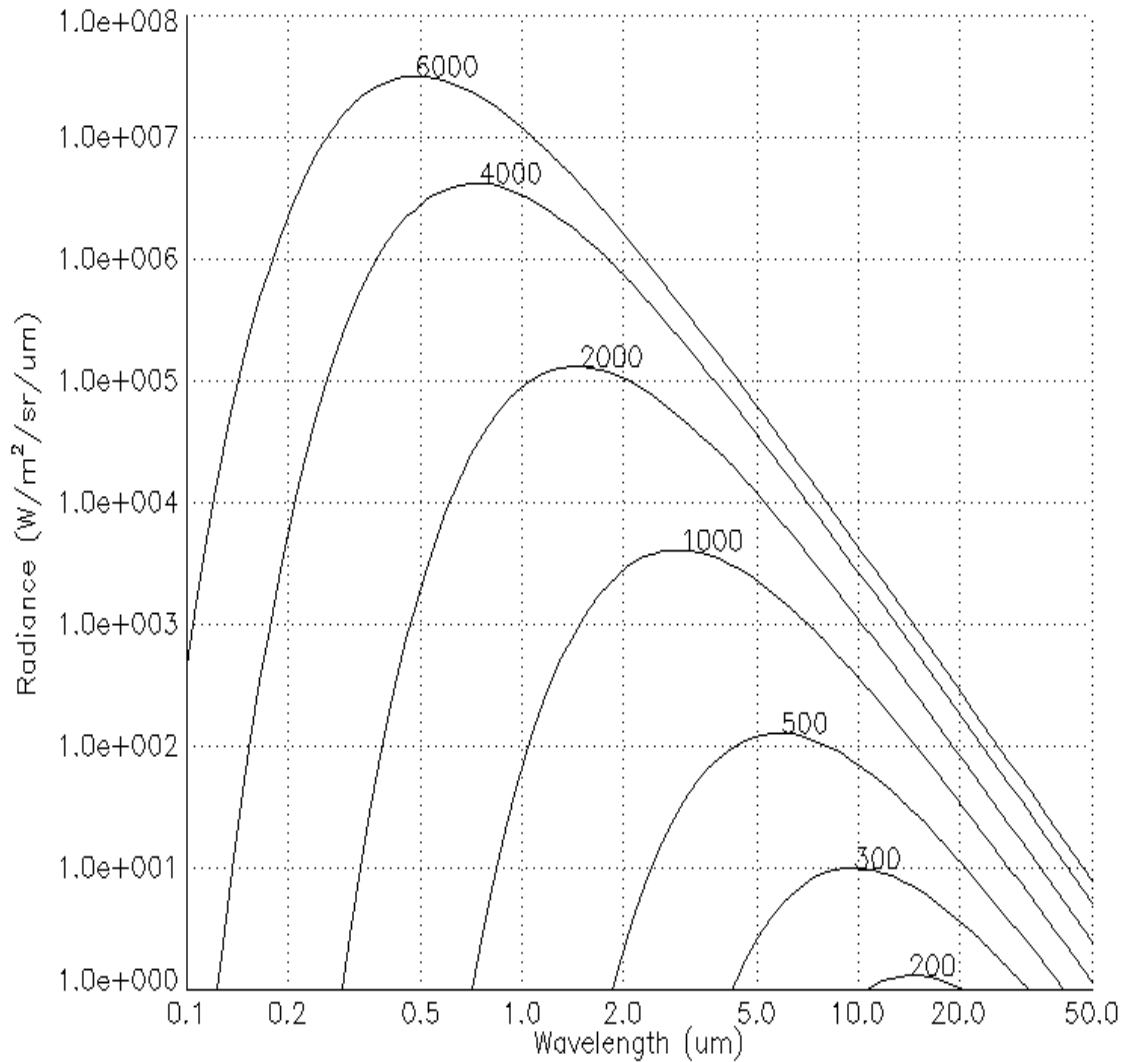
11.00 microns

Temperature	Radiance
300.00	9.573229e+000
Kelvin	W/m ² /sr/um



Normalized black body spectra representative of the sun (left) and earth (right), plotted on a logarithmic wavelength scale. The ordinate is multiplied by wavelength so that the area under the curves is proportional to irradiance.





Planck Calc...

4.00 microns

Temperature	Radiance
6000.00	1.416394×10^5
Kelvin	$\text{W/m}^2/\text{sr}/\mu\text{m}$

Planck Calc...

4.00 microns

Temperature	Radiance
300.00	7.219866×10^{-1}
Kelvin	$\text{W/m}^2/\text{sr}/\mu\text{m}$

BT11=290K and BT4=310K.

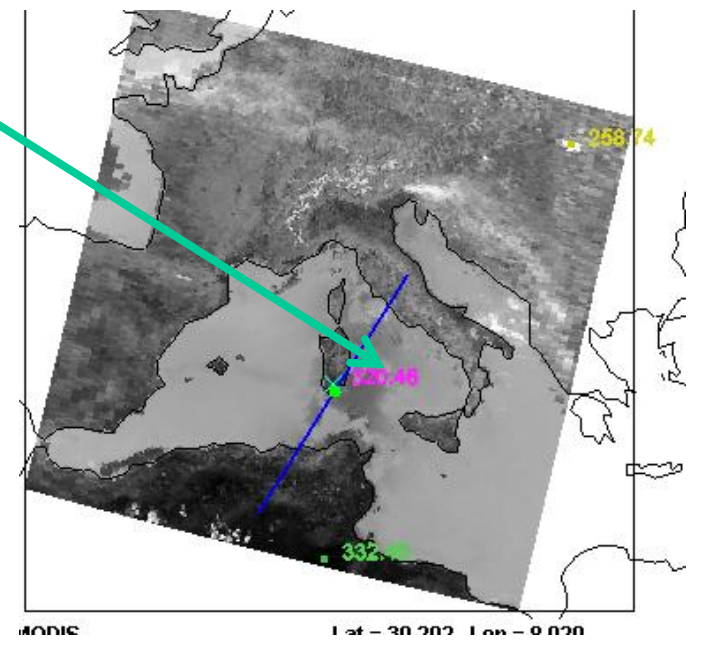
What fraction of R4 is due to reflected solar radiance?

$$R4 = R4_{\text{refl}} + R4_{\text{emiss}}$$

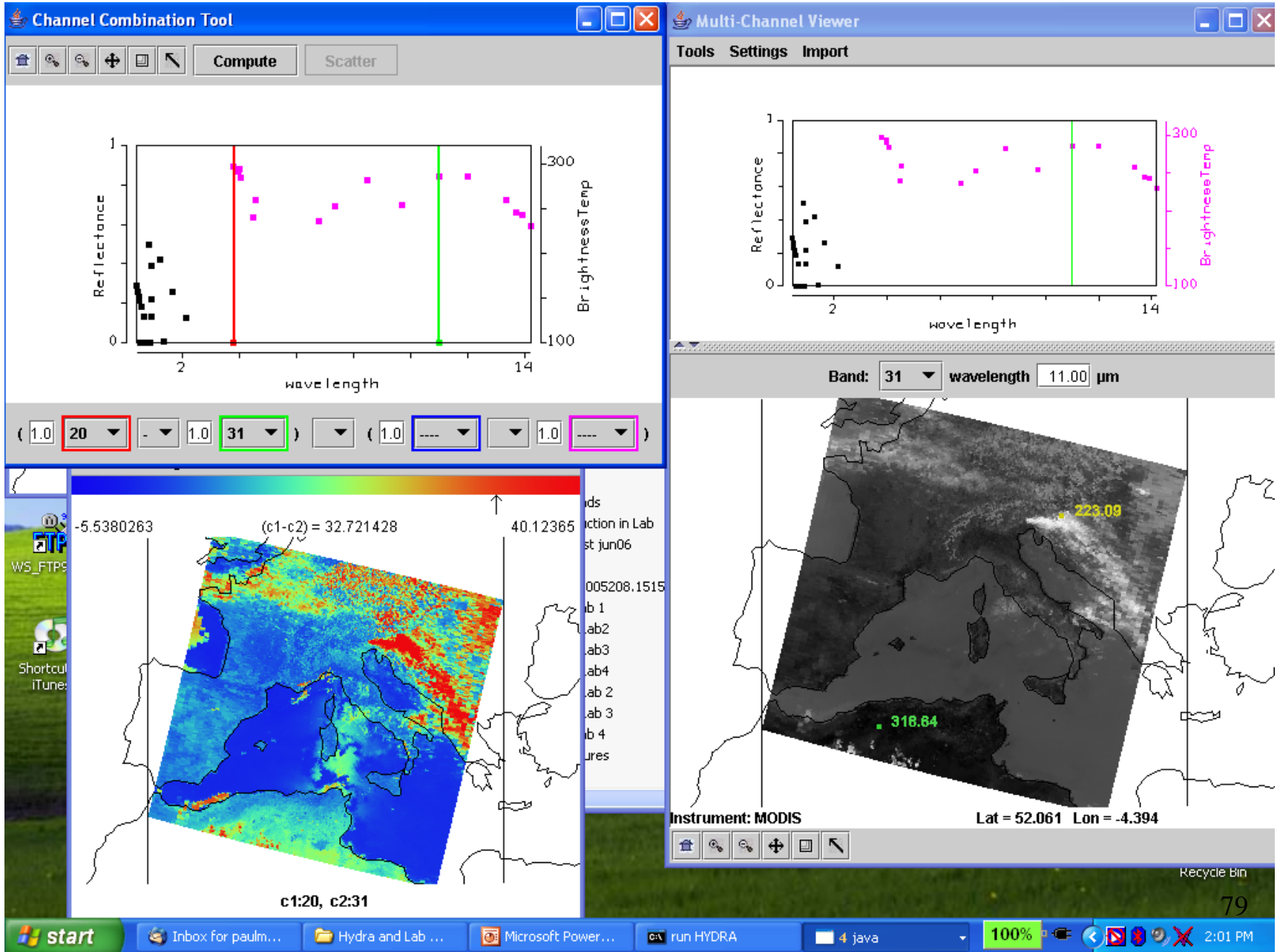
$$BT4_{\text{emiss}} = BT11$$

$$R4 \sim T^{**12}$$

$$\text{Fraction} = [310^{**12} - 290^{**12}] / 310^{**12} \sim .55$$

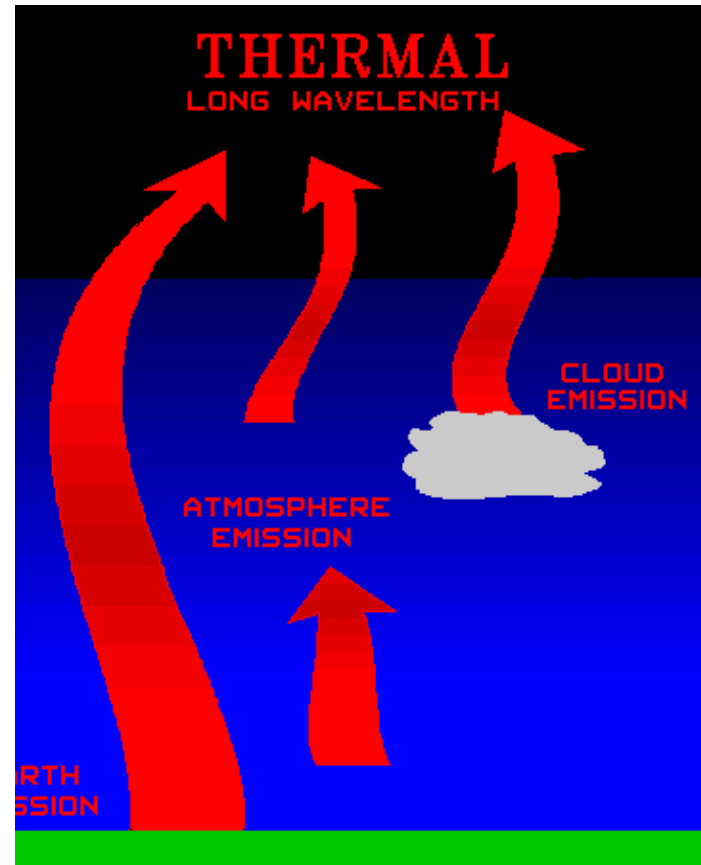


SW minus LW IRW



Infrared (Emissive Bands)

Radiative Transfer Equation
in the IR



Emission, Absorption, Reflection, and Scattering

Blackbody radiation B_λ represents the upper limit to the amount of radiation that a real substance may emit at a given temperature for a given wavelength.

Emissivity ε_λ is defined as the fraction of emitted radiation R_λ to Blackbody radiation,

$$\varepsilon_\lambda = R_\lambda / B_\lambda .$$

In a medium at thermal equilibrium, what is absorbed is emitted (what goes in comes out) so

$$a_\lambda = \varepsilon_\lambda .$$

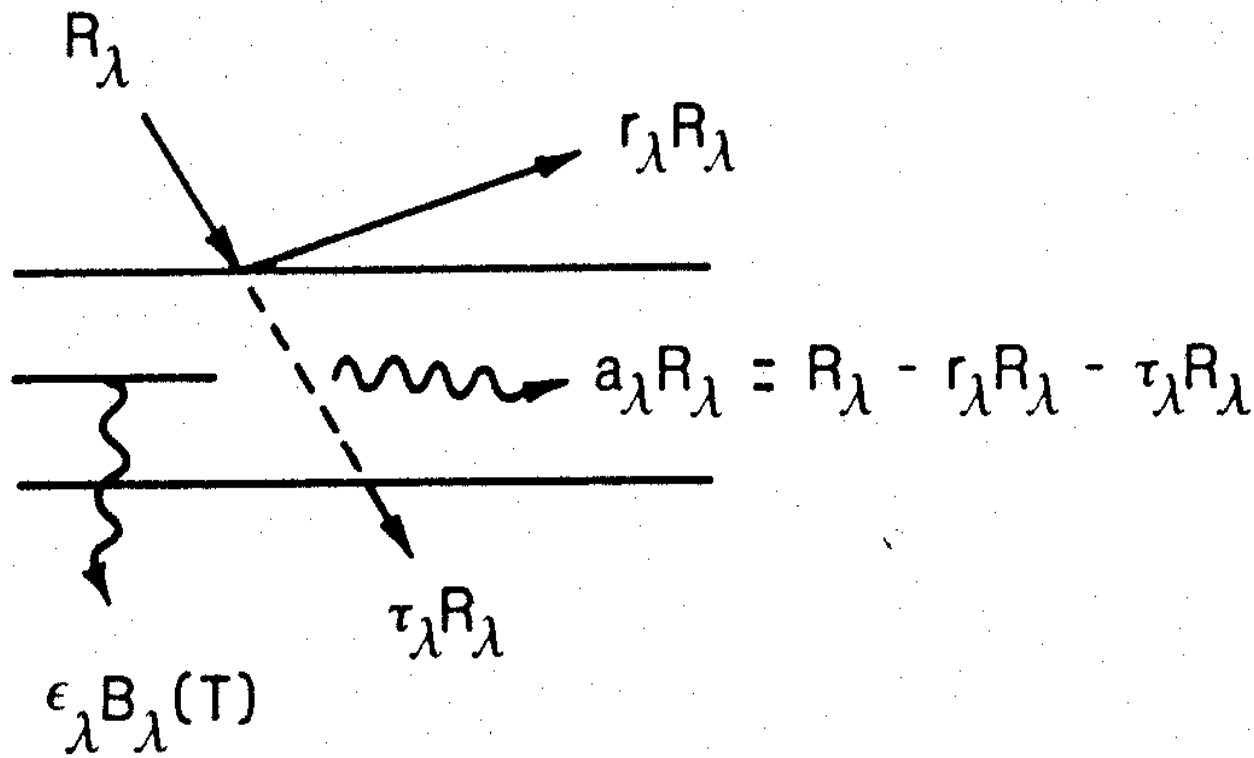
Thus, materials which are strong absorbers at a given wavelength are also strong emitters at that wavelength; similarly weak absorbers are weak emitters.

If a_λ , r_λ , and τ_λ represent the fractional absorption, reflectance, and transmittance, respectively, then conservation of energy says

$$a_\lambda + r_\lambda + \tau_\lambda = 1 .$$

For a blackbody $a_\lambda = 1$, it follows that $r_\lambda = 0$ and $\tau_\lambda = 0$ for blackbody radiation. Also, for a perfect window $\tau_\lambda = 1$, $a_\lambda = 0$ and $r_\lambda = 0$. For any opaque surface $\tau_\lambda = 0$, so radiation is either absorbed or reflected $a_\lambda + r_\lambda = 1$.

At any wavelength, strong reflectors are weak absorbers (i.e., snow at visible wavelengths), and weak reflectors are strong absorbers (i.e., asphalt at visible wavelengths).



‘ENERGY
CONSERVATION’

Transmittance

Transmission through an absorbing medium for a given wavelength is governed by the number of intervening absorbing molecules (path length u) and their absorbing power (k_λ) at that wavelength. Beer's law indicates that transmittance decays exponentially with increasing path length

$$\tau_\lambda (z \rightarrow \infty) = e^{-k_\lambda u (z)}$$

where the path length is given by $u (z) = \int_z^\infty \rho dz$.

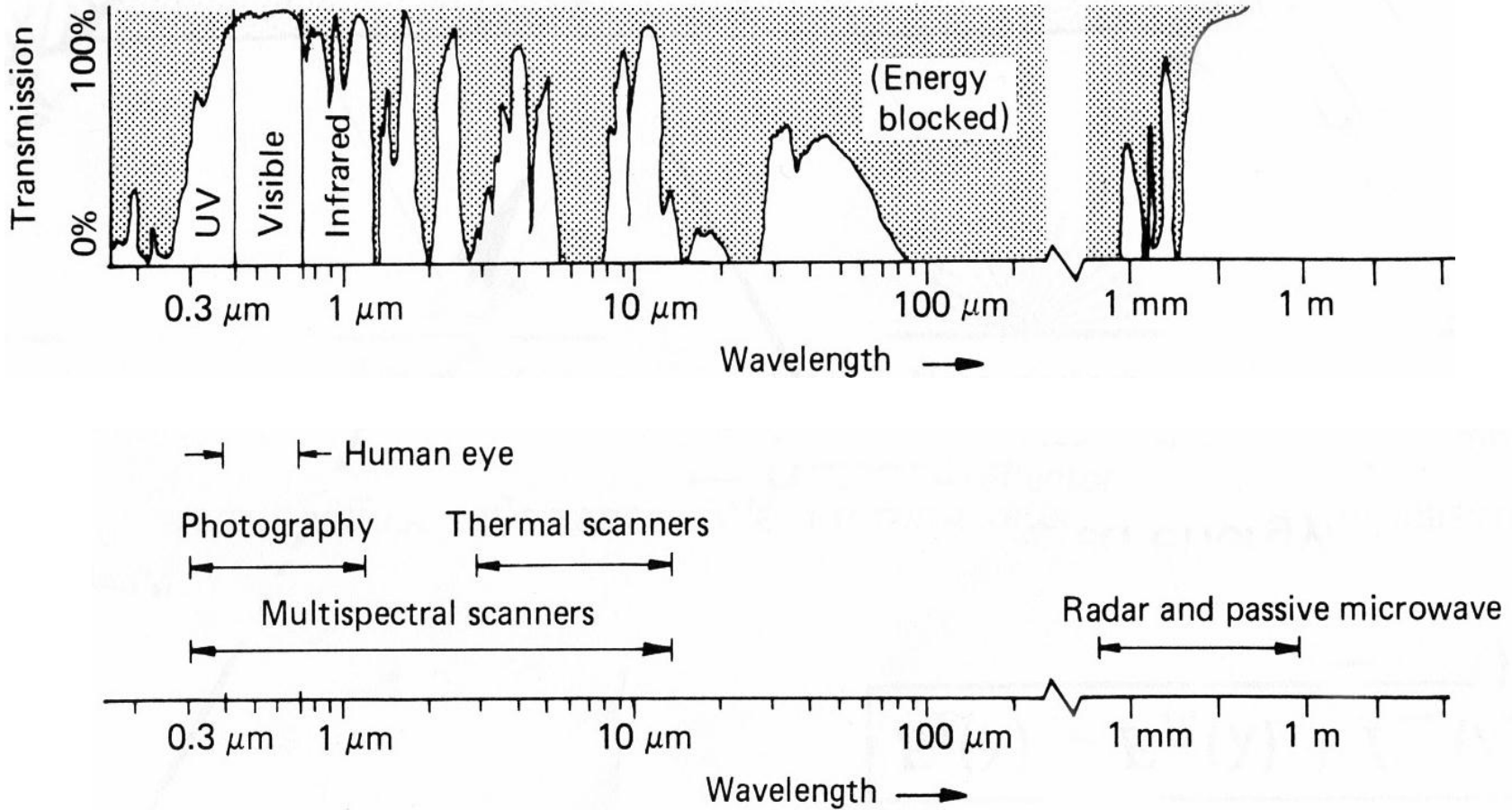
$k_\lambda u$ is a measure of the cumulative depletion that the beam of radiation has experienced as a result of its passage through the layer and is often called the optical depth σ_λ .

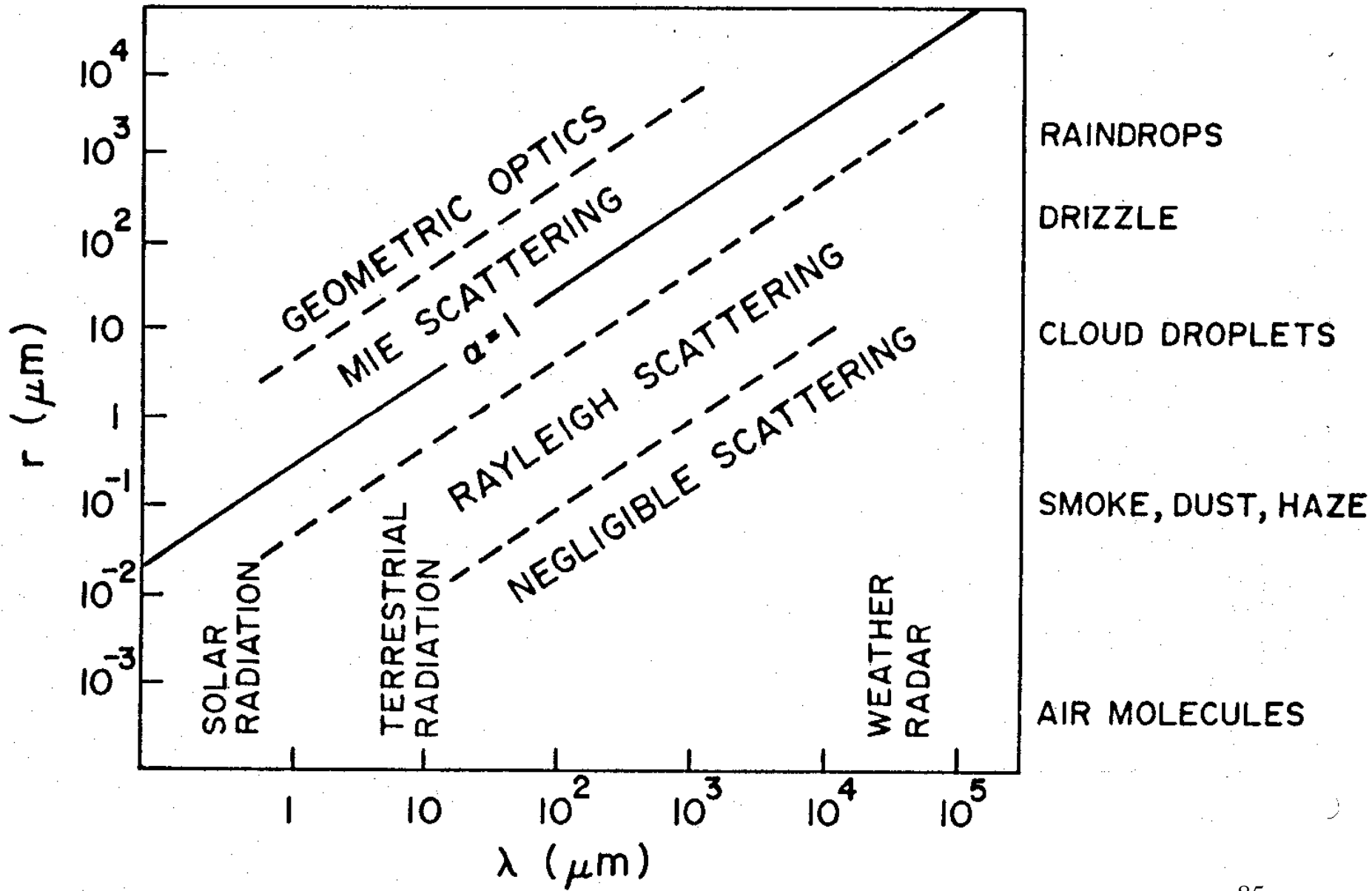
Realizing that the hydrostatic equation implies $g \rho dz = -q dp$

where q is the mixing ratio and ρ is the density of the atmosphere, then

$$u (p) = \int_0^p q g^{-1} dp \quad \text{and} \quad \tau_\lambda (p \rightarrow 0) = e^{-k_\lambda u (p)}$$

Spectral Characteristics of Atmospheric Transmission and Sensing Systems



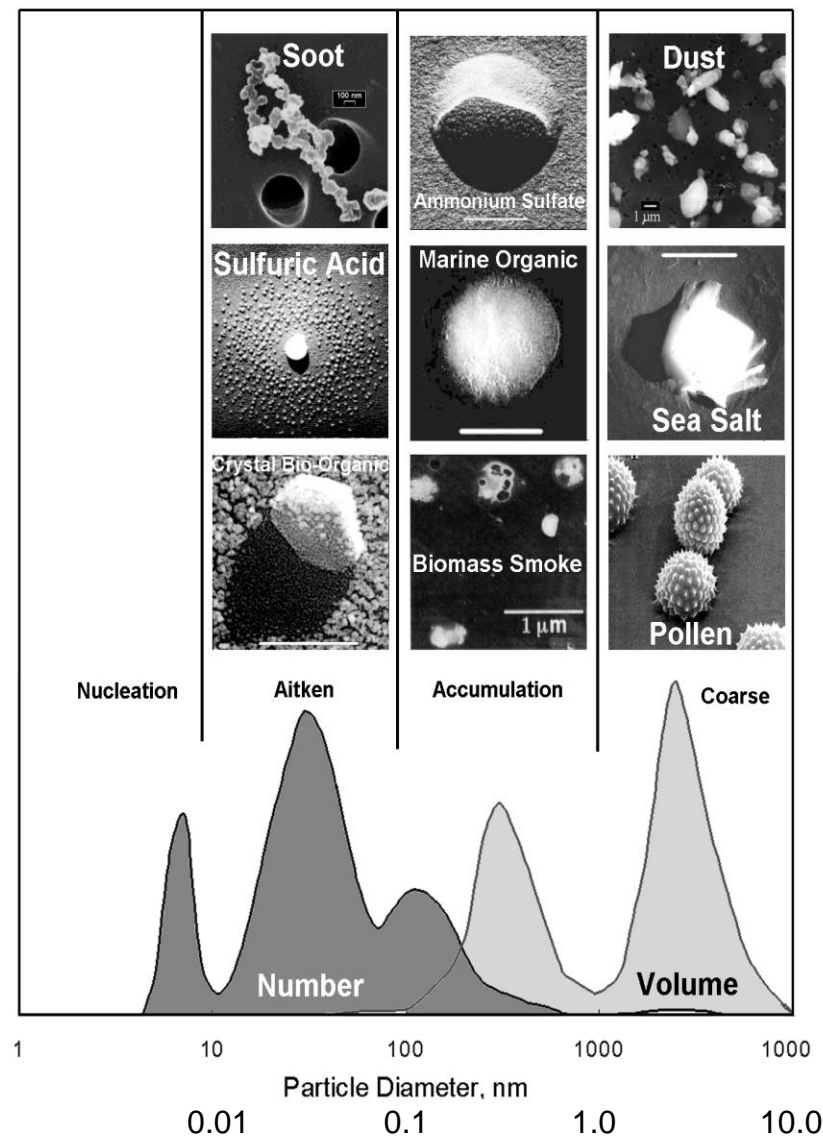


Aerosol Size Distribution

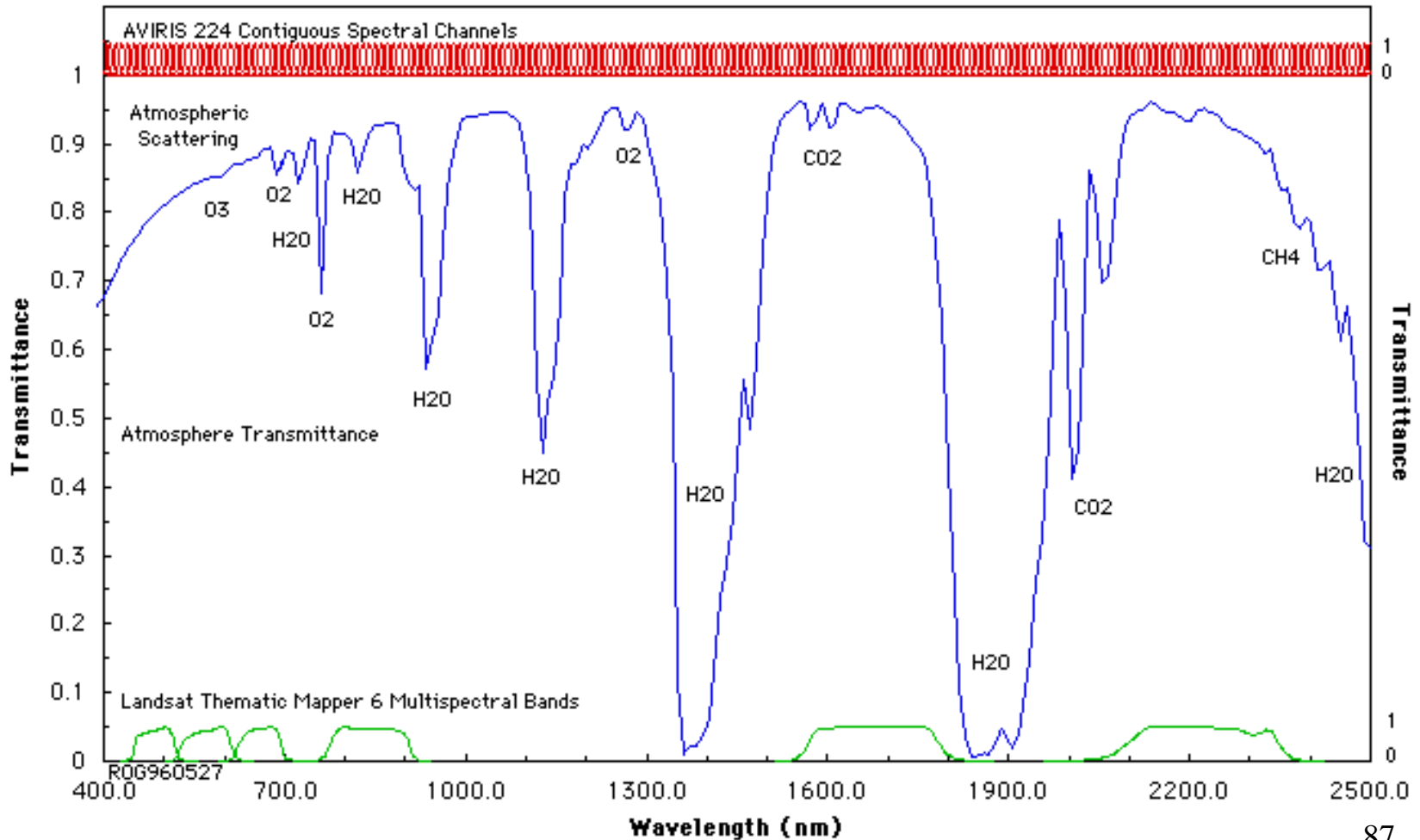
There are 3 modes :

- « **nucleation** »: radius is between 0.002 and 0.05 μm . They result from combustion processes, photo-chemical reactions, etc.
- « **accumulation** »: radius is between 0.05 μm and 0.5 μm . Coagulation processes.
- « **coarse** »: larger than 1 μm . From mechanical processes like aeolian erosion.

« fine » particles (nucleation and accumulation) result from anthropogenic activities, coarse particles come from natural processes.



Measurements in the Solar Reflected Spectrum across the region covered by AVIRIS

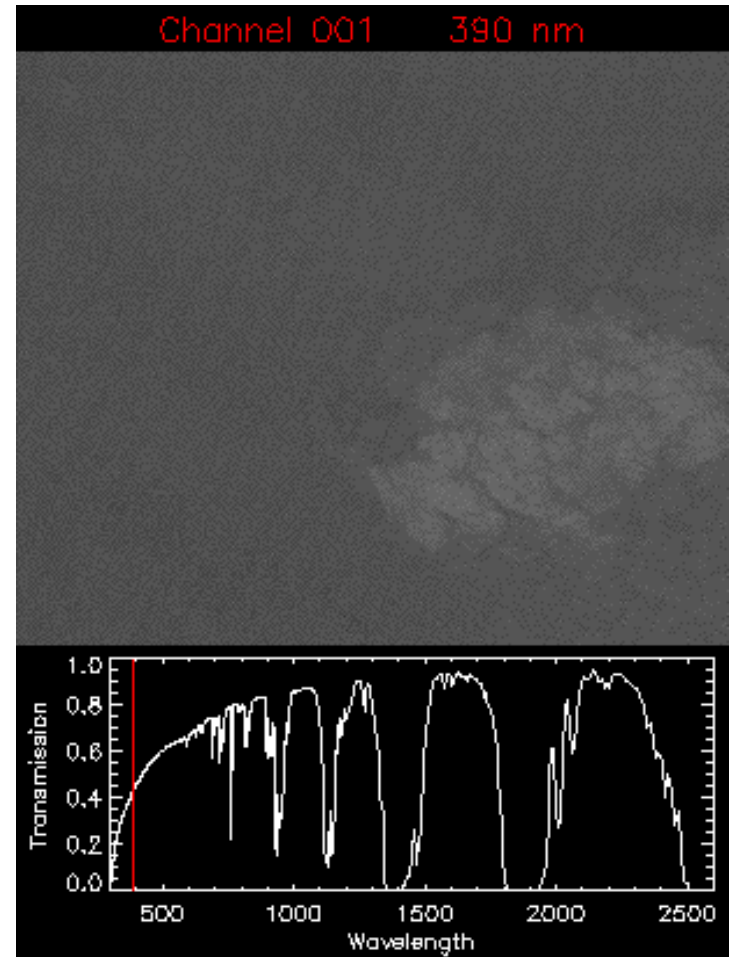


AVIRIS Movie #1

AVIRIS Image - Linden CA 20-Aug-1992

224 Spectral Bands: 0.4 - 2.5 μm

Pixel: 20m x 20m Scene: 10km x 10km



AVIRIS Movie #2

AVIRIS Image - Porto Nacional, Brazil

20-Aug-1995

224 Spectral Bands: 0.4 - 2.5 μm

Pixel: 20m x 20m Scene: 10km x 10km

